ORTA DOĞU TEKNİK ÜNİVERSİTESİ
FEN BİLİMLERİ ENSTİTÜSÜ MÜDÜRLÜĞÜ

TEZ ŞABLONU ONAY FORMU
THESIS TEMPLATE CONFIRMATION FORM

1. Şablonda verilen yerleşim ve boşluklar değiştirilmemelidir.
2. **Jüri tarihi** Başlık Sayfası, İmza Sayfası, Abstract ve Öz'de ilgili yerlere yazılmalıdır.
3. İmza sayfasında jüri üyelerinin unvanları doğru olarak yazılmalıdır. Tüm imzalar **mavi pilot kalemle** atılmalıdır.
4. **Disiplinlerarası** programlarda görevlendirilen öğretim üyeleri için jüri üyeleri kısmında tam zamanlı olarak çalıştıkları anabilim dalı başkanlığının ismi yazılmalıdır. Örneğin: bir öğretim üyesi Biyoteknoloji programında görev yapıyor ve biyoloji bölümünde tam zamanlı çalışıyorsa, İmza sayfasına biyoloji bölümü yazılmalıdır. İstisnai olarak, disiplinler arası program başkanı ve tez danışmanı için disiplinlerarası program adı yazılmalıdır.
5. Tezin **son sayfasının sayfa** numarası Abstract ve Öz'de ilgili yerlere yazılmalıdır.
6. Bütün chapterlar, referanslar, ekler ve CV sağ sayfada başlamalıdır. Bunun için **kesmeler** kullanılmıştır. **Kesmelerin kayması** fazladan boş sayfaların oluşmasına sebep olabilir. Bu gibi durumlarda paragraf (¶) işaretine tıklayarak kesmeleri görünür hale getirin ve yerlerini **kontrol edin**.
7. Figürler ve tablolar kenar boşluklarına taşmamalıdır.
8. Şablonda yorum olarak eklenen uyarılar dikkatle okunmalı ve uygulanmalıdır.
9. Tez yazdırılmadan önce PDF olarak kaydedilmelidir. Şablonda yorum olarak eklenen uyarılar PDF dokümanında yer almamalıdır.
10. **Bu form aracılığıyla oluşturulan PDF dosyası arkalı-önlü baskı alınarak tek bir spiralli cilt haline getirilmelidir.**
11. Spiralli hale getirilen tez taslağınızdaki ilgili alanları imzalandıktan sonra, Tez Juri Atama Formu ile birlikte bölüm sekreterliğine teslim edilmelidir.
12. Tez taslaklarının kontrol işlemleri tamamlandığında, bu durum öğrencilere METU uzantılı öğrenci e-posta adresleri aracılığıyla duyurulacaktır.
13. Tez yazım süreci ile ilgili herhangi bir sıkıntı yaşarsanız, **Sıkça Sorulan Sorular (SSS)** sayfamızı ziyaret ederek yaşadığınız sıkıntıyla ilgili bir çözüm bulabilirsiniz.

1. Do not change the spacing and placement in the template.
2. Write **defense date** to the related places given on Title page, Approval page, Abstract and Öz.
3. Write the titles of the examining committee members correctly on Approval Page. **Blue ink** must be used for all signatures.
4. For faculty members working in **interdisciplinary programs**, the name of the department that they work full-time should be written on the Approval page. For example, if a faculty member staffs in the biotechnology program and works full-time in the biology department, the department of biology should be written on the approval page. Exceptionally, for the interdisciplinary program chair and your thesis supervisor, the interdisciplinary program name should be written.
5. Write **the page number of the last page** in the related places given on Abstract and Öz pages.
6. All chapters, references, appendices and CV must be started on the right page. **Section Breaks** were used for this. **Change in the placement** of section breaks can result in extra blank pages. In such cases, make the section breaks visible by clicking paragraph (¶) mark and **check their position.**
7. All figures and tables must be given inside the page. Nothing must appear in the margins.
8. All the warnings given on the comments section through the thesis template must be read and applied.
9. Save your thesis as pdf and Disable all the comments before taking the printout.
10. **Print two-sided the PDF file that you have created through this form and make a single spiral bound.**
11. Once you have signed the relevant fields in your thesis draft that you spiraled, submit it to the department secretary together with your Thesis Jury Assignment Form.
12. This will be announced to the students via their METU students e-mail addresses when the control of the thesis drafts has been completed.
13. If you have any problems with the thesis writing process, you may visit our **Frequently Asked Questions (FAQ)** page and find a solution to your problem.

☒ **Yukarıda bulunan tüm maddeleri okudum, anladım ve kabul ediyorum. / I have read, understand and accept all of the items above.**

Name : **Anıl**
Surname : **Hatiboğlu**
E-Mail : **anil.hatiboglu@gmail.com**
Date : **13.09.2021**
Signature : _____

INVESTIGATION OF THE PERMEABILITY OF THE CELL MEMBRANE FOR DIFFERENT CRYOPROTECTANT AGENTS IN A CONTINUOUS THERMO-FLUIDIC MICRO-CHANNEL SYSTEM

A THESIS SUBMITTED TO
THE GRADUATE SCHOOL OF NATURAL AND APPLIED SCIENCES
OF
MIDDLE EAST TECHNICAL UNIVERSITY

BY

ANIL HATİBOĞLU

IN PARTIAL FULFILLMENT OF THE REQUIREMENTS
FOR
THE DEGREE OF MASTER OF SCIENCE
IN
MICRO AND NANOTECHNOLOGY

SEPTEMBER 2021

Approval of the thesis:

INVESTIGATION OF THE PERMEABILITY OF THE CELL MEMBRANE FOR DIFFERENT CRYOPROTECTANT AGENTS IN A CONTINUOUS THERMO-FLUIDIC MICRO-CHANNEL SYSTEM

submitted by **ANIL HATİBOĞLU** in partial fulfillment of the requirements for the degree of **Micro and Nanotechnology** i**n , Middle East Technical University** by,

Prof. Dr. Halil Kalıpçılar
Dean, Graduate School of **Natural and Applied Sciences** _____

Prof. Dr. Almıla Güvenç Yazıcıoğlu
Head of the Department, **Micro and Nanotechnology** _____

Prof. Dr. Haluk Külah
Supervisor, **Micro and Nanotechnology, METU** _____

Assoc. Prof. Dr. Selis Önel
Co-Supervisor, **Chemical Engineering, Hacettepe University** _____

Examining Committee Members:

Prof. Dr. Almıla Güvenç Yazıcıoğlu
Micro and Nanotechnology, METU _____

Prof. Dr. Haluk Külah
Micro and Nanotechnology, METU _____

Assoc. Prof. Dr. Selis Önel
Chemical Engineering, Hacettepe University _____

Assoc. Prof. Dr. Ender Yıldırım
Mechanical Engineering, METU _____

Assoc. Prof. Dr. Özgür Ekici
Mechanical Engineering, Hacettepe University _____

Date: 13.09.2021

I hereby declare that all information in this document has been obtained and presented in accordance with academic rules and ethical conduct. I also declare that, as required by these rules and conduct, I have fully cited and referenced all material and results that are not original to this work.

Name Last name : Anıl Hatiboğlu

Signature :

ABSTRACT

INVESTIGATION OF THE PERMEABILITY OF THE CELL MEMBRANE FOR DIFFERENT CRYOPROTECTANT AGENTS IN A CONTINUOUS THERMO-FLUIDIC MICRO-CHANNEL SYSTEM

Hatiboğlu, Anıl
Master of Science, Micro and Nanotechnology
Supervisor: Prof. Dr. Haluk Külah
Co-Supervisor: Assoc. Prof. Dr. Selis Önel

September 2021, 124 pages

Modeling cell membrane permeability in different solutions is a critical requirement in controlling the response of cells during preconcentration processes in biotechnological applications, such as drug delivery, fluorescence imaging, and cryopreservation . Current multi-step methods employed in loading cells with high concentrations of cryoprotectant agents (CPAs) prior to cryopreservation for long term storage affect cell viability as a result of extended exposure times associated with these methods. One of the objectives of this research to observe the response of different types of cells in a continous microfluidic system allowing for reduced exposure times to the CPAs and to model the transport of CPA through the cell membrane.

In this study, a micro thermo-fluidic device designed for faster and continuous preconcentration of cells with CPAs is used to study cell membrane permeability. Cells are encapsulated in uniform aqueous droplets with a low CPA concentration, The concentration of the CPA in the droplet is increased along the microchannel by controlling the temperature, and thus the water solubility of the oil phase. Selective diffusion of water out of the droplet causes the droplet to shrink and get concentrated

in CPAs. The response of the cell to the changes in the extracellular concentration is observed and analysed. The dynamic extracellular CPA concentration data is integrated in a permeability model to calculate the dynamic permeability of the cell membrane to a specific CPA.

Two-phase flow conditions for droplet generation are optimized to determine the flow rate to achieve the desired droplet size. A linear relationship is found between flow rates and the size of the droplets, regardless of the size and geometry of the microfluidic device. The performance of encapsulation of cells in the droplets based on the flow rate is assessed. The undesired phenomena, such as the encapsulation of cells in multiples and the sedimentation inside the microchannels, are found to be associated with the low flow rates.

Employing a continuous two-phase microfluidic system has proved valuable in observing the response of the cell to increasing CPA concentrations. Encapsulation in smaller droplets has yielded a higher increase in the intracellular CPA concentration. A conventional mathematical model for the permeability of the cell membrane is modified by using the dynamic extracellular concentrations obtained from the microfluidic system. Membrane permeability parameters are determined for MDA-MB231 cells using glycerol as the CPA, where concentration is increased from 1 M to 2.05 M in the aqueous droplets with heating to 40°C in the microfluidic channels.

Keywords: Droplet Microfluidics, Cell Encapsulation, Cell Membrane, Membrane Permeability, Cryoprotectant Agents

ÖZ

HÜCRE ZARI GEÇİRGENLİĞİNİN SÜREKLİ BİR TERMO-AKIŞKAN MİKROKANALLI SİSTEMDE FARKLI DONMADA KORUYUCU MADDELER İLE İNCELENMESİ

Hatiboğlu, Anıl
Yüksek Lisans, Mikro ve Nanoteknoloji
Tez Yöneticisi: Prof. Dr. Haluk Külah
Ortak Tez Yöneticisi: Doç. Dr. Selis Önel

Eylül 2021, 124 sayfa

Hücre zarı geçirgenliğinin farklı solüsyonlar içinde modellenmesi, ilaç taşınımı, floresan görüntüleme, donmada koruma gibi biyoteknoloji uygulamalarında önderişim işlemi sırasında hücre tepkisini kontrol etmek açısından kritik bir ihtiyaçtır. Güncel çok aşamalı yöntemlerde, uzun süreli dondurarak saklama öncesi hücrelere yüksek derişimde donmada koruyucu maddelerin yüklenmesi uzayan maruz kalma süreleri nedeniyle hücrelerin canlılığını etkilemektedir. Bu çalışmanın hedefleri farklı hücrelerin tepkilerinin donmada korucu maddelere maruz kalma süresini düşüren sürekli mikroakışkan sistemde gözlemlenmesi ve bu şartlar altında hücre zarından donmada koruyucu madde taşınımının modellenmesidir.

Bu çalışmada, daha hızlı ve hücrelerin donmada koruyucu madde ile sürekli önderiştirilmesi için tasarlanan mikro termo-akışkan cihaz, hücre zarı geçirgenliğini incelemek için kullanılmıştır. Hücreler, düşük donmada koruyucu madde derişimine sahip eş boyutlu sulu damlacıklara hapsedilmiştir. Donmada koruyucu madde derişimi sıcaklığın ve buna bağlı olarak soğa yağı içinde su çözünürlüğünün kontrol edilmesi ile mikrokanal boyunca artırılmıştır. Suyun damlacıktan dışarı seçimli difüzyonu, damlacığın küçülmesine ve içeride kalan donmada koruyucu madde derişiminin artmasını sağlamıştır. Hücre dışı derişimin değişimine hücrenin verdiği

tepki incelenmiş ve analiz edilmiştir. Dinamik hücre dışı donmada koruyucu madde derişimi verileri bir gerçirgenlik modeline entegre edilerek hücre zarının spesifik bir donmada koruyucu maddeyi dinamik geçirgenliği hesaplanmıştır.

Damlacık oluşumu için iki fazlı akış koşulları optimize edilerek istenen damlacık boyutu için kullanılması gereken akış hızları belirlenmiştir. Akış hızı ve damlacık boyutu arasında, microakışkan cihaz boyutu ve geometrisinden bağımsız olarak doğrusal bir ilişki bulunmuştur. Akış hızına bağlı olarak damlacık içinde hücre enkapsülasyon performansı incelenmiştir. Birden fazla hücrenin tek damlacık içinde enkapsülasyonu ve microkanal içinde hücrelerin çökelmesi gibi istenmeyen durumların düşük akış hızı kullanımı ile ilişkili olduğu gösterilmiştir.

Sürekli bir iki fazla mikroakışkan sistemin kullanılması hücrenin artan donmada koruyucu madde derişimine verdiği tepkileri gözlemlemede değerli olduğunu göstermiştir. Damlacık içinde enkapsüle edilen hücrelerde, damlacık küçüldükçe daha yüksek donmada koruyucu madde derişimlerine ulaşılmıştır. Hücre zarı geçirgenlik modelleri için mevcut olan konvansiyonel bir model dinamik hücre dışı derişimin kullanımı ile modifiye edilmiştir. Hücre zarı geçirgenlik parametreleri, derişimin 1 M'dan 2.05 M'a çıkarıldığı sulu damlacıklarda ve 40°Cye ısıtılan mikroakışkan kanal içerisinde, donmada koruyucu madde olarak gliserol kullanılarak MDA-MB231 hücreleri için elde edilmiştir.

Anahtar Kelimeler: Damlacık Mikroakışkanları, Hücre Enkapsülasyonu, Hücre Zarı, Hücre Zarı Geçirgenliği, Donmada Koruyucu Maddeler

To my grandfather, for being the most hardworking, gentleman, happy and kind person whom I had the honor of knowing and living with

ACKNOWLEDGMENTS

The author wishes to express his deepest gratitude to his supervisor Professor Haluk Külah and co-supervisor Professor Selis Önel for their guidance, advice, criticism, encouragements, and insight throughout the research.

The author would like to thank Professor Mehmet Toner, the director of the BioMEMS Resource Center and the Center for Engineering in Medicine and Surgery at Massachusetts General Hospital (MGH) and Harvard Medical School, where the microfluidic devices used in this study were developed.

The author would like to thank Professor Can Özen and Selin Gerekçi (Biotechnology Program, METU), Professor Müge Yemişçi Özkan (Institute of Neurological Sciences and Psychiatry, Hacettepe University), and Professor Handan Sevim and Professor Esin Akbay Çetin (Department of Biology, Hacettepe University) for providing the cells as this work could not be completed without their useful advice and support.

The author would like to thank Dr. Erhan Şenlik, Dr. Güneş Kibar, Ali Can Atik, and Bahar Özden for their precious help and suggestions during the study.

The author also appreciates the undergraduate fellows, who found the chance to join the lab to observe and learn things during this study, which brings encouragement of sharing the experience and knowledge gained during the long adventure.

The author feels grateful and lucky to have the emotional support, companionship, friendship and love of Betül Aktaş at the hardest times. With her presence, every struggle and achievement was a delightful memory.

This work is partially funded by Scientific and Technological Research Council of Turkey under grant numbers TUBİTAK 214M323 and 220M002.

TABLE OF CONTENTS

ABSTRACT v

ÖZ vii

ACKNOWLEDGMENTS x

TABLE OF CONTENTS xi

LIST OF TABLES xiv

LIST OF FIGURES xv

LIST OF ABBREVIATIONS xviii

LIST OF SYMBOLS xix

CHAPTERS

1 INTRODUCTION 1

1.1 Research Background 1

1.2 Cryopreservation of Cells 4

1.3 Preparation of Cells for Cryopreservation in Microfluidic Environment 7

1.4 Droplet Microfluidics 7

1.5 Motivation and Objectives of the Study 8

1.6 Outline of the Thesis 10

2 LITERATURE REVIEW 11

2.1 Microfluidic Devices 12

2.2 Two Phase Flow in Microfluidic Devices 13

2.3 Cell Membrane Permeability Models 17

2.3.1 Two-Parameter Model 17

2.3.2 Kedem-Katchalsky Model 18

2.4 Determination of Membrane Permeability Parameters using Cryoprotectant Agents 20
2.5 Cell Encapsulation 25
3 MATERIALS AND METHODS 27
3.1 Design and Use of the Microfluidic Device 27
3.2 Fabrication of Microfluidic Devices 29
3.3 Microfluidic System Setup 32
3.4 Solution Preparation 32
3.5 Droplet Generation in Microfluidic Device 33
3.6 Droplet Size Measurements 34
3.7 Cell Culturing, Cytometry and Handling 38
3.7.1 Jurkat Cells 40
3.7.2 K562 Cells 41
3.7.3 MDA-MB231 Cells 41
3.7.4 L929 Cells 42
3.7.5 Mouse Brain Microvessels 43
3.8 Integration of Cell Solution to Microfluidic System 44
3.9 GUI Designed for Model Solvers 47
4 RESULTS AND DISCUSSION 53
4.1 Aqueous Droplet Generation 53
4.1.1 Droplet Generation in X-Channel Device 56
4.1.2 Droplet Generation in Serpentine Device 58
4.1.3 Aqueous Droplet Solubility in Soybean Oil 64
4.2 Droplet Shrinkage in Serpentine Device 67

4.2.1 Droplet Shrinkage in 25 µm-Device 69
4.2.2 Droplet Shrinkage in 50µm-Device 71
4.2.3 Droplet Shrinkage in 100 µm-Device 74
4.3 Cell Encapsulation Performance of the Microfluidic Device 77
4.4 Cell Membrane Permeability in Microdroplet Environment 84
4.4.1 CPA Concentration in Continuous Media.....84
4.4.2 Microfluidic Model for the Cell Membrane Permeability 87
5 CONCLUSION.....91
REFERENCES 95
APPENDICES
A. Python script for droplet size detection using image processing 99
B. Python script for cell membrane permeability solver 102

LIST OF TABLES

TABLES

Table 3.1 Unit conversion between pixels and micrometers for digital camera 38
Table 3.2 Concentrations of cell solutions used in experiments 38
Table 3.3 Cell membrane permeability parameters used in the solver..... 50
Table 4.1 Shrinking data of droplets with three different molarities 67
Table 4.2 Droplet diameter and volume change across the 50 µm-device..... 73
Table 4.3 Droplet diameter and volume change across the 100 µm-device..... 76
Table 4.4 Number of encapsulated cells in droplets at various flow rates 78
Table 4.5 Flow rates used in each step 81
Table 4.6 Experimental shrinking rates of aqueous droplets in a heated channel... 86
Table 4.7 Estimated cell membrane permeability parameters of MDA-MB231 cells at 40°C with 1M glycerol 90

LIST OF FIGURES

FIGURES

Figure 1.1 Solidification of cell culture solution used in microfluidic experiments without (a) and with (b) CPA 6
Figure 1.2 Aqueous droplet generation in a) t-channel device [15] b) co-flowing device [16] c) flow-focusing device [17] 8
Figure 2.1 Comparison of different flow regimes in microchannels, a) dripping regime b) jetting regime 15
Figure 2.2 Simulation results of radii of shrinking droplets at various flow rates .. 17
Figure 2.3 Volume change and CPA concentration plots of 2-parameter (top) and Kedem-Katchalsky (bottom) models 20
Figure 2.4 Study of Xu [23] where cell images are processed to obtain experimental cell volume change data 22
Figure 3.1 Regions of the microfluidic device 28
Figure 3.2 Microfluidic device and its placement on 3D printed holder with thermocouples and the heater 29
Figure 3.3 Plasma activation setup of microfluidic device fabrication 30
Figure 3.4 Microfluidic device fabrication steps 31
Figure 3.5 Microfluidic system setup with all equipments ready to use 32
Figure 3.6. Snapshot taken from DMV video processing tool during analysis of a video recorded at the experiments 36
Figure 3.7 Droplet size detection with image processing 37
Figure 3.8 Jurkat cells imaged before encapsulation experiments (scale is 50μm). 40
Figure 3.9 K562 cells traveling from the inlet towards the junction 41
Figure 3.10 MDA-MB231 cells traveling to the junction 42
Figure 3.11 L929 cells just before encapsulation in a droplet 43
Figure 3.12 Brain microvessel encapsulated inside a microdroplet 44
Figure 3.13 Integrated NEMIX Syringe Stirrer module 45

Figure 3.14 Schematic of syringe pump and microfluidic system with cell solution 46
Figure 3.15 Syringe pump and microfluidic device on inverted microscope during cell encapsulation experiment 47
Figure 3.16 A user interface designed in Python for solving membrne permeability models..... 49
Figure 4.1 Adjusted flowrates during droplet generation..... 54
Figure 4.2 Adjusted flow rates after obtaining stable droplet generation 55
Figure 4.3 X-Channel devices with (a) 100 µm (b) 50µm (c) 25 µm junction width used in the experiments 57
Figure 4.4 Droplet diameter as a function of volumetric flow rate for three junction widths 58
Figure 4.5 Serpentine devices used in the experiments with (a) 100 µm (b) 50µm (c) 25 µm junction width..... 59
Figure 4.6 Pressure contours at the auxiliary flow channel junction (middle channel flow rate =10 µL/min, each auxiliary channel flow rate = 1 µL/min) 60
Figure 4.7 Pressure contours at the auxiliary flow channel junction (middle channel flow rate =10µL/min, each auxiliary channel flow rate = 5µL/min) 61
Figure 4.8 Pressure contours at the auxiliary flow channel junction (middle channel flow rate =10µL/min, each auxiliary channel flow rate = 10µL/min) 61
Figure 4.9 Pressure contours at the auxiliary flow channel junction (middle channel flow rate =10 µL/min, each auxiliary channel flow rate = 15 µL/min) 62
Figure 4.10 Droplet sizes in 100µm-device (Q_w=0.8 µL/min ,Q_o=16 µL/min)..... 63
Figure 4.11 Interdroplet distances in 50µm-device (Q_w=0.4 µL/min ,Q_o=8 µL/min) 63
Figure 4.12 X-junction type device and the clamped tubings to stop the flow..... 64
Figure 4.13 Approximate dimensions for the solvent volume and solubility calculation..... 65
Figure 4.14 DMSO and pure water droplet sizes with respect to time..... 66
Figure 4.15 Droplet sizes for three different glycerol molarities and pure water ... 67

Figure 4.16 Experimental shrinking sdroplet radii at various flow rates 69
Figure 4.17 Droplets traveling at different regions of the 25 µm device and shrinking 70
Figure 4.18 Histograms showing the droplet sizes at cold and hot regions 70
Figure 4.19 Droplets traveling at different regions of the 50 µm device and shrinking recorded with 10x lens 71
Figure 4.20 Droplets traveling at different regions of the 50 µm device and shrinking recorded with 4x lens 72
Figure 4.21 Locations of the measurements from 50 µm device and histograms of droplet sizes 73
Figure 4.22 Droplets traveling at different regions of the 100 µm device and shrinking 74
Figure 4.23 Locations of the measurements from 100 µm device and histograms of droplet sizes 75
Figure 4.24 Number of encapsulated cells per droplet at flow rates 3/3/0.3 µL/min (blue), 4.5/4.5/0.45 µL/min (orange), 9/9/0.9 µL/min (gray) 79
Figure 4.25 Cells traveling inside the dispersed phase just before encapsulation .. 80
Figure 4.26 Encapsulation during decreased dispersed phase flow rates (steps 1-5) 82
Figure 4.27 Encapsulation during increased dispersed phase flow rates (steps 6-9) 83
Figure 4.28 MDA-MB231 cells encapsulated in aqueous glycerol droplets with increasing concentration 85
Figure 4.29 Cell size measurement from surface areas in several frames 86
Figure 4.30 Volume change and CPA concentration plots of proposed model with human embriyonic stem cells encapsulated in droplets with diameter of 100µm (top), 50µm (middle) and 35µm (bottom) 89
Figure 4.31 Comparison of experimental and theoretical cell volume response to glycerol exposure 90

LIST OF ABBREVIATIONS

CPA	Cryoprotectant Agent
DMSO	Dimethyl Sulfoxide
EG	Ethylene Glycol
PDMS	Polydimethylsiloxane
PG	Propylene Glycol

LIST OF SYMBOLS

A	Surface area
C_0	Initial solute concentration in droplet (mol/m³)
C_c^e	Extracellular permeable solute concentration (mol/m³)
C_c^i	Intracellular permeable solute concentration (mol/m³)
C_s^e	Extracellular non-permeable solute concentration (mol/m³)
C_s^i	Intracellular non-permeable solute concentration (mol/m³)
L_p	Hydraulic Conductivity (µm/atm/min)
N_c	Number of Moles of CPA molecules (mol)
P_s	Solute permeability (cm/min)
Q_o	Oil (Continuous) phase volumetric flow rate (µL/min)
Q_w	Water (Dispersed) phase volumetic flow rate (µL/min)
R	Universal gas constant (J/mol/K)
r	Droplet radius (µm)
T	Temperature (K)
V	Droplet volume (pL)
V_b	Osmotically inactive volume (-)
V_c	Isotonic cell volume (µm³)
U_0	Characteristic Velocity of the Flow (m/s)
δV	Droplet shrinking rate (µm³/s)
ΔV	Droplet volume change (%)
$\varnothing$	Droplet diameter (µm)
γ	Surface tension between two liquid phases (N/m)
η	Viscosity of the Continuous Phase (Pa·s)
σ	Reflection coefficient (-)

CHAPTER 1

INTRODUCTION

1.1 Research Background

Modeling cell membrane permeability in different solutions is a critical requirement in understanding, predicting, and controlling the response of cells during preconcentration processes. One of the fields, where cells need to be loaded with carbohydrates is cryopreservation. High concentrations of cryoprotectant agents (CPAs) are required to increase the glass transition temperature to prevent crystallization at the applied low temperatures in cryopreservation. It is currently the most preferred method for long term safe storage of cells despite the use of high CPA concentrations. Multi-step CPA loading methods are employed to prepare and preconcentrate the cells prior to freezing. Step wise incrementation of the concentration of the extracellular solution that is spread over time allows for the osmotic adjustment of the cells to the required high CPA concentrations, but the extended exposure times to the CPAs cause harm to the cells and affect viability negatively. Application of a continuous method to eliminate both the step change in concentration and the long exposure times could provide a better means of CPA loading, but the response of the cell must be investigated.

In this thesis, it is aimed to investigate the membrane permeability parameters of mammalian cells using a novel micro thermo-fluidic device designed for faster and continuous preconcentration of cells with CPAs and heating method, with the use of several cryoprotectant agents (CPAs) and a modified membrane permeability model based on time dependent data collected in the microfluidic system. Current models on the permeability of cell membrane depend on parametric equations. Parameters that affect the permeability of the cell membrane can be listed as its permeability to the solvent, in general water, and to the solute and its reflection coefficient. Cell

membrane permeability has been sudied, both theoretically and experimentally, for different materials including cryoprotectant agents (CPAs).

CPAs are vital for safe preservation of mammalian cells at cryogenic temperatures. The intra- and extra-cellular environments need to be loaded with high concentrations of CPAs to raise the glass transition temperature of water but in a gradual sense to prevent excess plasmolysis, swelling, and intoxication of the cell. These molecules can be permeable or non-permeable through the cell membrane.

Cell membrane is a phospholipid bilayer which allows all cellular activities requiring interaction with extracellular environment. Mammalian cells use their membranes and its integral components for molecular transport activities in both directions. Therefore, intracellular and extracellular media is in osmotic balance. Changes in osmotic equilibrium is balanced by water and molecular transport through the cell membrane. Even though membrane transport is also a discipline in engineering for separation processes with artificial membranes used, cell membranes are more complex than artificial ones and require their own models to investigate solute and solvent transport [1] [2]. Cell membrane transport can be utilized in many biotechnological applications, such as drug delivery, fluorescence imaging and cryopreservation. These applications require proper handling, microscopy, and chemicals usage on cells during experiments since they are more vulnerable to harmful effects in-vitro conditions.

Consequently, one of the objectives of this research is to observe the response of different types of cells in a continous microfluidic system allowing for reduced exposure times to the CPAs and to model the transport of CPAs through the cell membrane. A micro thermo-fluidic device designed for faster and continuous preconcentration of cells with the CPAs was used to observe and study the permeability of the cell membrane. The following procedure was foolowed to reach this goal:

1. The flow conditions in the microfluidic device was optimised to produce uniform droplets of desired size.

2. Cells encapsulation studies based on flow rate and droplet size were done with different types and properties of cells.

3. Cells were encapsulated in the aqueous droplets with a low CPA concentration. Heating experiments were conducted to increase the concentration of the CPA in the aqueous solution along the microchannel by controlling the temperature and the shrinkage of the droplets. Water solubility of the oil phase increases with temperature allowing for selective diffusion of water out of the droplet and causing an increase in the concentration of CPA in the aqueous droplet, and thus around the cell.

4. The response of the cell to the changes in CPA concentration was observed on an inverted microscope using a high speed camera and image analysis tools.

5. The data from image analysis was used to determine the change in volume of cells, and thus the shrinkage rate of the droplets and the increase in the extracellular concentration in the droplet.

6. The dynamic extracellular CPA concentration data was integrated in a permeability model to calculate the dynamic permeability of the cell membrane to a specific CPA.

In this thesis, it is aimed to investigate the membrane permeability parameters of mammalian cells using a novel microfluidic device and heating method, with the use of several cryoprotectant agents (CPAs) and a new membrane permeability model suited for microfluidic environment. Current models on the permeability of cell membrane depend on parametric equations. Parameters that affect the permeability of the cell membrane are defined as its permeability to the solvent, in general water, and to the solute, and its reflection coefficient. Cell membrane permeability has been sudied, both theoretically and experimentally, for different materials including cryoprotectant agents (CPAs). CPAs are vital for safe preservation of mammalian cells at cryogenic temperatures. The intra- and extra-cellular environments need to be loaded with high concentrations of CPAs to raise the glass transition temperature

of water but in a gradual sense to prevent excess plasmolysis, swelling, and intoxication of the cell. These molecules can be permeable or non-permeable through the cell membrane. Cell membrane is a phospholipid bilayer which allows all cellular activities requiring interaction with extracellular environment. Mammalian cells use their membranes and its integral components for molecular transport activities in both directions. Therefore, intracellular and extracellular media is in osmotic balance. Changes in osmotic equilibrium is balanced by water and molecular transport through cell membrane. Even though membrane transport is also a discipline in engineering for separation processes with artificial membranes used, cell membranes are more complex than artificial ones and require their own models to investigate solute and solvent transport. Cell membrane transport can be utilized in many biotechnological applications such as drug delivery, fluorescence imaging and cryopreservation. These applications require proper handling, microscopy and chemicals usage on cells during experiments since they are more vulnerable to harmful effects in-vitro conditions.

1.2 Cryopreservation of Cells

Approximately 80% of the cytoplasm is water [3] and thermodynamic properties of water dictates that both intracellular and extracellular water freezes by forming ice crystals in standard conditions as the glass transition temperature of water is accepted around T_g=136K [4]. This phase transformation of water affects the cells by the formation of sharp ice crystals which can cause lethal damage to organelles. In addition, the freezing of water occur in such a way that molecules dissolved in cytoplasmic water are repelled as water solidifies [5] [6], causing concentration of molecules high enough to result in intoxication of the cell. In order to overcome this, it is essential to solidify aqueous content by vitrification. One way to to achieve vitrification in either pure water or dilute aqueous solutions is to use rapid cooling methods to achieve glass transition [7], requiring cooling rates as high as 10^6-10^7

°C/sec however it is not practical in biological samples [8]. Also, handling at elevated temperatures is not possible due to the limit of glass transition temperature. Another way to achieve vitrification has been discovered in the metabolical processes in nature. A few animal types are known to be capable of surviving freezing conditions. Some frog and turtle species, a salamander and a snake species have adaptations for freeze tolerance by triggering synthesis of some cryoprotectant molecules in their liver and delivered to blood stream and other tissues [9]. These discoveries expanded research around cryoprotectant molecules and preservation of cells from freeze injury. Cryoprotectant molecules have direct effect on water by modifying hydrogen bonds between water molecules [10] so that freezing occurs in the form of vitrification without the need of rapid cooling to very low temperatures. Before the actual experiments, a small sample of cell solution were put onto microscope slides and kept there until the water inside cell culture solution evaporates. Figure 1.1 shows two different droplets observed under the microscope, where both droplets are left to dry in ambient temperature and pressure. The droplet on Figure 1.1(a) did not involve any Cryoprotectant agent (CPA) and formed crystalline structures upon solidification. The droplet on Figure 1.1(b) contains the same cell culture solution with 1 M glycerol, however did not show any formation of sharp crystalline structures, showing the impact of CPA molecules in aqueous solutions. CPAs are a wide range of chemicals, which consist of alcohols, sugar and sugar alcohols, polymers, sulfoxides, amides and amines [6]. Some of CPAs has limited use in due to being not applicable to variety of cell types. However, conventional protocols exposed cells to high concentration of CPAs in single [11] or multiple steps [12] [13]. Increasing solution in one step would require a huge jump if a high concentration is needed for vitrification, resulting in osmotic shock and intoxication.Increasing concentration in multiple steps also requires the isolation of cells and reintroducing them to a new solution, which increases the duration that cells are exposed to CPAs before cryopreservation and induces mechanical damage to cells during the handling with the use of micropipettes, centrifuge and similar tools.

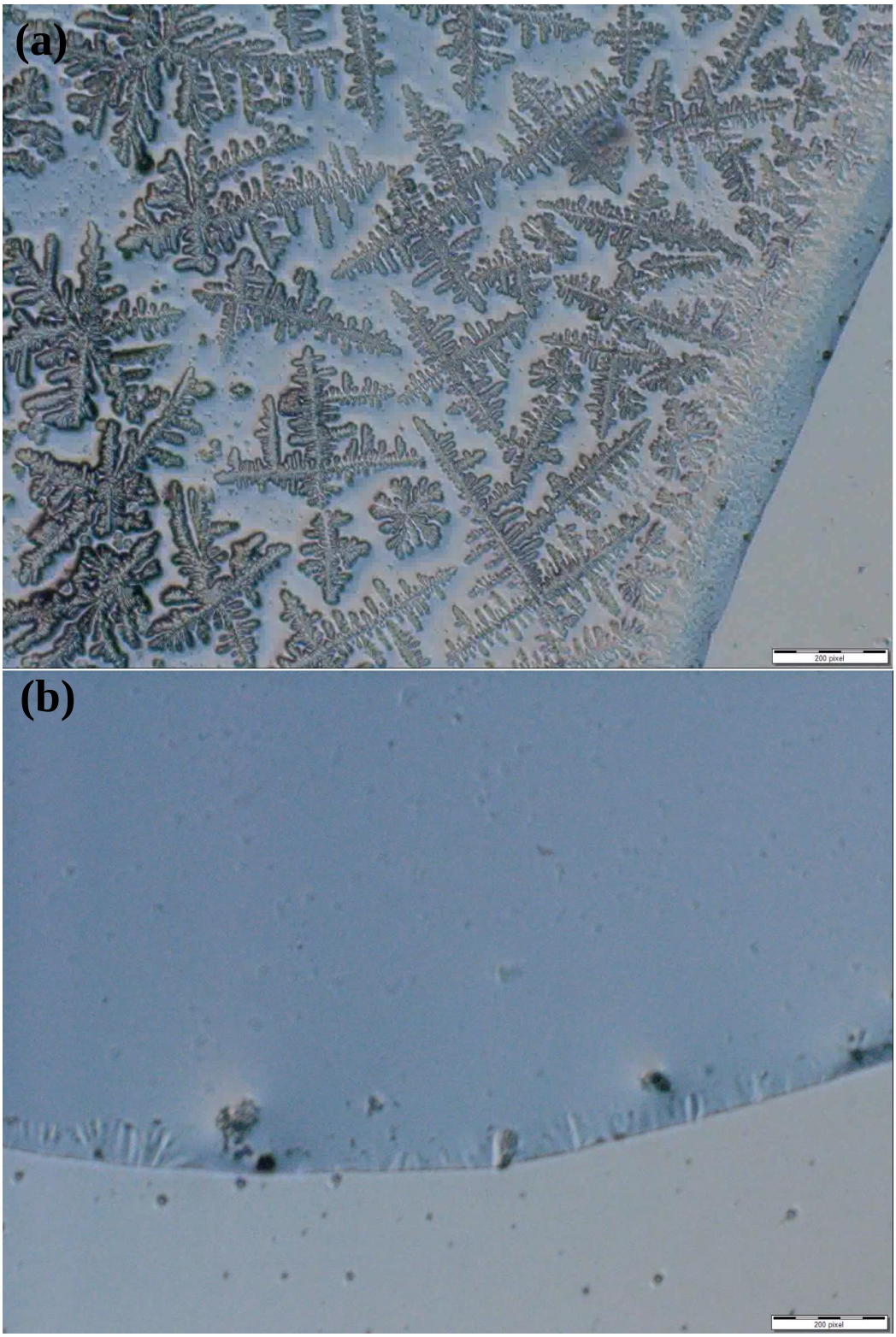

Figure 1.1 Solidification of cell culture solution used in microfluidic experiments without (a) and with (b) CPA

1.3 Preparation of Cells for Cryopreservation in Microfluidic Environment

Unlike conventional methods, it is possible of load CPAs with a continuously increased concentration [14], where CPA concentration inside aqueous droplets could be increased by increasing the solubility of water to the surrounding medium, which is not miscible with CPA molecules. The success of microfluidic devices on monodispersed droplet generation enables a novel method to load CPA molecules to cells by encapsulating them in the droplets and controlling the extracellular CPA concentration (inside of droplet) via heating in a specially designed thermo-fluidic microchannel.

1.4 Droplet Microfluidics

Droplets of micrometer scale diameter, or picoliter scale volume, is a trending area of fluid mechanics. Physics are mostly explained with microfluidics concepts and having laminar flow in very small confined channels allow for an unconventional approach to many biological and biochemical phenomena. Droplet generation in microfluidic devices can provide thousands of monodispersed droplets with equal sizes and equal inter-droplet distances. This monodispersity ensures the same confined conditions in each droplet, which can either be used as reactors or encapsulators. With the use of optical microscopy, droplets can be obversed and analyzed in real time. The geometry of droplet generation devices involving microfluidic channels has evolved troughout the years Figure 1.2 shows very early examples of different microfluidic droplet generation devices. The device used in this study can be described as the flow-focusing type like in Figure 1.2c), where a continuous phase causes droplets to break-up and form a spherical shape at a narrow junction.

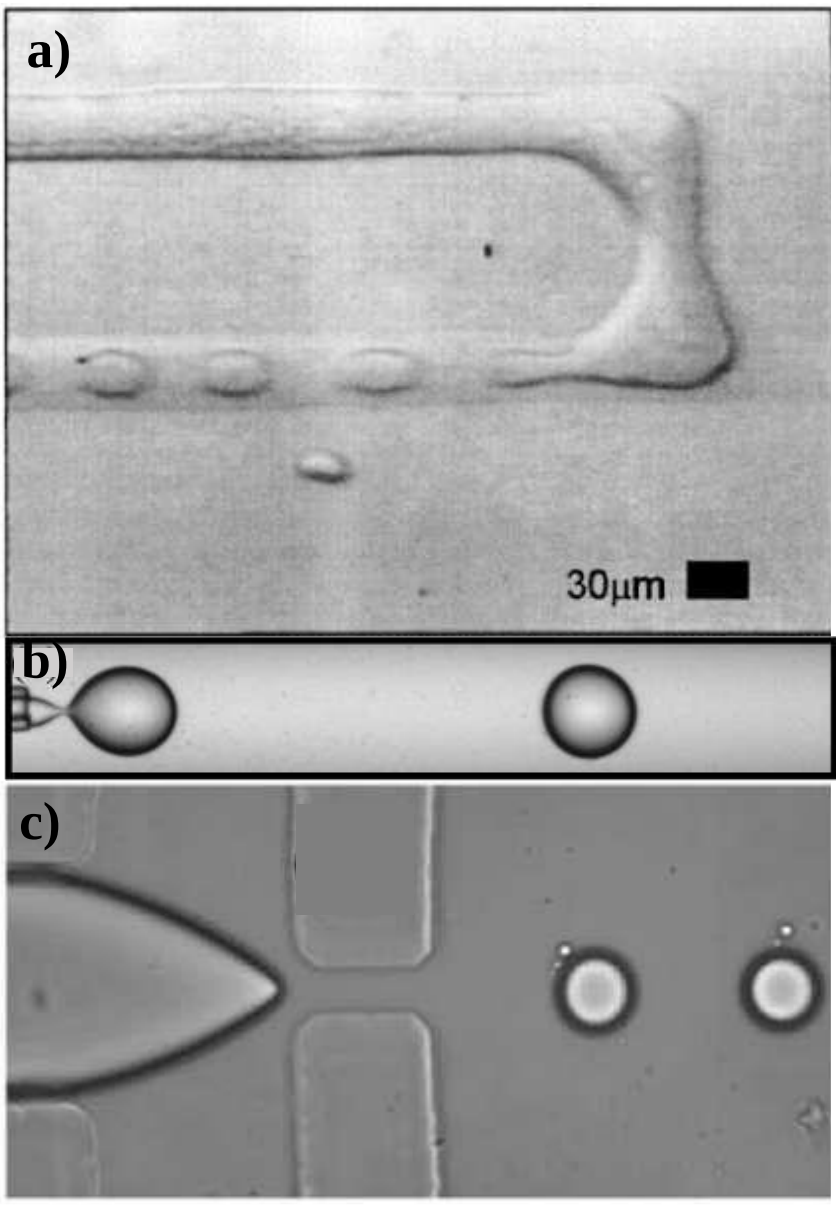

Figure 1.2 Aqueous droplet generation in a) t-channel device [15] b) co-flowing device [16] c) flow-focusing device [17]

1.5 Motivation and Objectives of the Study

Handling of mammalian cells in biomedical or pharmaceutical applications has become more convenient with the use of microfluidic platforms due to several

reasons. Most microfluidic devices are fabricated using PDMS (polydimetyl siloxane) material [18], which allows for transmittance of visible light through the device, and thus, allows for observing substances that flow inside on an inverted microscope. The environment is isolated from ambient. Therefore, contamination or fluctuations in ambient conditions are less of a concern during the experiment. Having laminar flow properties and fast response to the changes make the parameters used in microfluidic devices easily controllable. Also, the use of a novel heating technique in a microfluidic device is one of the main motives that can expand the research in droplet microfluidics, cell encapsulation, and cell membrane permeability studies.

Conventional methods used in preconcentration of cells with CPAs involve some drawbacks as part of the procedures followed, which affect cell viability. Cells are exposed to CPAs in a step-wise manner for a long duration in order to load high concentations, since sudden exposure to high concentration yields to osmotic shocks and swelling. However, long durations while increasing CPA concentration step by step also cause intoxication of cells and mechanical damages during all cell handling steps. These include recentrifugating and preparing cells to the next higher concentration after reaching equilibrium at the current CPA concentration, then repeating the procedure until reaching to desired concentration. By using the novel heating method in microfluidic devices, the motive is to continuously increase the CPA concentration in intra-cellular environment, by eliminating the long exposure times and the step-wise loading procedure.

Old models for cell membrane permeability do not represent the microfluidic environment well as a result of the lack of representing state of the art knowledge in cell biology. More recent discoveries in cell biology helps to understand the membrane properties better, which were unknown back when the currently used cell membrane permeability models had been developed. Microfluidic devices are also new field of study, which can be implemented to a vast amount of work done in conventional ways. Performing membrane permeability studies in microfluidic devices also require new models to explain the environment and conditions better.

To achieve these motives, one of the required tasks is to examine the generation and shrinkage behavior of droplets in the microfluidic device. Use of various CPAs in the aqueous phase in the microchannels and increasing the concentration by controlling the shrinkage of the droplets is assessed. Based on the flow rate, cell encapsulation performance in droplets is determined. Using experimental data extracted for the shrinkage rate of aqueous droplets with different CPAs, a novel mathematical model is presented to describe the permeability of the cell membrane using a dynamic extracellular CPA concentration.

1.6 Outline of the Thesis

The next chapter introduces literature review of similar studies and their relation to the thesis work. Following parts include the objectives and the results of the experiments and are divided into four chapters, starting with the utilization of microfluidic device in Chapter 3, explaining the design, fabrication and additional equipments and tools required for the experiments. The description part is followed by the preliminary studies in Chapter 4 to understand droplet generation and shrinkage behavior of microfluidic devices, where the effect of flow rates, heating and the use of different CPAs are observed. Once the microfluidic device and the experimental use is familiar enough, encapsulation of cells inside droplets are performed and discussed in Chapter 5. Cell membrane permeability is studied with encapsulated cells inside shrinking droplets with a novel heating method in Chapter 6. Due to being a new method and including a microfluidic environment that is different than conventional methods in membrane permeability and CPA preconcentration studies, a new mathematical model based on the differences caused by the microfluidic environment is presented and exemplified with literature data. The thesis is finally summarized with the main conclusions and findings providing possible future ideas to expand this work.

CHAPTER 2

LITERATURE REVIEW

In the literature, most studies performed in microfluidic devices make use of cell trapment inside microchannels and a solution containing a CPA with a certain concentration flows through the cells, while maintaining solute transfer across the membrane [19]. This process can be reverted to wash cells with less dilute solutions to remove CPA from the cell. However, performing a preconcentration in a continuous system, where cells encapsulated in monodispersed droplets, in which the same solution conditions are maintained, is a novel tool to prepare cells to survive from cryogenic temperatures. This method offers a faster process for loading the cells with CPAs without causing the damages that were possible with the conventional methods.

The microfluidic devices employed in this study undergo a series of experiments to figure out their performances in controlling the generation, the volume and the shrinkage of droplets, the encapsulation of cells, and the concentration of CPAs. Some studies [20] involve the encapsulation of cells based on size selectivity, i.e. separating different cell types before encapsulation. In preconcentration of cells with CPA molecules, it is more convenient to work with a single cell type since each cell type has completely different responses to CPA exposure. Therefore, in the experiments each cell type was studied individually.

New osmotic virial equations were developed for the use of solutions with a mixture of several CPAs [2]. In this work, only one CPA type is used in each experimental case to reduce complexity and due to being one of the first studies combining droplet microfluidics, cell encapsulation, and preconcentration of cells in a continuous media. The well-accepted Kedem-Katchalsky model [21] that forms the basis for the model used in this study is an improved model to describe the cell membrane

permability by introducing the solute-solvent interaction during transport. The use of a novel microfluidic system, where cells are exposed to dynamically changing extracellular CPA concentration required modifications to the permeability model developed by Kedem-Katchalsky, which is proposed in this study.

2.1 Microfluidic Devices

Fabrication techniques of microfluidic devices depend on the application field. Bulk techniques, preferred for biological applications, are based on direct modification of a substrate material to shape the desired structures. Surface techniquesare based on deposition of various layers of materials in the form of thin films and their definition into the desired structural shape. Folch [22] described a microfabrication method which enabled the soft lithography based PDMS device production of larger than 50 μm deep channels.PDMS is a liquid phase material at room temperature. Mixing with a curing agent and pouring onto a mold were key steps to develop a microchannel device with soft lithography method. In this method, negative of the channel geometries are formed onto the mold. Either anisotropic etching of silicon or the SU8 photoresist patterning are used as common methods to create a microchannel mold. Even though those microfabrication methods were mainly developed for MEMS applications and for the MEMS devices itself, employing those for the fabrication of mold enabled the production of low cost and highly reproducible microfluidic devices. The most important parameter one should be concerned about in the fabrication is that the flatness of the final sealing surface. Since microfluidic device encounters with various changes of pressure of flowing liquids, sealing might be at most quality. Although the fabrication steps are mostly identical for microfluidic devices, tools and materials required to execute the experiment greatly vary. Microfluidic devices can utilize single or multiphase flows depending on the application. In droplet microfluidics, which is also one of the focuses of the thesis, two immiscible liquid phases regarding their mechanical properties such as surface tension and viscosity and independent control on the flow

rates of the phases are main aspects to determine since the behavior of the generated droplets heavily depends on those aspects.

Nie [23] investigated the viscosity effect on the generation of droplets in a microfluidic flow-focusing device. In a droplet generator microchannel, there exist different flow regimes such as dripping and jetting regimes. Fluid properties and flow rate are the key elements dictating how the droplets would be generated. Using several liquids of various dynamic viscosities, droplet volumes are plotted as a function of flow rate and capillary number. In general, liquids of higher viscosity form larger droplets and the diameter tends to lose dependency to the flow rate or capillary number.

Basu [24] developed a software which makes the processing of recorded videos of droplets in microfluidic devices possible. Software includes the tools for background manipulation, droplet detection, position, velocity, size and circularity measurements. By assigning ID numbers to each droplet detected, droplet generation frequency can also be found given the video frames per second. Software allows to exports the results as written reports or the plots. Scatter plots for the information about individual droplets or the histograms for the properties of all droplets can be generated.

2.2 Two Phase Flow in Microfluidic Devices

In this study, droplet generation and shrinkage is important to understand the behavior of the microfluidic devices, given that the fluids used in encapsulation and permeability studies should be investigated.

Droplet generation in microfluidics is based on having a two-phase flow in laminar flow regime, providing that miscibility of the liquid phases is either negligible or very low. Two separate phases are used to form the droplet, while the continuous phase acts as the carrier fluid and the dispersed phase acts as the droplet.

Monodispersed droplets, which have equal size and equal inter-droplet distances, can be generated by controlling the flow rates of the two phases independently.

In fluid mechanics, dimensionless numbers play an important role while performing experiments and modeling. Flow behavior can be explained by expressing relations between two physical phenomena as a dimensionless ratio. In microfluidics and the generation of micro droplets, Capillary number (Ca) plays an important role, by being a measure of the relation between viscous forces and interfacial forces . Capillary number can be written in equation form as:

$$Ca = \frac{\eta U_0}{\gamma} \tag{1}$$

where, $\eta, U_0,$ and γ represent the viscosity of the continuous phase, characteristic velocity of the flow, and the surface tension between the two phases, respectively. At high capillary numbers, viscous effects become dominant and tends to drag the flow of the dispersed phase along the continuous phase. Since surface tension forces are not strong enough, continuous phase cannot enclose the dispersed phase to form a stable spherical shape early enough so break-up of droplet is delayed, which is called as the jetting regime. On the other hand, at lower capillary number values, surface tension effect overcomes the viscous drag, forming spherical droplets at the vicinity of the junction, which is called as the dripping regime. The flow regimes are illustrated in Figure 2.1. The importance of capillary number emerges from the fact that it is related with the size of the droplets formed in micro channels. As at the junction of the two phases, the viscous and interfacial stresses compete with each other, a force balance can be written in pressure form [18] given by:

$$\frac{\gamma}{R} \sim \frac{\eta U_0}{h} \tag{2}$$

where *h* is the width of the junction and acts as the viscous shear gradient along the stream, and *R* denotes the characteristic droplet size.

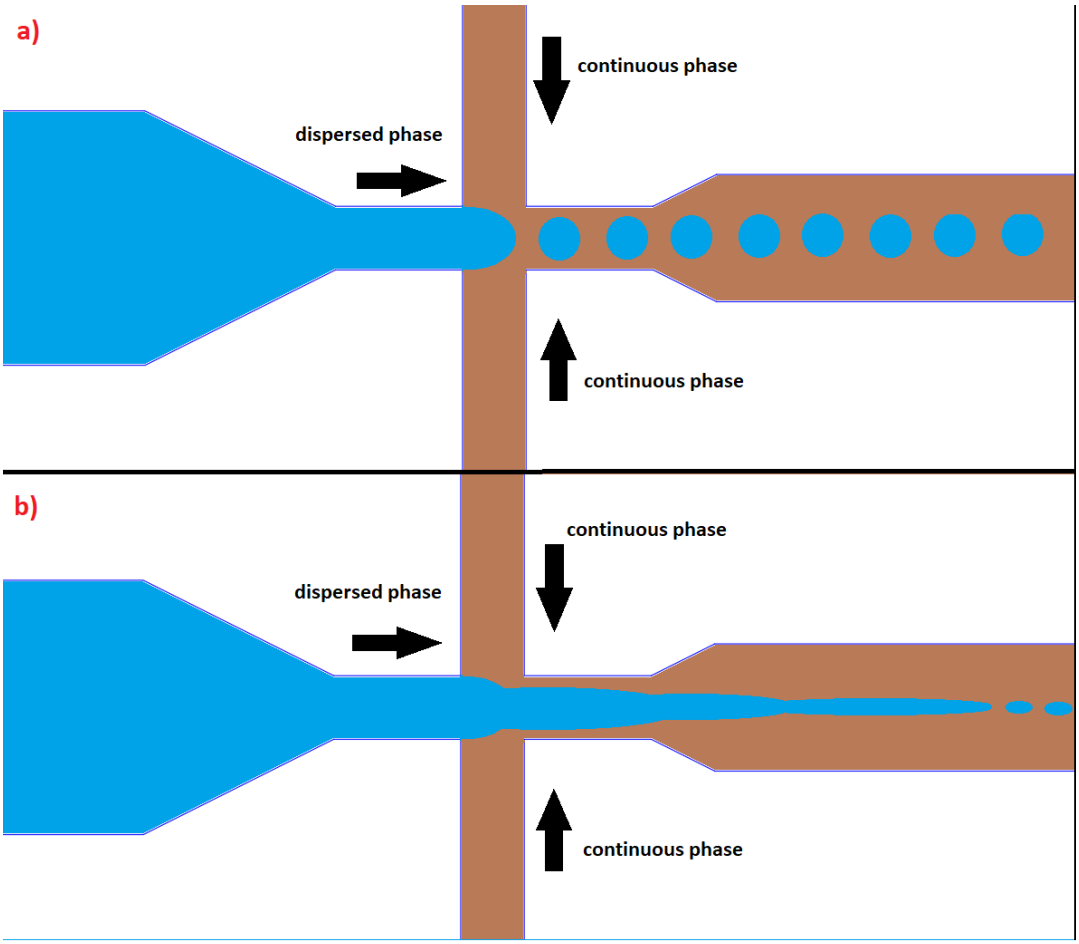

Figure 2.1 Comparison of different flow regimes in microchannels, a) dripping regime b) jetting regime

Reforming the above equation, the capillary number can be shown to be inversely proportional with the characteristic droplet size and can be approximated by:

$$R \sim h \frac{\gamma}{\eta U_0} = h \frac{1}{Ca} \tag{3}$$

In the experimental setup of the microfluidic environment, the capillary number has a direct influence in the droplet size since it involves the flow velocity and it can be controlled through adjusting volumetric flow rate.

The other critical number in droplet microfluidics is the Weber number. It correlates the inertial forces to interfacial forces by [16],

$$We = \frac{\rho U_o^2 h}{\gamma} \quad (4)$$

and is useful as well as the capillary number in adjusting the flow rate of the system to form droplets.

Nie et al [23] investigated the viscosity effect on the generation of droplets in a microfluidic flow-focusing device. In a droplet generator microchannel, there exist different flow regimes, such as dripping and jetting regimes. Fluid properties and the flow rate are the key elements dictating how the droplets would be generated. Using several liquids of various dynamic viscosities, droplet volumes are plotted as a function of flow rate and capillary number. In general, liquids of higher viscosity form larger droplets and the diameter tends to lose dependency to the flow rate or capillary number.

Okumuş [25] performed a simulation study in his thesis about the droplet shrinkage in microfluidic devices. Figure 2.2 shows some shrinking droplets in microchannel at various flow rates as a simulation result, including a condition that is equivalent to stationary, where the velocities of the droplet and the continuous phase are eqaul to each other,. Droplet shrinkage is based on the solubility of water in soybean oil. The below graph shows the difference between the cases of mass transport by molecular diffusion only, when the droplets (dispersed phase) and the oil (continous) phase flow with the same velocity, i.e. there is no velocity difference and, thus, no convection, and the case of mass transport by molecular diffusion plus convection when there is a velocity difference between the droplet and the continuous phase. Although droplet radius decreases in all cases, increased flow rate has a dominant effect by the addition of convective mass transport on the amount of shrinkage at a given time.

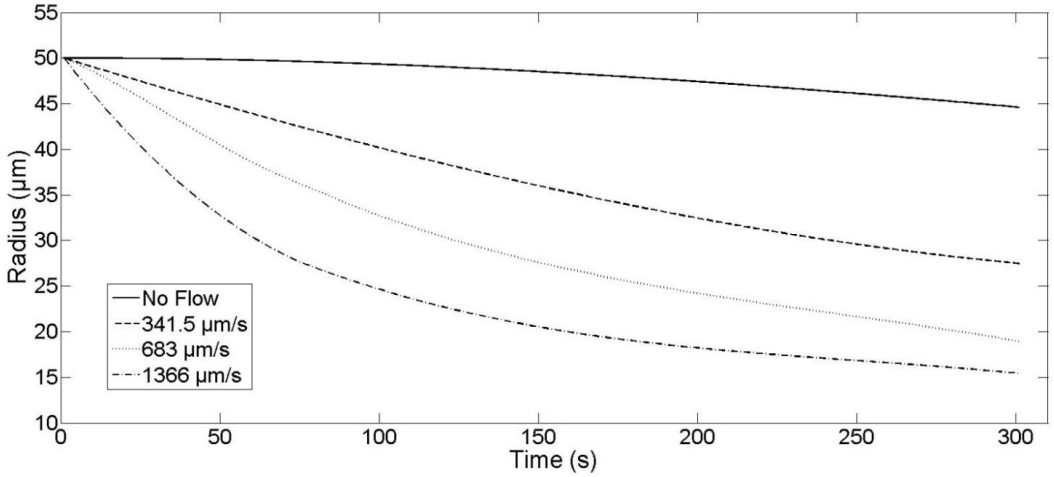

Figure 2.2 Simulation results of radii of shrinking droplets at various flow rates

2.3 Cell Membrane Permeability Models

2.3.1 Two-Parameter Model

The wo-parameter model is one of the oldest models in cell membrane permeability, used by Jacobs in 1930s [26]. In this model, water and permeable solute flux are defined in two separate equations, where non-permeable solutes are also present. Water permeability is described by

$$\frac{dV_c}{dt} = -L_p ART[(C_s^e - C_s^i) + (C_c^e - C_c^i)] \tag{5}$$

and solute permeability is described by

$$\frac{dN_c}{dt} = P_s A(C_c^e - C_c^i) \tag{6}$$

where membrane permeability parameters L_p and P_s are hydraulic conductivity and solute permeability, respectively. A is the surface area of the cell, R is universal gas constant, T is the ambient temperature. C denotes the concentration of solutes, with the subscripts s and c, whether they are non-permeable or permeable, respectively.

Extracellular and intracellular solute concentrations are denoted by the superscripts *e* and *i*, respectively. Even though this model has been used extensively, it does not describe the solute-solvent (water) interaction. Since the existence and diversity of channels in the biological membranes are specific to the type of cell, the two-parameter model underestimates the importance of complexity of cell membranes and the necessity of having a better explanation to the phenomena occurring across the cell membrane.

2.3.2 Kedem-Katchalsky Model

Kedem and Katchalsky [21] improved the mathematical expressions developed on cell membrane permeability. Living in an aqueous environment, cells always interact with the outside through their membranes and the chemical balances. Biological membrane behavior was mathematically described by the water and solute flow equations. Kedem and Katchalsky felt an insufficiency on current membrane permeability models, which only includes two parameters, each for the permeation of water and solute. Together with thermodynamics point of view considering the irreversible processes, a three parameter model was developed, containing the filtration coefficient, or hydraulic conductivity (Lp), solute permeability(ω) and the reflection coefficient (σ).

In cell membrane, cotransport channels exist where both water and permeable solutes can be transported together. In this case, a coupled model is required to define the phenomena more precisely. Studies show that membranes modified with Nystatin [27] or Amfotericin B [27] [28] have increased permeability to water, electrolytes and non-electrolytes and show similar characteristics to the permeability of human red blood cell membranes. Therefore, cotransport is an important aspect of membrane permeability and its addition helped to develop a new model by Kedem and Katchalsky, even though it became more complex compared to the two-parameter model. Water permeability using the reflection coefficient (σ) is described by

$$\frac{dV_c}{dt} = -L_p ART[(C_s^e - C_s^i) + \sigma(C_c^e - C_c^i)] \quad (7)$$

and solute permeability using the reflection coefficient (σ) is described by

$$\frac{dN_c}{dt} = P_s A(C_c^e - C_c^i) + \frac{(1-\sigma)}{2}\frac{dV}{dt}(C_c^e + C_c^i) \quad (8)$$

where the membrane permeability parameters L_p, P_s, and σ are the hydraulic conductivity, solute permeability, and reflection coefficient, respectively. A is the surface area of the cell, R is the universal gas constant, T is the ambient temperature. C denotes the concentration of solutes with the subscripts s and c, whether they are non-permeable or permeable, respectively. Extracellular and intracellular solute concentrations are denoted by the superscripts e and i, respectively.

The main difference between the two-parameter model and the Kedem-Katchalsky model is the addition of the reflection coefficient. The reflection coefficient takes into account the interaction between the solute and the solvent (water) during their transport across the cell membrane. Therefore, the parameter also couples Equation 9 and 10, making the solution more complex than the two-parameter model. Figure 2.3 shows the cell volume and intracellular CPA concentration during the CPA loading process, while cell is reaching osmotic balance. Plots are regenerated using literature data to discuss the differences between the models. The most noticable thing in the plots is that the cell volume reaches the lowest value after CPA exposure. 2-parameter model gives 1618.1 μm^3 as the lowest volume, while in the Kedem-Katchalsky model the lowest volume is 1639.9 μm^3. The difference stems from the fact that the two-parameter model ignores the reflection coefficient, which includes the solute-solvent interaction. Under the assumptions of the two-parameter model, transport of water occurs without any interaction with the CPA, therefore cell is expected to lose more water during osmotic balance recovery.

The difference between the two-parameter and the Kedem-Katchalsky models becomes more apparent for cell types for which the reflection coefficient (σ) approaches to zero. Theoretically, when σ=1, the two models should give the same result as the coupling parameter in Eq. 10 cancels out and Eq.10 reduces to Eq. 8.

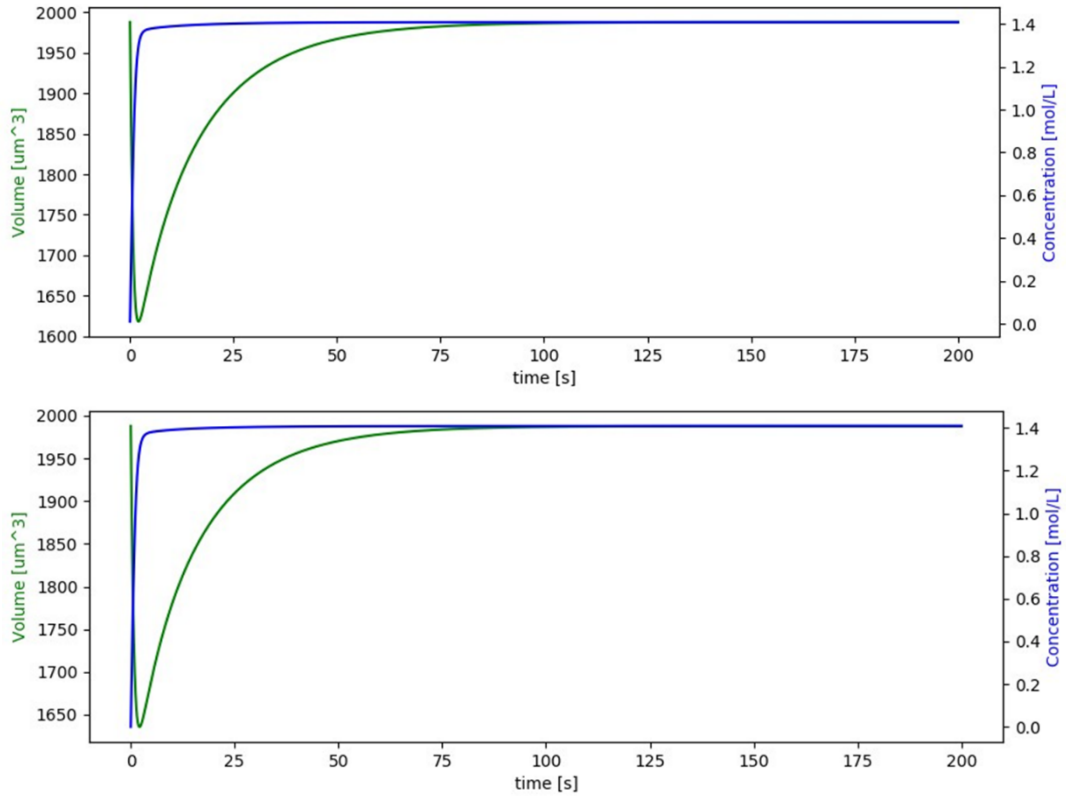

Figure 2.3 Volume change and CPA concentration plots of 2-parameter (top) and Kedem-Katchalsky (bottom) models

2.4 Determination of Membrane Permeability Parameters using Cryoprotectant Agents

Fleming Glass [29] worked on a theoretical model, which deals with the diffusive extraction of a cryoprotectant from the cell solution. They used a microfluidic flow system, where cell solution and a washer solution flow in parallel. Together with a fully developed laminar flow assumption, they investigated the cryoprotectant

diffusivity from cell region to the washer region. Their study based on the parameters that may be used to optimize the microfluidic device geometry. Peclet number (Pe), cell volume fraction in the cell-laden flow (V_i/V_t), and the cell stream flow rate fraction (f_q) are the controlled parameters. Design of the device geometry includes the channel width, flow rate and the number of stages that provides the molecular transport. According to the optimization of those parameters, several two or three stage devices are possible with specific channel width. In addition, cell volume fraction inside the cell stream is a parameter that determines the optimal Peclet number and cell flow rate fraction.

Elmoazzen [30] generated a new membrane transport equation, covering the non-dilute solute permeability. On the basis of cryopreservation applications, non-dilute, or in other words high concentration solutions are more frequent to observe. This brought the idea of using existing models for a different field, which actually requires an improved model. In the new model, authors suggested both a new total volume change transport equation and a nondilute solute transport equation. Total volume change was in consistency with the experiment performed with human corneal epithelial cells exposed to 2 molal Dimethyl Sulfoxide for 5 minutes.

Xu et al. [31] investigated the influence of different cryoprotectant agents on cell membrane permeability parameters. Two different cell cultures, human embryonic stem cells (hESCs) and human induced pluripotent stem cells (hiPSCs) are used in the experiments. Their methodology required the calculation of the osmotically inactive volume of each cell line. By conducting experiments on steady-state responses of cell membrane to the several different concentrations of non-permeable solutes, Boyle-Van't Hoff model provided the osmotically inactive volume of the cells. This volume was used as a parameter in determining the intracellular concentrations of permeable and non-permeable solutes. As non-permeable cryoprotectant agents, dimethylsulfoxide (with two different concentrations), 1,2 propanediol and glycerol were used. First, cell viability upon exposure to each CPA

was measured with respect to the control group of cells without CPA loading. Cell membrane response to the water and non-permeable solute fluxes were compared with the Kedem-Katchalsky models at different temperatures ranging from 8°C to 30°C. Figure 2.4 shows human embriyonic stem cell volume change response to 10% glycerol. Cell volume change as a function of time is very well suited to the response obtained from microfluidic model when the permeability and ambient parameters are used as input.

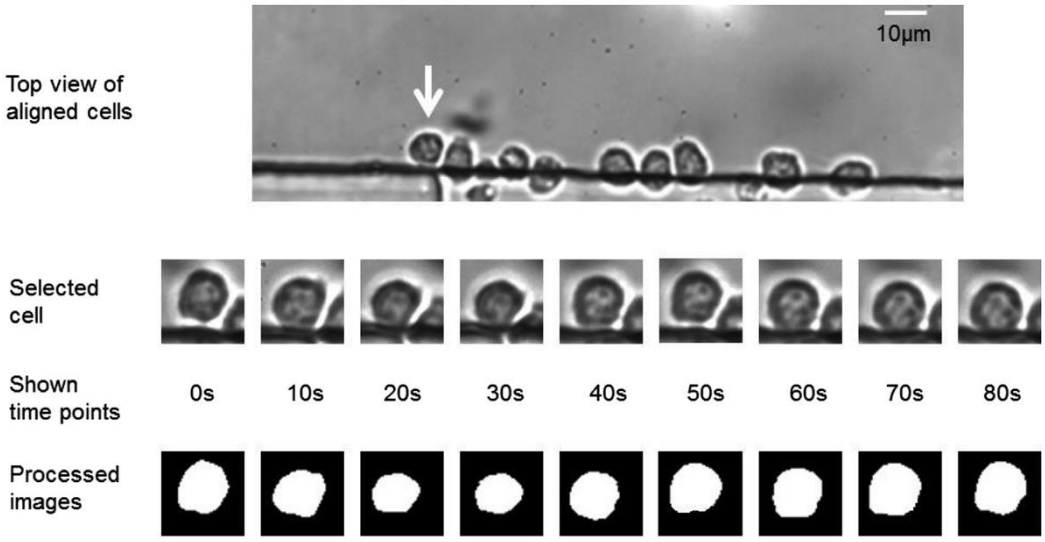

Figure 2.4 Study of Xu [23] where cell images are processed to obtain experimental cell volume change data

Young et al. [19] designed and fabricated a microfluidic device, suggesting a novel way to introduce necessary cryoprotectant agent into HepG2 (hepatocellular carcinoma human liver) cells by preventing the toxication and osmotic injury that mostly occur during standard CPA loading procedures. In the order of flow direction, micro channel design comprised of three inputs, a mixing regime, a serpentine-shaped channel regime and one outlet. In the three-way junction, CPA solutions were feeded from the sides, while cell solution were feeded from the middle. Due to the laminar properties of microchannel flow, three distinct phases enters into the serpentine channel. Serpentines are efficient designs to increase the distance

travelled in a small area. Therefore, throughout the serpentine, CPA solution at left and right sides diffuses into the cell solution at the middle. In order to observe the phenomena, fluorescent dyes were introduced into the CPA solution. At the entrance of serpentine structure, intensity measured from the the channel made peak at the sides and zero intensity observed at the center. This indicates, cell solution did not involve any contribution from CPA solution. As the flow proceeded, intensity gradient along the channel cross section decreased and stabilized at a point. Then, the point at which the concentrations of CPA and cell solutions were equal, was determined. Adjusting the flow rates of each inlet, it was possible to control the CPA concentration in the cell solution. Once the CPA concentration in the cell solution is a known parameter, then CPA can be used as a permeable solute through the cell membrane. CPA concentration in the cell solution is the concentration at the extracellular environment. Concentration difference between extracellular and intracellular region triggers the osmotic pressure and therefore water and solute flux across the membrane. Kedem-Katchalsky model was used to numerically calculate the cell volume and CPA concentration. Later, by looking to the initial, pre-freeze and after-thaw viability of the cells, the method was considered an efficient alternative to the standard CPA loading procedures.

Elliot et al. [2] developed a novel equation for the calculation of osmolalities of solutions involving multiple compounds. They enhanced the use of osmotic virial cross coefficients such that separate two compund solution information is sufficient for the prediction of multiple compound solutions. Osmolality is an important parameter on the development of cryopreservation procedure of cells. Osmolality of permeable solutes, or cryoprotectant agents, influences the water and solvent flux across the cell membrane. Multisolute osmotic virial equation can be used to determine the osmolality information in ternary CPA solutions, such as Glycerol + Dimethyl Sulfoxide + Water.

Bajpayee et al.[14] developed a method for the preparation of cells to the cryopreservation process. They used the solubility property of water in organic oils. Most organic oils dissolve a small amount of water in the room temperature. At higher temperatures, this property enhances to allow dissolving more water in the same media. Soybean oil were vigorously mixed with deionized water in order to dissolve it at the capacity of oil, which is 0.3% water by volume at 25°C, and kept at rest. With the addition of surfactant, SPAN80, the water emulsions that would be created in the oil was stabilized better. After the preparation of saturated oil, additional 'dispersed phase' was added to create polydispersed emulsion phase. Dispersed phase was used at different glycerol concentrations of 0 mol/L, 1 mol/L and 2 mol/L in water droplets. Theory behind shows that upon shrinking of droplets, that is, as the droplet loses its water content by diffusion, glycerol concentration starts to increase. This phenomenon is possible with the confinement of all glycerol inside the droplet. Since glycerol does not dissolve in soybean oil, it is possible to protect all glycerol content in aqueous droplet. As a cryoprotectant, glycerol were compared with the dimethylsulfoxide (DMSO) in terms of its solubility in soybean oil and selected to be used in the experiments. Both pure water and aqueous-glycerol droplets are used in the shrinkage experiments and it has been shown that pure water droplets can no longer be seen after a time. This is due to the fact that all water content has dissolved in soybean oil. However, aqueous-glycerol droplets show different kind of behavior due to their glycerol content and water-glycerol binding effect, which was stated as the binding of 2.63 water molecules for each glycerol molecule exist in the droplet.

2.5 Cell Encapsulation

Edd et al. [32] reported a method that allows the encapsulation of cells to water droplets in a microfluidic device. Single cell encapsulation is a unique technique in terms of providing an isolated environment to each cell, which actually isolates the cells in a chemical sense. Unlike tissues, organs or naturally living organisms, single cells only interact with the surrounding environment and chemical compounds without the influence of other cells. Microfluidic channels allowed the high-throughput generation of water droplets inside which cells can be trapped individually. The method described a passive generation of cell encapsulation after a self-sorting system. System enabled cells to be sorted by having a high-aspect ratio channel. When the cell diameter was comparable with the width of micro channel, it is possible to organize cells along one side of the channel by hydrodynamic interactions. By adjusting the droplet generator frequency, it is possible to reach high efficiencies on the encapsulation of single cells in aqueous picoliter droplets.

Kamalakshakurup et al. [20] developed a novel method to obtain single cell encapsulation with an additional feature of size selectivity. Designing an extended junction, where the dispersed phase, involving the cells and oil phase meet, allowed the creation of three-dimensional hydrodynamic vortices at the center, where only the outermost streamlines managed to break up with the vortices and proceeded to the outlet channel. It was possible to adjust a parameter called as d_{gap} such that it allows the release of certain sized particle. So called Trap&Release technique were examined using blood cells. Since blood involves many different kinds of cells, such as platelets, red blood cells(RBC), white blood cells(WBC) etc, which deviates from each other in terms of their sizes, It is possible to selectively release only one type of blood cell high a high efficiency.

Gilmore et al. [33] studied on the water permeability of the membranes of human spermatozoa cells. They found the osmotically inactive fraction of sperm cells by employing Boyle Van't Hoff (BVH) plots and investigated the solute permeability by using several cryoprotectant agents, which are Glcyerol, Dimethyl Sulfoxide, Propylene Glycol and Ethylene Glycol. Then effect of each solute on the water permeability was examined. For each CPA, experimental cell volume was measured and then fitted to a theoretical curve, excerpted from Kedem-Katcalsky model, which enabled to find the corresponding solute permeabiltiy and water permeability, i.e, hydraulic conductivity.

Heo et al. [34] designed and fabricated a microfluidic device which can store oocytes in a chamber prior to a CPA loading. Cryopreservation of oocytes are important to protect the fertility of women undergoing chemotherapy since it damages oocytes as well. In order to transfer back the oocytes after chemotherapy, a viable cryopreservation technique is necessary. This technique offers an environment in which proper CPAs are loaded to the oocytes in order to reduce toxicity and osmotic injury during operation. A secondary PDMS layer including a valve control was used to trap the oocytes inside the chamber, where the CPA concentration was continuously increased. Using cell membrane permeability models including osmolality values of the CPAs are used to figure out volumetric change of oocytes.

CHAPTER 3

MATERIALS AND METHODS

3.1 Design and Use of the Microfluidic Device

Microfluidic devices used in this study are intended to generate droplets using two immiscible liquids by merging them at a narrow junction. To achieve this, three devices with different junction widths are used to generate a wide range of droplet sizes. The narrowest part of junction region, where droplet generation takes place also gives their names to devices and mentioned with the same notation throughout the work (e.g. 25 μm device has the narrowest junction width of 25 μm). As it will be mentioned in the following chapter, basic X-junction devices and serpentine devices share the same geometry at the junction region. The design of the microfluidic devices that involve an auxiliary oil channel and a serpentine section is done by Dr. Selis Önel as part of her research at the Center for Engineering in Medicine and Surgery (CEMS) and the BioMEMS Research Center associated with Harvard Medical School and Massachusetts General Hospital (MGH) and directed by Dr. Mehmet Toner. The droplet generation section of these devices involving an X-crossing is based on a simple flow-focusing microfluidic device developed in these centers.

Figure 3.1 and Figure 3.2 are the schematics of the microfluidic device redrawn in Solidworks 2016 for this work for illustration purposes and and identifies the regions of microfluidic device based on their functions. Except for the droplet formation region, where the geometries are the same for both the simple device and the new serpentine device, figures mainly show the parts and equipments used for the serpentine device. The device mainly consists of four segments. Channel inlet region contains three punched holes and two of those inlets are connected to a X-shaped

junction via narrow channels. Those channels join each other at the droplet formation region, from which the first observable features of the device emerge.

The third inlet port is connected to the upcoming stream from droplet formation region by making a ‘Y’ shaped junction. The design of this so called ‘auxiliary flow’ helps to establish a steady flow by having a velocity direction towards the direction of the main flow. After all three channels join, the flow goes through the serpentine and outlet region, where the serious mixing and heating occurs before the droplets are collected at the outlet. All four sections are transparent and can be observed on an inverted microscope. Since several tubings are attached to the device, it is likely to have accidental touches and slips if the device is put onto a planar holder. Therefore, a 3D printed holder was designed to provide a tight platform for both the transparent heater and the microfluidic device, meanwhile allowing all the light transmission required for vision and observation.

Figure 3.2 also shows two thermocouple ports, which are a second fabrication layer in the mold, having a different channel length than fluidic layer. Thermocouple layer does not connect to the fluid flow and only allows a probe from the side edge of the device to measure temperature locally.

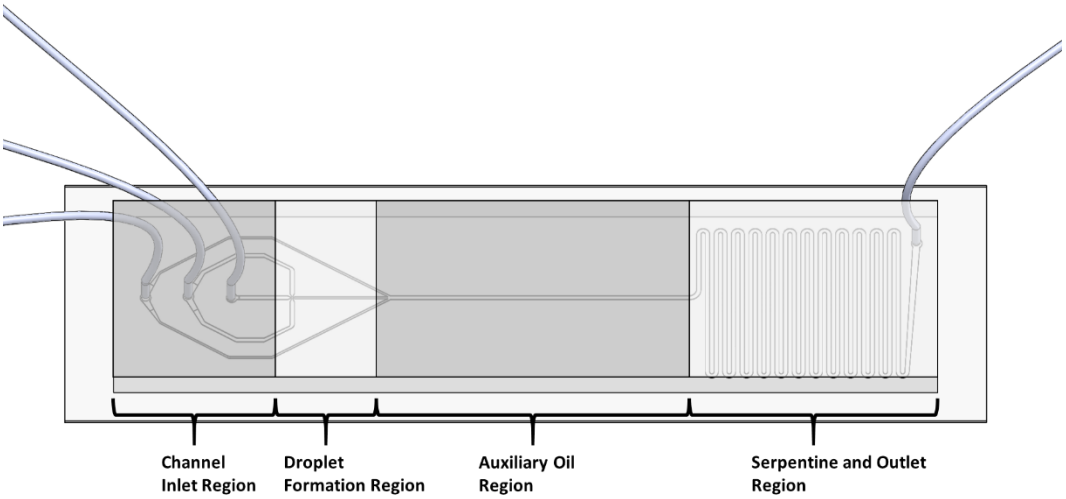

Figure 3.1 Regions of the microfluidic device

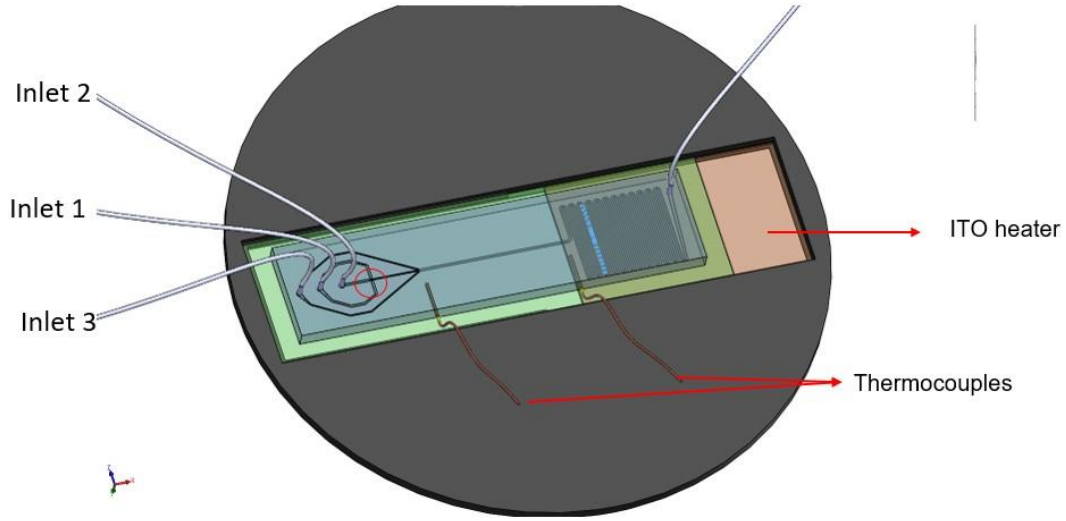

Figure 3.2 Microfluidic device and its placement on 3D printed holder with thermocouples and the heater

3.2 Fabrication of Microfluidic Devices

Standard (polydimethyl siloxane) PDMS fabrication methods were followed to fabricate the devices. A curable thermoset material was obtained by vigorously mixing PDMS elastomer (Sylgard 184, Dow Corning, Midland, MI) with its curing agent for cross-linking (10:1 ratio). Figure 3.4 shows each step in the fabrication of microfluidic device, with the equipment shown in Figure 3.3. First, the mix was poured onto the male SU-8 mold with the microchannel geometry on it. The mold was degassed in a vacuum chamber for at least two hours to remove the air bubbles in the polymeric mix. Curing process was carried out in the oven at 80 °C. The molds were removed from the oven after 4 hours and left for cooling at room temperature. Cured PDMS was removed from the SU-8 mold using a surgical knife and the micro-channel devices were peeled off. Inlet and outlet holes were opened on each device using a 75-gauge punch. Surfaces of the glass slide and the PDMS device that has the microchannel geometry were cleaned from any dust particles with tape. They

were placed on a plasma cleaner tray with the surfaces to be bonded facing the top. Plasma cleaner (Harrick Plasma Inc. PDC-32G-2 Model, USA) was set to 700 mTorr at high power for 40-50 s. With the completion of surface activation, plasma cleaner was turned off and brought to atmospheric pressure. The PDMS part and the glass slide were removed quickly and the PDMS surface with the geometry on it was allowed to chemically bond with the glass slide. The devices were kept in the oven at 80 °C overnight for stabilization of bonding.

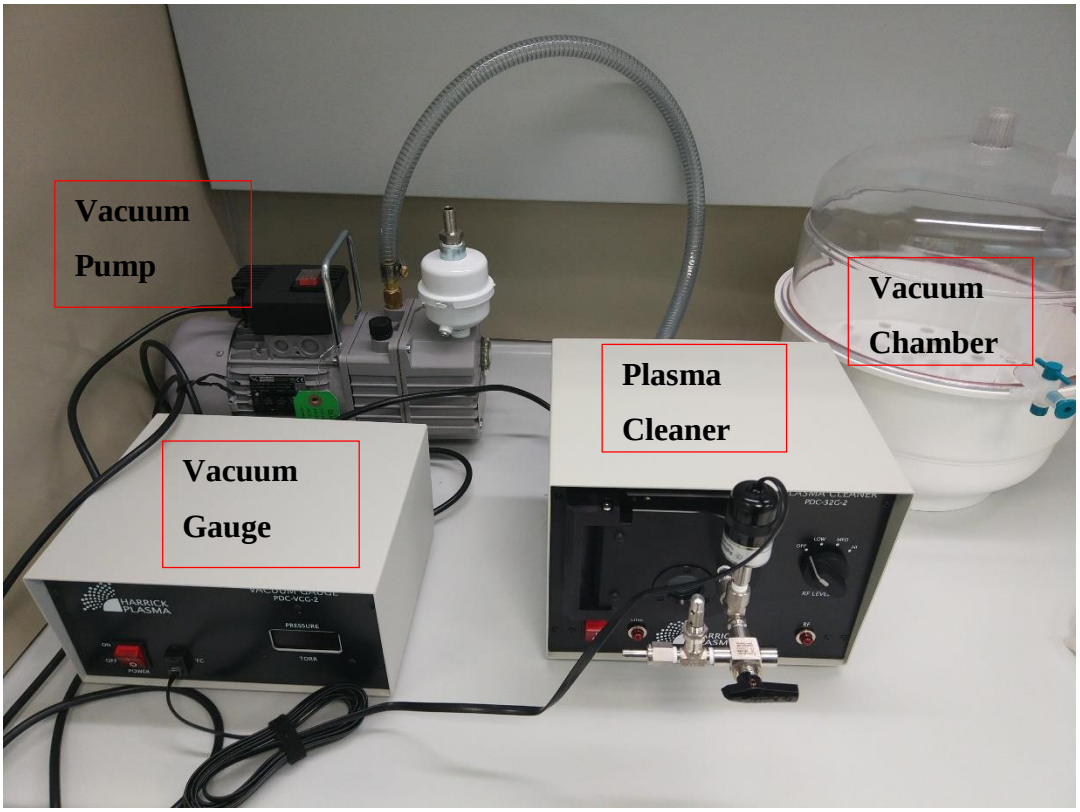

Figure 3.3 Plasma activation setup of microfluidic device fabrication

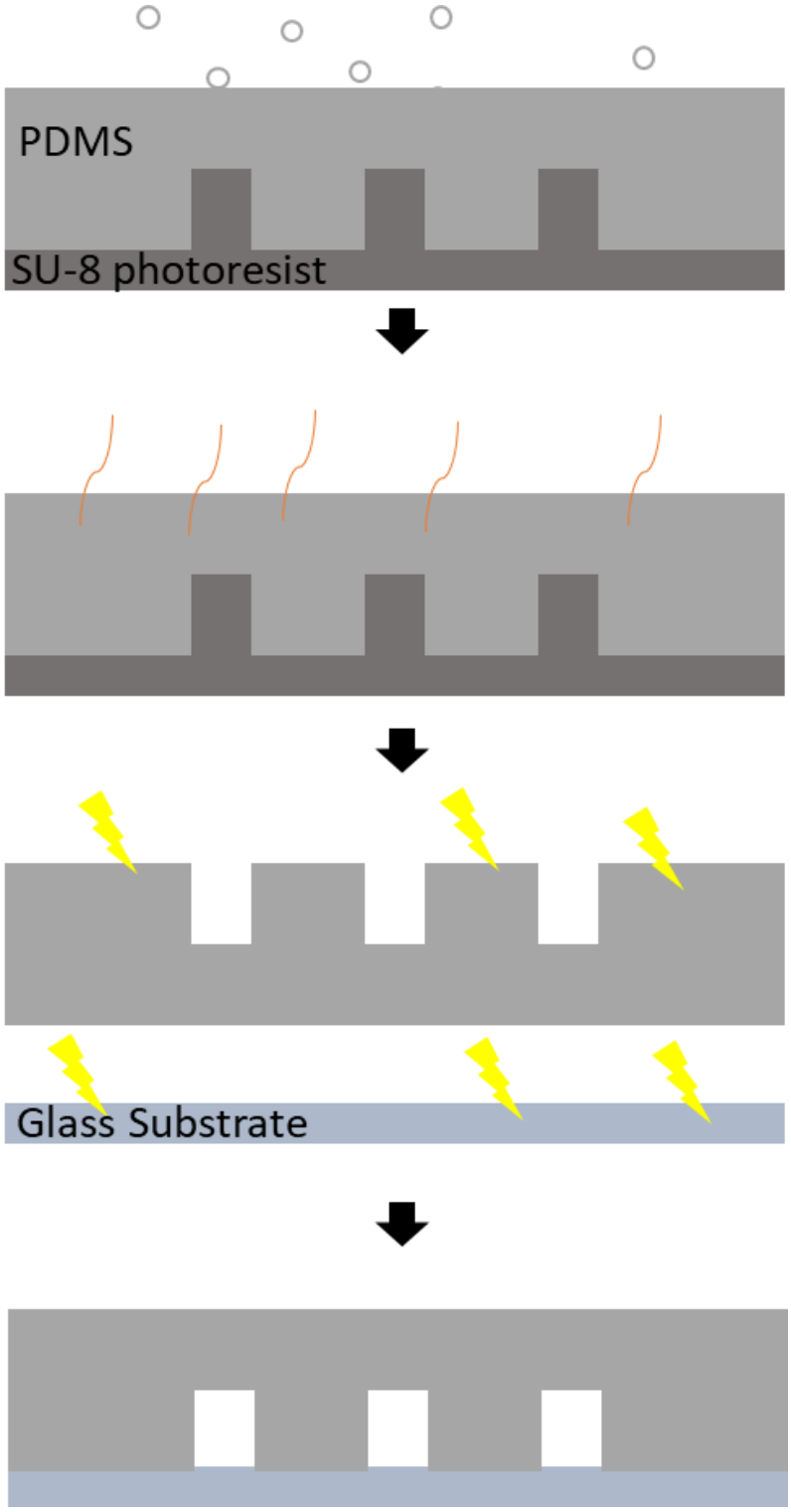

Figure 3.4 Microfluidic device fabrication steps

3.3 Microfluidic System Setup

Microfluidic setup consist of a computer controlled Nemesys BASE120 (CETONI GmbH) syringe pump system, Tygon® tubings, microfluidic device, PID controlled indium-tin oxide (ITO) heater and its controller (Cell MicroControls, Norfolk, VA) and Olympus IX73 inverted microscope with a DP73 high-speed camera. Devices used are shown in Figure 3.5

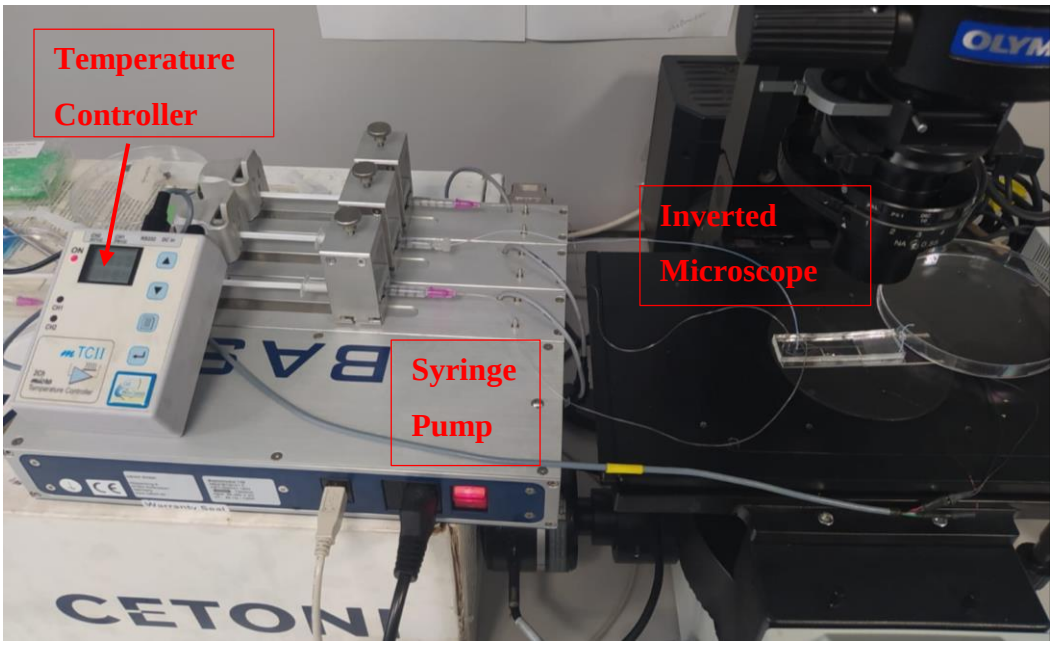

Figure 3.5 Microfluidic system setup with all equipments ready to use

3.4 Solution Preparation

Droplet generation requires two immiscible phases which are put into syringes. Dispersed phase in the early stage experiments was pure distilled water, in later stages aqueous droplets were prepared with appropriate amounts of CPAs. Soybean oil (Sigma Aldrich, St. Louis, MO) was used as continuous phase in the experiments. Soybean oil consists of triglycerides, allowing it to dissolve water a certain amount of water, which can be greatly enhanced by increasing the temperature. Since the partial heating of microfluidic device and the droplet shrinking is one of the main

objectives of the work, soybean oil is a great candidate for being used in continuous phase.

For the purpose of the experiments, soybean oil was saturated with water by following a protocol used in a similar study [14], where 0.3% of water solubility in soybean oil at room temperature is achieved. Procedure includes the addition of 1% water in pure soybean oil and vigorous mixing until it looks like a cloudy formation. The mixture was then kept at rest for at least 72 hours to separate the phases and to have saturated oil. Finally, surfactant SPAN80 (Sigma Aldrich, St. Louis, MO) was added (0.1% v/v) to soybean oil which had already been saturated. This final process ensures the droplet integrity during experiments.

3.5 Droplet Generation in Microfluidic Device

In this study, droplet generation and shrinkage form a crucial part of the work to understand and optimize the behavior of microfluidic devices, given that the fluids used in encapsulation and permeability studies should be investigated. Two different devices with different geometries are used. Initial experimets are done using simple devices that only has an X-junction for better understanding and and adjustment of the flow rates required. Actual experiments are done using the more complicated devices including an auxiliary oil channel and a serpentine section for heating. While droplet generation is a result of the microfluidic design, droplet shrinkage requires heating of the system to a higher temperature to increase the water solubity of the oil phase. Two separate phases, soy bean oil and an aqueous phase are used to form the aqueous monodispersed droplets, which have equal size and equal inter-droplet distances. The flow rates of the two phases are adjusted and controlled independently using an auotomaticly controlled syringe pump and optimized to obtain droplets of desired size based on the flowrates. The flow rates were incremented at various time steps until reaching the 20:1 oil to aqueous phase flow rate ratio, which is the design parameter for the devices used. After reaching a stable flow regime, i.e. the dripping

regime described in the previous sections, flow rates are adjusted with a 20:1 ratioto control the droplet size.

In the experimental setup of the microfluidic environment, the capillary number has a direct influence on the droplet size since it involves the flow velocity and it can be controlled through adjusting volumetric flow rate. In the experiments, the capillary number goes up to 0.13, 0.3 and 0.05 for 25 μm, 50 μm and 100 μm devices, respectively. Capillary numbers smaller than 0.3-0.4 range can be safely said to be in the dripping regime for Weber numbers lower than 1, which was also satisfied in the experiments showing a 0.0002-0.0003 range, ensuring that the experiments were performed in the dripping regime.

3.6 Droplet Size Measurements

In microfluidic devices, provided that the liquid phases are moving along the channel, droplets travel as microspheres, and their sizes can be defined as diameter or volume of a sphere. When the droplets are observed under the microscope, it is possible to follow their movement in real-time. However, droplets form and move so fast to measure using the eyepiece as seen in their images can be recorded in image or video formats, and image processing can be performed.

The video processing tool Droplet Morphometry and Velocimetry (DMV) [24] for the droplet size measurement for the microchannels is used for some of the videos recorded during the experiments as seen in Figure 3.6. The DMV software offers many features for the analysis of droplet generation, including the measurement of droplet diameter, surface area, interdroplet distance, shape eccentricity, circularity, position and velocity data. For the scope of the thesis, the software has most of the tools required. However, the assessment of droplet size during the experiments are required. That is, the video processing with live images while droplets are generated at the same time is needed in order to control the flow rates to obtain desired droplet

sizes. Even though flow rates are computer controlled, the syringe pump and the microfluidic device system has many components and are prone to mistakes during an experiment such as air bubble remnants inside syringes, improper tightening of the syringes, wrong dimensions (internal diameter, stroke length etc) registered for syringes. Such kind of mistakes still allow to obtain droplets in microfluidic devices, however it is difficult to understand the geenrated droplets are actually not the result of given flow rates but affected by some unwanted inputs. Using DMV software, it is required to conduct the experiment and record the results before the analysis. During the experimental process, too many videos are required for different flow rates, different regions of the channel and for different temperatures. Therefore, a live image processing is needed to ensure the droplets obtained are the correct outcome of controlled parameters. In order to do that, a python script is developed for the scope of the thesis, which can detect droplets and measure droplet size and interdroplet distances from live camera streams and imported videos, as used to be in DMV software. After obtaining a stable flow and droplet generation by following the steps illustrated in Figure 4.1 and ensuring the correct droplet sizes are obtained using the live video droplet size processing., videos in OLYMPUS Stream Motion software can be recorded in .avi file format. Each video was taken to record droplets for a specific flow rate and it is indicated in the file name. Then, the videos are imported to a python script to be processed frame by frame, using Hough Circle Detection algorithm, as shown in Figure 3.7. The python script used for the droplet size detection is given in Appendix A.

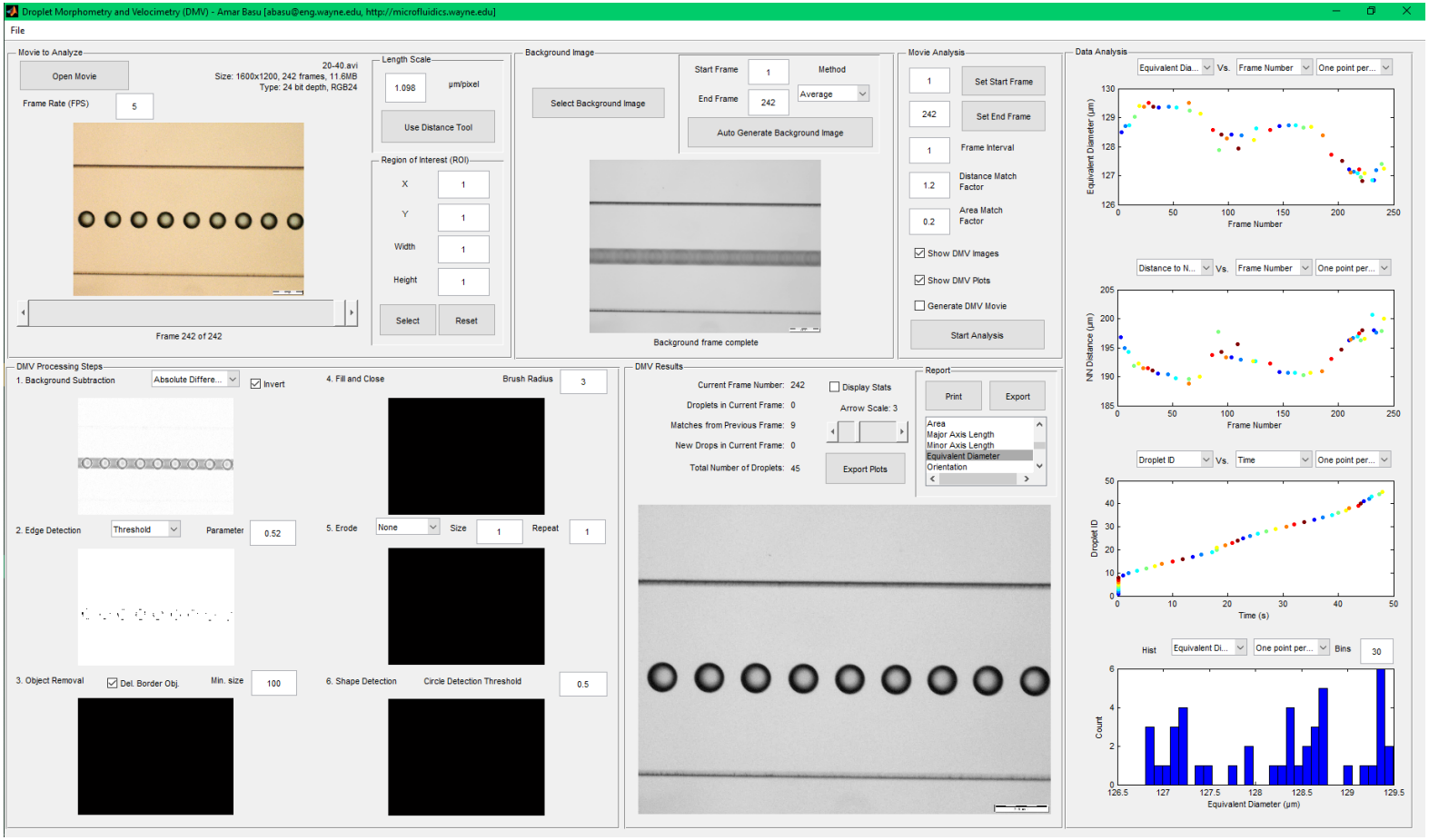

Figure 3.6. Snapshot taken from DMV video processing tool during analysis of a video recorded at the experiments

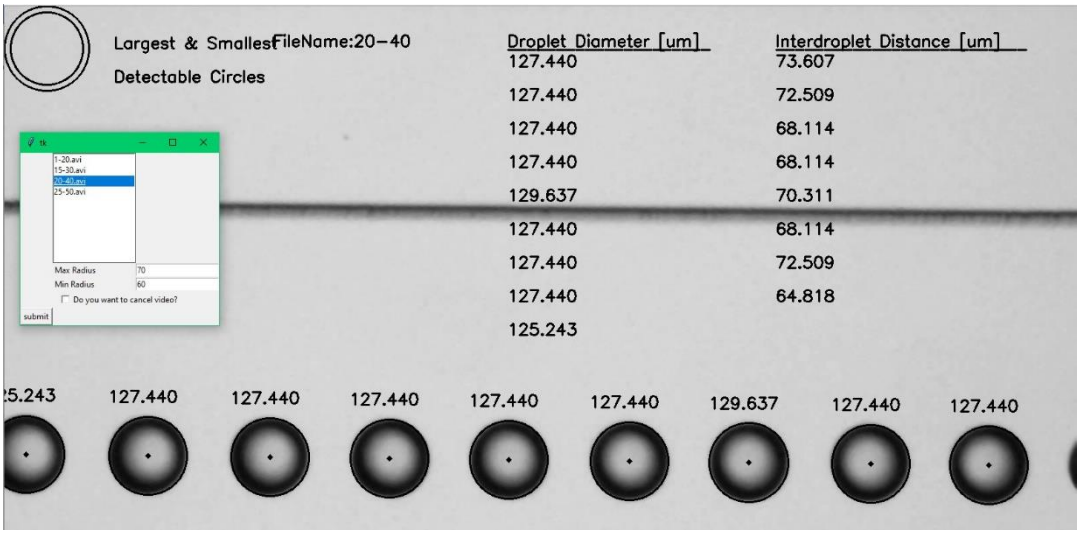

Figure 3.7 Droplet size detection with image processing

Specific to the droplet experiments, droplet sizes and interdroplet distances are calculated. OLYMPUS IX73 inverted microscope used in the experiments has four different magnification lenses, being 4x, 10x, 20x and 40x. Python image processing algorithms detect circles based on their center locations and radii in pixels. Therefore, a conversion from pixels to micrometers was implemented into the code. Table 3.1 shows the unit conversion for each lens of the microscope. The default width of the video frame is 1600 pixels and its conversion is given in µm. When a droplet size is measured in pixels, it is converted to micrometers by a ratio based on the magnification of the lens used. Size and position of all droplets are stored in an array to extract information such as average droplet size or monodispersity. In order to present the monodispersity of droplets, histograms were plotted at the end of code execution.

Table 3.1 Unit conversion between pixels and micrometers for digital camera

Lens	Size in pixels	Size in μm
4x	1600	1575.80
10x	1600	703.12
20x	1600	351.56
40x	1600	175.78

3.7 Cell Culturing, Cytometry and Handling

In the experiments, five different cell lines were used. Jurkat and K562 cell lines were obtained from METU Central Laboratory in the Department of Biology. MDA-MB231 and L929 cell lines were obtained from Hacettepe University Department of Biology. Mouse brain microvessels were obtained from Hacettepe University School of Medicine. Concentrations used in the experiments are given in Table 3.2.

Table 3.2 Concentrations of cell solutions used in experiments

Cell Type	Concentration [cell/mL]
Jurkat	$1 \cdot 10^6$
K562	$1 \cdot 10^6$
MDA-MB231	$7.5 \cdot 10^6$
L929	$2.5 \cdot 10^6$

Cell culturing requires the use of a certain environment which provides essential tools for cells to survive in-vitro. Jurkat and K562 cell lines require RPMI 1640, while MDA-MB231 and L929 cell lines require DMEM medium for culturing and growth.

If the cells will be cultured for the first time, 20% of the medium consists of FBS (Fetal Bovine Serum), which is a growth supplement for cell culturing. The same cell line can be cultured repetitively, providing that cell life cycle is sustained. To ensure that, any possible contamination should be avoided. Therefore, 1% v/v of non-essential aminoacids and antibiotics were added to the medium. All micropipettes and other tools to handle liquids while the preparation was exposed to UV light and cleaned with alcohol after use.

Cell counting is important to see if the culture has approached to a critical limit above which the product of their metabolism starts to affect the population negatively. In order to perform cell counting, cell solution inside the flask where they had been cultured was agitated gently and put onto a hemocytometer. Under microscope, number of cells confined in certain areas was counted with three separate measurement and the average was calculated. For Jurkat Cells, average of 16.7 cells per unit area on hemocytometer was found. In order to find the total number of cells in the solution, this number is multiplied by 10000 and the result was 167000 cells per mililiter. In microfluidic experiments, we found out that this concentration of cells were quite low to perform their encapsulation in micro droplets.

Cell culture flasks were disposed and culture was moved to a new flask every two weeks, two prevent issues like the wear of plastic container might result in cells to stick to the rough surfaces. Due to the metabolism waste of cells and that the medium is contaminated with this waste, the medium is also changed every time, while removing the dead cells as well. Cells were transferred to new flasks via micropipettes, which were removed from their hygenic paper packaging and used without any contact to human body. Using plastic centrifuge tubes, (T75 Flasks, Thermo Fisher Scientific, MA USA) cell solutions were centrifugated for 7 minutes. Centrifuge speed is set to RCF = 700 as standard in order not to induce mechanical damage to the cells. After the centrifugation, top portion of the content, called supernatant, was vacuumed via a glass pipette and aspirator, then disposed through a hose. Glass pipettes are single use only. The aspirator and the disposing hose are flushed and disinfected using ethyl alcohol.

3.7.1 Jurkat Cells

Jurkat cells are a type of leukaemic T-cell line, which were identified in 1980s and contributed many things to the T-cell receptor signaling pathway studies [35]. Jurkat cells are able to stay as suspension in their cell culture solutions for enough duration, therefore handling in microchannels were expected to be possible. Figure 3.8 shows a portion of Jurkat cells under optical microscope before being out into syringes for encapsulation. Size of Jurkat cells varies between 5-10 µm and they can stay in suspension long enough to perform experiment.

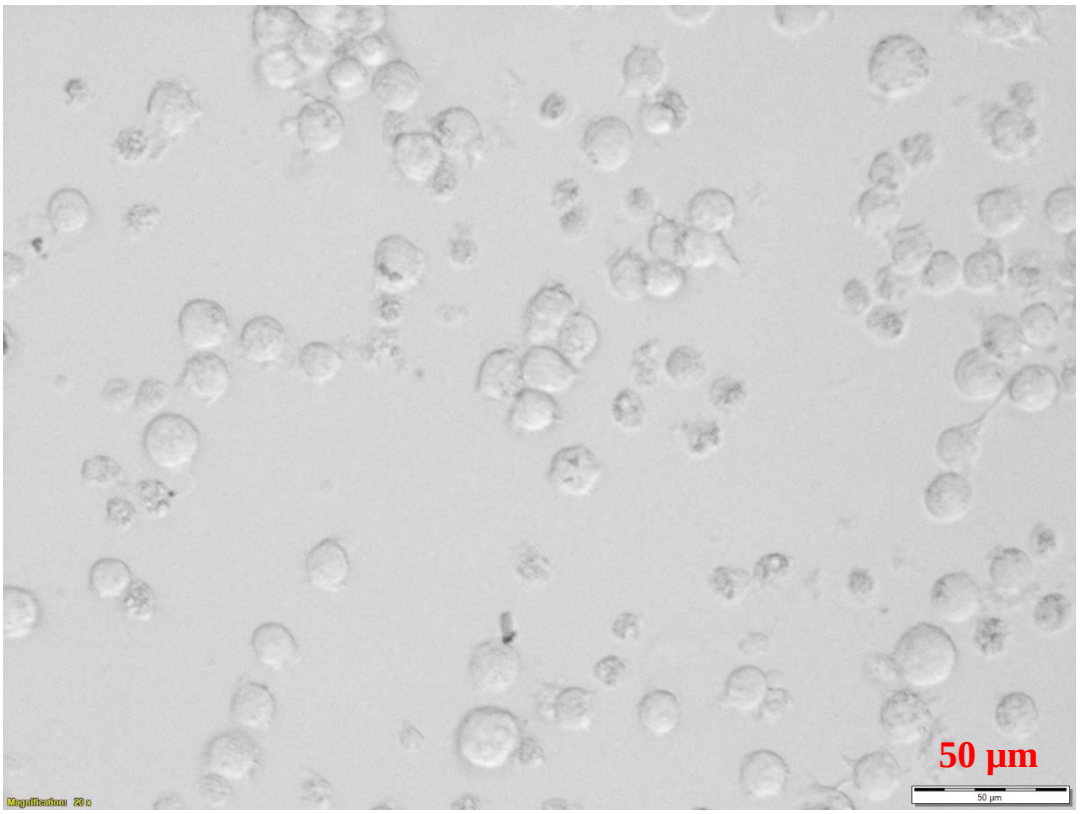

Figure 3.8 Jurkat cells imaged before encapsulation experiments (scale is 50µm).

3.7.2 K562 Cells

K562 cells are a human blood cell line, causing chronic myelogenous leukemia, and can be grown in RPMI1640 medium. Size of K562 cells varies between 5-10 µm like Jurkat cells. Figure 3.9 shows K562 cells traveling in flow direction, where in the left portion some of the cells might settle down due to lower flow velocity at larger portions of the channel.

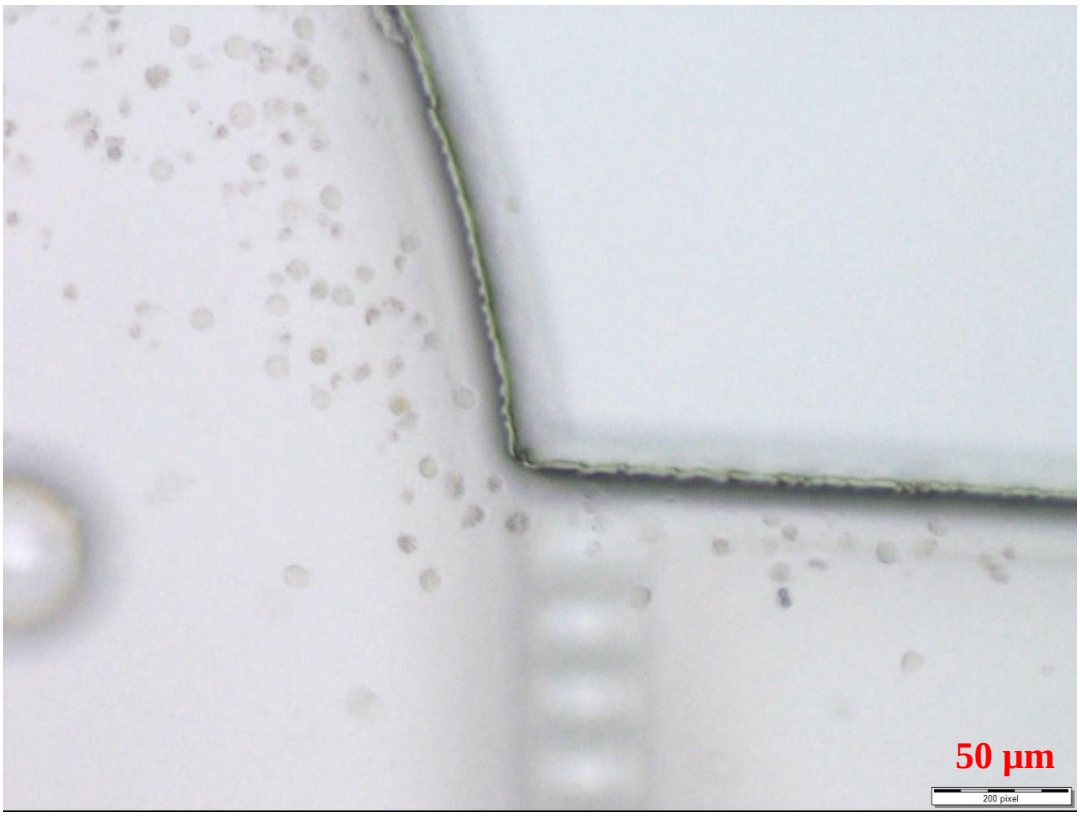

Figure 3.9 K562 cells traveling from the inlet towards the junction

3.7.3 MDA-MB231 Cells

MDA-MB231 cells are a human breast cancer cell line and can be grown in DMEM medium. Their diameters were mostly around 7-15 µm, however larger cells were in the solution since their viability was not too much and number of dead cells were a bit high in the solution, which has already undergone serious swelling and their

cytoplasm spilled around the solution. Figure 3.10 shows while they move across microchannel.

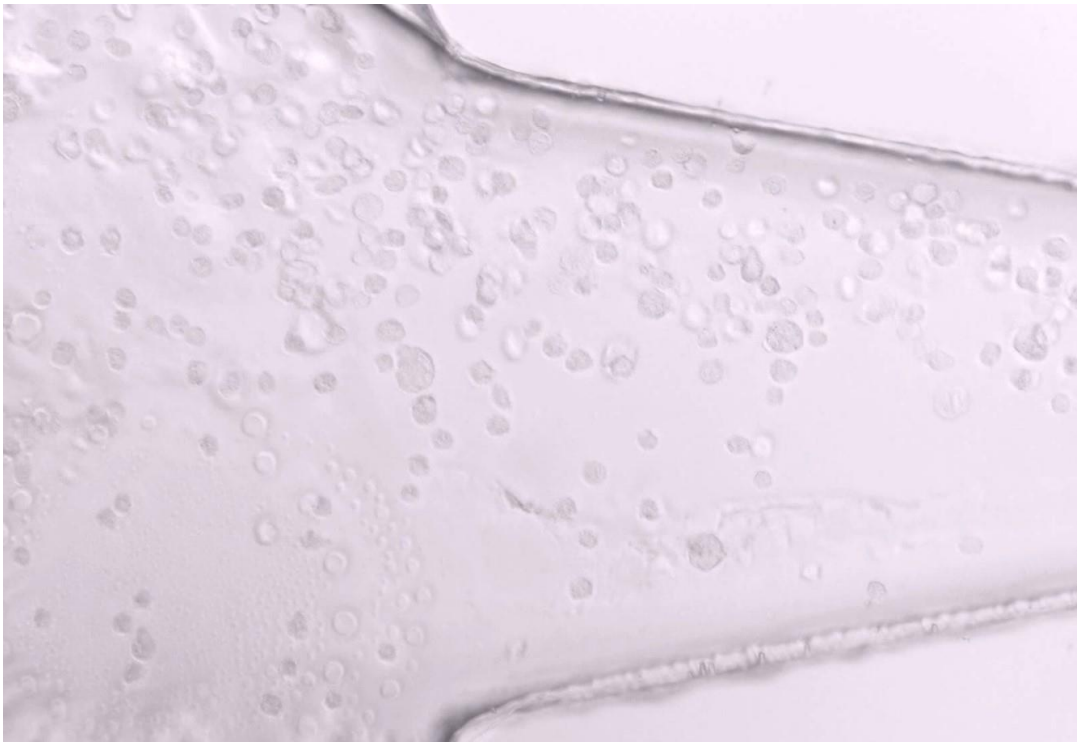

Figure 3.10 MDA-MB231 cells traveling to the junction

3.7.4 L929 Cells

L929 cells are a mouse fibroblast cell line, which can be cultured in DMEM growth medium. In microfluidic experiments, their diameters were observed around 10-15µm, which is suitable to encapsulate inside droplets that are formed with the device. However, as seen in Figure 3.11, in suspension most cells were not separated and encapsulated in a bulk form, even though they were used at lower concentration compared to MDA-MB231 cell line.

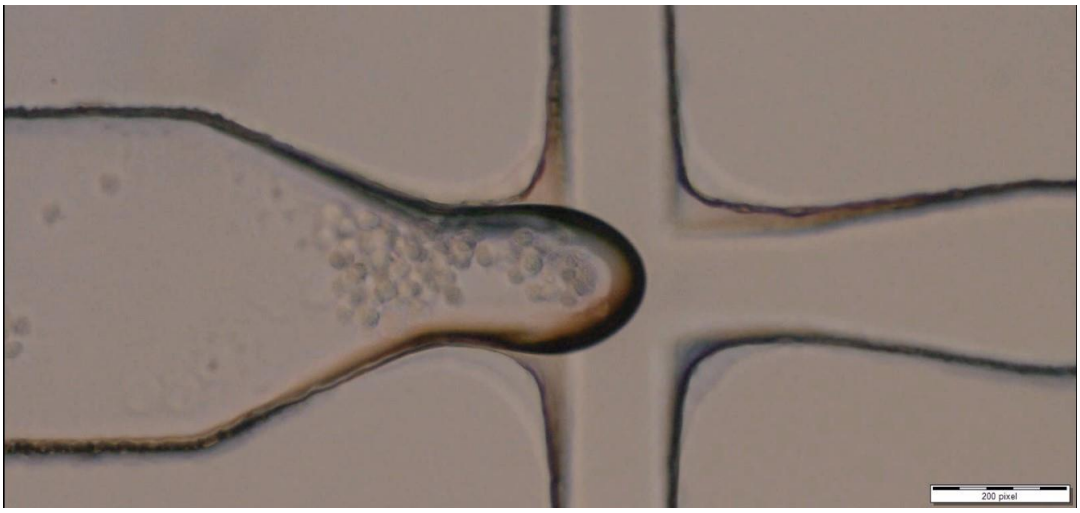

Figure 3.11 L929 cells just before encapsulation in a droplet

3.7.5 Mouse Brain Microvessels

Brain microvessels are a part of blood-brain barrier which separates circulation system from the central nervous system and prevents the toxic substances in the blood to enter brain tissues. This barrier consists of three types of cells, namely astrocytes, pericytes and endothelial cells. Those cells encircle the microvessel and form a secure and selective structure for the substances that are to be transferred to brain tissues. Since they cannot form a spherical shape, it is unlikely to use permeability models on the microvessels, although the CPA loading inside microdroplets are still a promising method which might be used for the cryopreservation of brain microvessels.

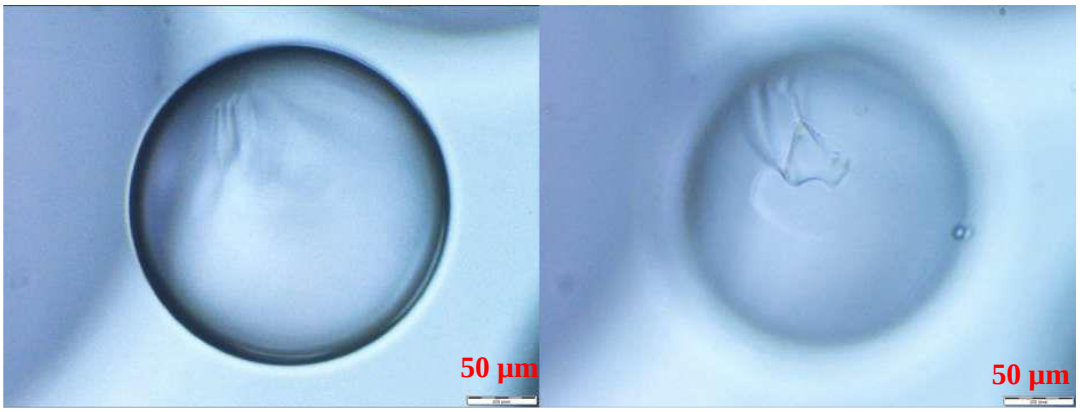

Figure 3.12 Brain microvessel encapsulated inside a microdroplet

3.8 Integration of Cell Solution to Microfluidic System

Performing microfluidic experiments using cell solutions require some preparations. First, oil syringes are filled using the same procedure explained in Solution Preparation section. The syringe used to contain cell solution is either a sterile, single-use plastic syringe or to prevent cell sedimentation, an ILS borosilicate glass syringe with an integrated mixer, which is rotated by a concentric magnet, covering the syringe from outside and motorized via a pulley-belt system, shown in Figure 3.13. Since this syringe has been used regularly and not a single use syringe, it is flushed with isopropyl alcohol, water and a fresh cell culture medium before the loading of actual cell solution. Preparation of cells involve processes to make them ready to use inside syringes, ensuring that cell concentration is enough to maintain cell supply along with the carrier fluid inside micro channels. Schematic and the placement of the equipments during cell encpsulation experiments can be seen in Figure 3.14.

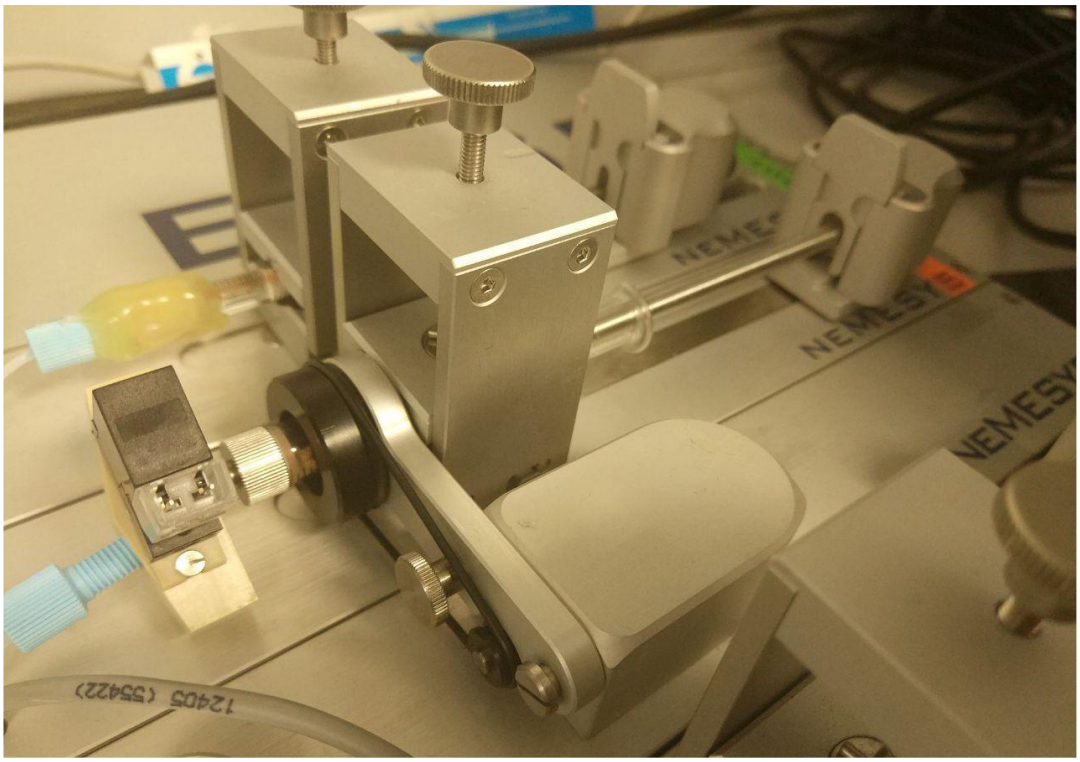

Figure 3.13 Integrated NEMIX Syringe Stirrer module

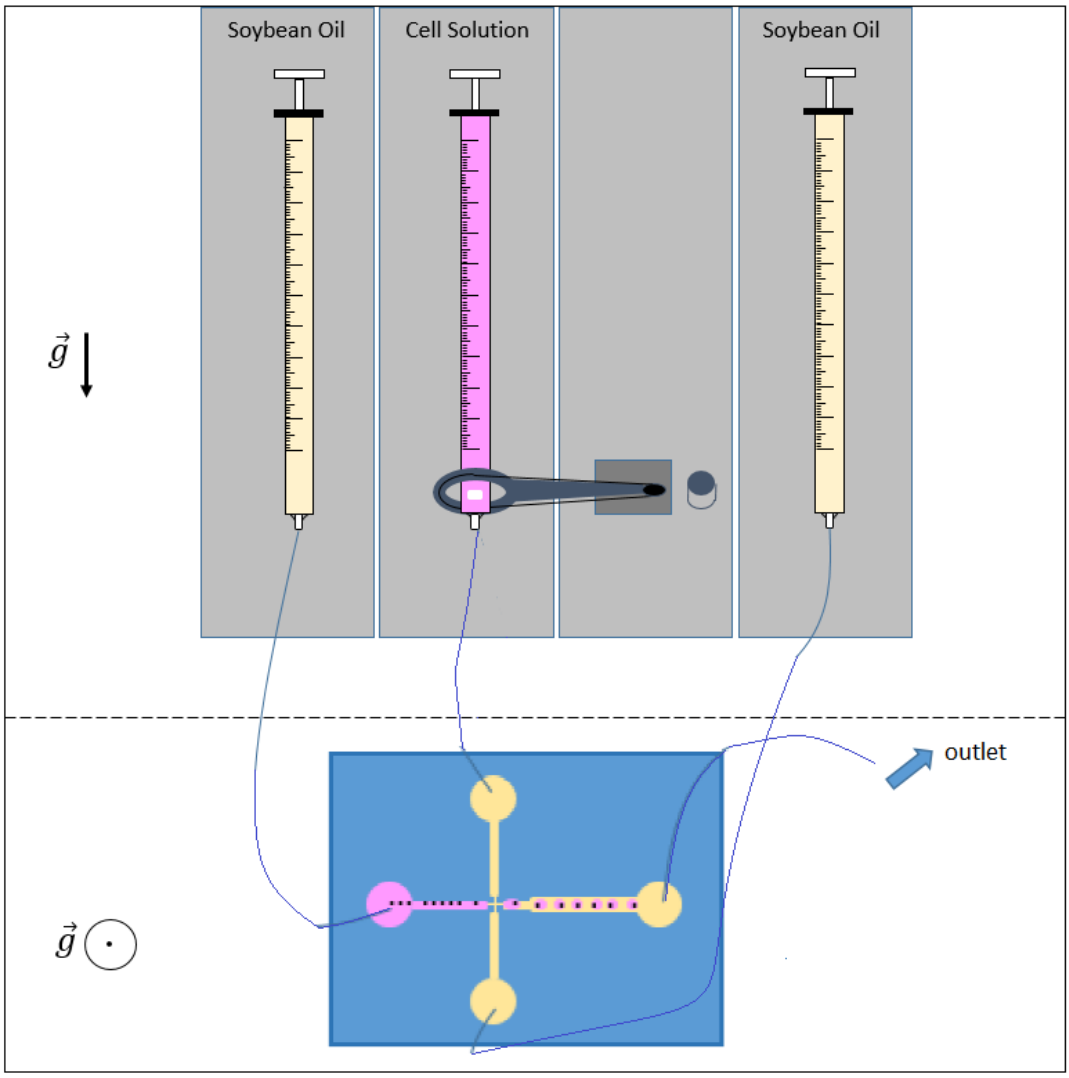

Figure 3.14 Schematic of syringe pump and microfluidic system with cell solution

Figure 3.15 shows all equipments ready to use in experiment. Two plastic single use syringes were used for oil phases and ILS borosilicate glass syringe with integrated mixer was used for the cell solution. All liquid phases were transported to microchannels via Tygon tubings.

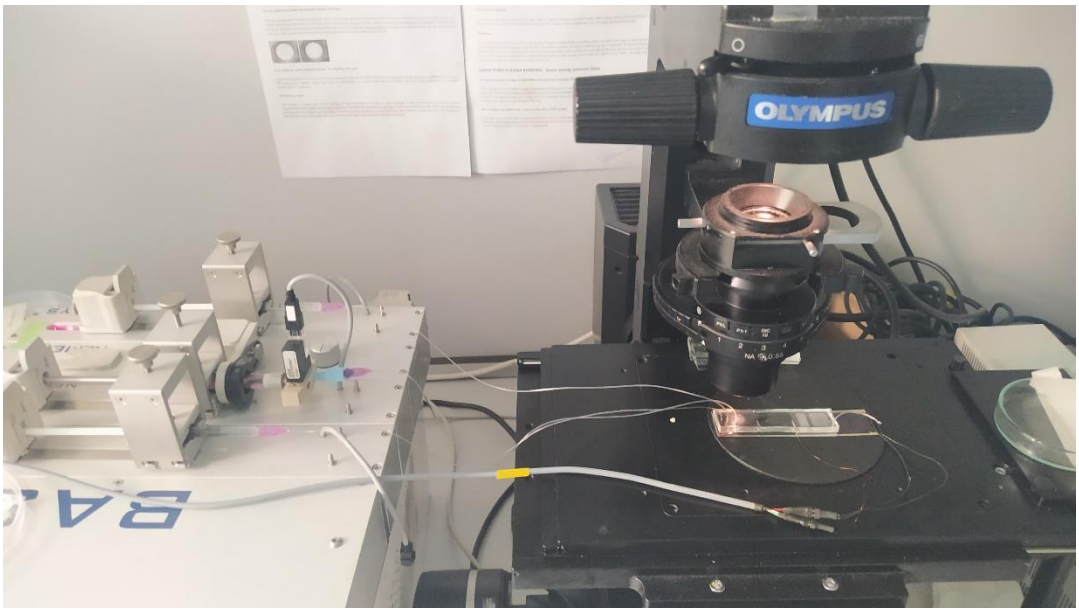

Figure 3.15 Syringe pump and microfluidic device on inverted microscope during cell encapsulation experiment

3.9 GUI Designed for Model Solvers

Here, a GUI (graphical user interface) designed to solve cell membrane permeability models is introduced. Cell membrane properties from related studies in the literature is collected and implemented to the software. Commonly used membrane permeability models are presented and the modified model suitable for the dynamic data collected from the microfluidic system is proposed, all of which can be used for solution of cell response to a CPA exposure. For the modified model only, shrinkage rates of aqueous droplets for three different CPA molecules, glycerol, ethylene glycol and propylene glycol are used as input to represent the dynamic extracellular CPA concentration, as opposed to constant concentrations used in conventional methods. Cell volume change inside a shrinking droplet is observed and the response is correlated to the modified model to obtain membrane permeability parameters.

Cell membrane permeability models in general are ordinary differential equations, solutions of which describe the changes in the cell volume and intracellular CPA concentration. Similar studies in the literature are a way to assess the models by introducing the parameters. Although some models employ only one of permeability models, the GUI designed provide access to three different permeability models and their solutions, providing that the parameters about cell type and the environmental conditions are given. It is possible to solve the model used in the literature and compare it to the proposed model for the thesis, where the dynamic extracellular concentration is a remarkable difference.

Figure 3.16 shows the graphical user interface that allows to enter cell membrane permeability parameters and the ambient parameters used in literature studies. It is also possible to manually enter numbers to change values or give new values used in the experiments. Using the same cell and ambient parameters, it is possible to solve both current models and the microfluidic model. The source code for the GUI and integrated solvers are given in Appendix B. Some of the values provided in the literature are given in Table 3.3, which were imported to the graphical user interface of model solver for easy access.

Images of encapsulated cells taken under microscope can be processed to see real-time volume response of cells to the CPA exposure. Matching these experimental volume change response with the model is a way to find cell membrane permeability parameters for the given cell type, at the specified temperature in the specific CPA concentration.

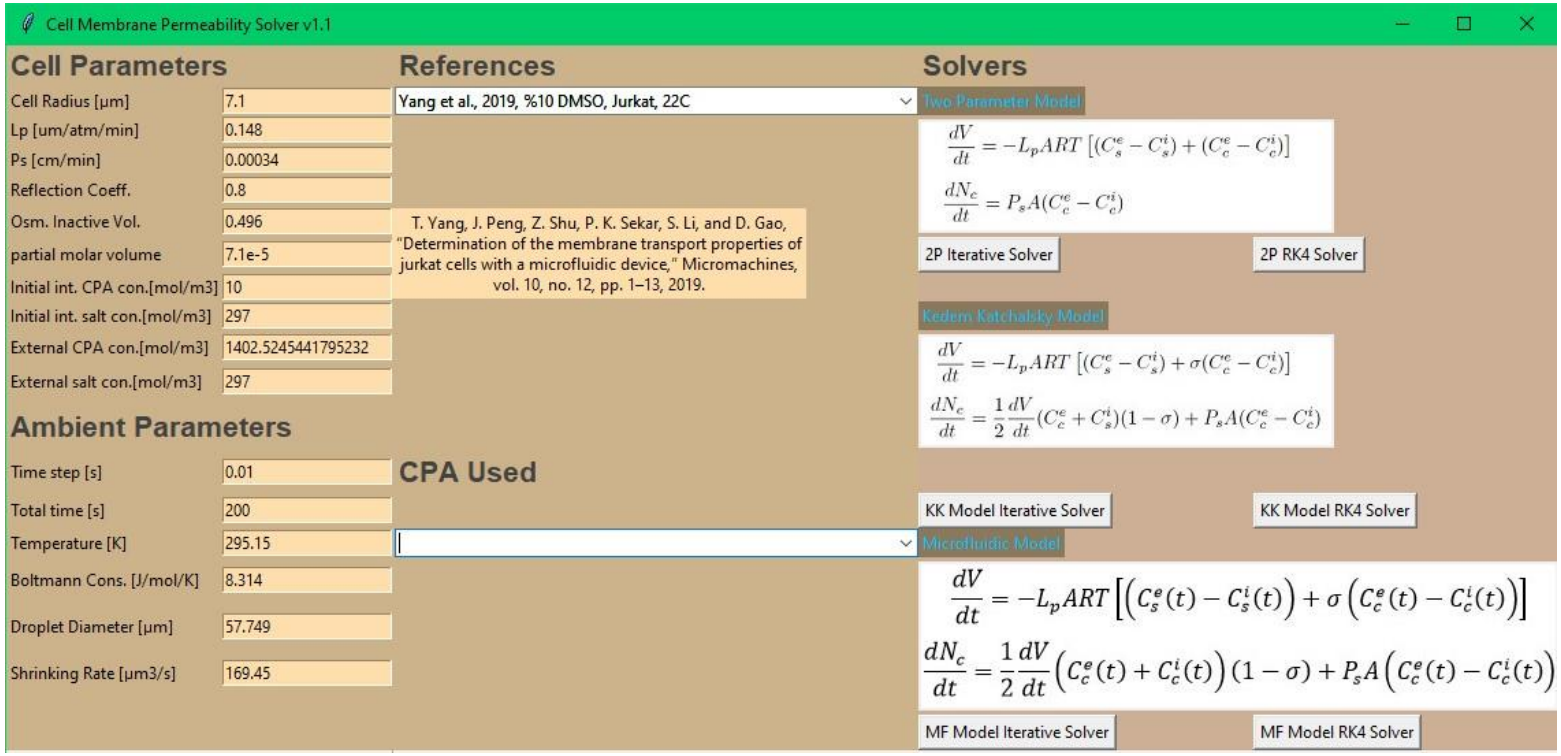

Figure 3.16 A user interface designed in Python for solving membrne permeability models

Table 3.3 Cell membrane permeability parameters used in the solver

Cell Type	CPA	Temp. [°C]	Isotonic Cell Radius [µm]	Hydraulic Conductivity Lp [µm/atm/min]	Solute Permeability Ps [cm/min]	Reflection Coefficient σ	Ref.
Jurkat Cell	DMSO	22	7.10	0.148	0.00034	0.8	[36]
Jurkat Cell	DMSO	22	5	0.158	0.00042	1	[37]
Human Embriyonic Stem Cell	Glycerol	24	7.80	1.224	0.088	0.92	[31]
Human Granulocyte	Glycerol	21	4.485	0.18	0.0001	1	[38]
Human Vaginal	Propylene Glycol	22	9.62	0.221	0.001168	1	[39]
Human Spermatozoa	Ethylene Glycol	22	1.89	0.74	0.0079	0.77	[33]

Whole experimental setup involves tools to generate, detect, measure and heat up the droplets in microfluidic devices. Droplet generation and shrinkage experiments were performed gradually to understand the behavior of each device used. X-junction devices are used for early droplet generation experiments due to the simplicity and ease of use. Having same junction design, serpentine devices involve more regions and parameters to control. Therefore, droplet shrinkage experiments in serpentine devices did not require to develop a droplet generation procedure, which is already done in the simple X-junction devices. Next chapter discusses the results obtained from experiments done on droplet generation and shrinkage, cell encapsulation and permeability studies.

CHAPTER 4

RESULTS AND DISCUSSION

4.1 Aqueous Droplet Generation

Droplet generation is a process where steady state flow conditions inside the microchannel should be met. Since the volumetric flow rate is controlled with a linear velocity of worm gear in syringe pump, applied force is required to cause a pressure change throughout the syringes, tubings and finally microchannels. Therefore, although it is experienced that 20:1 oil/water flow rate ratio ($Q_{o/}$ Q_w) is practically useful to generate droplets, it is not practical to start experiment with that much of a big flow rate ratio. Figure 4.1 shows the flow rates at various time steps followed until reaching 20:1 ratio various time steps followed until reaching 20:1 ratio with 5:0.25 µL/min flow rates. After reaching a stable flow regime, which is also mentioned as the dripping regime in the previous sections, flow rates can be adjusted to control the droplet size. Figure 4.2 shows how droplets with different sizes and interdroplet distances can be generated by keeping the 20:1 flow rate ratio at various flow rates.

Oil Flow Rate	Water Flow Rate	Droplet generation at constant oil flow rate with 4x camera
µL/min	µL/min	
5.00	2.50	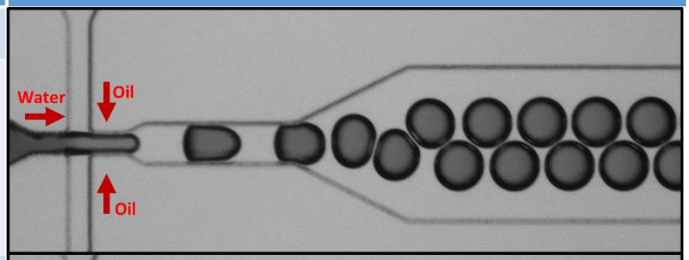
5.00	2.00	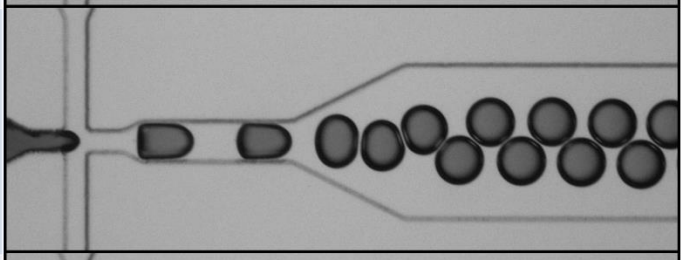
5.00	1.50	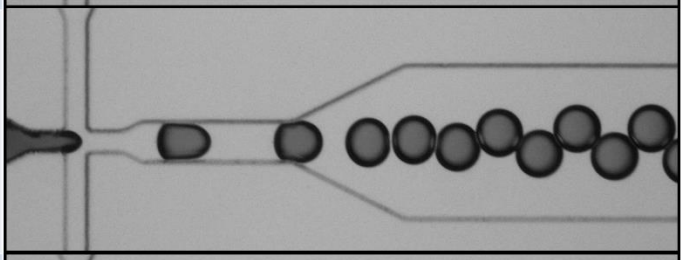
5.00	1.00	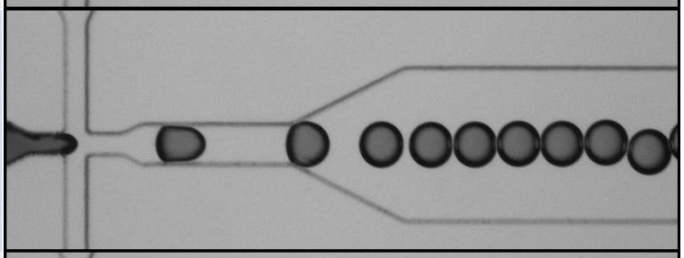
5.00	0.50	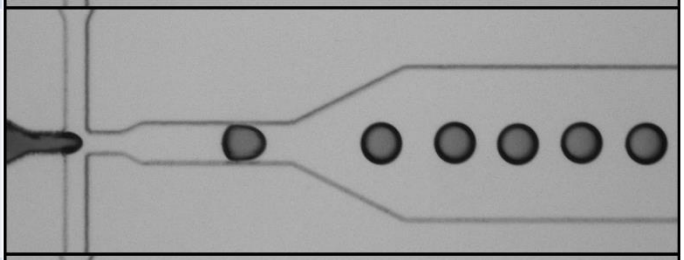
5.00	0.25	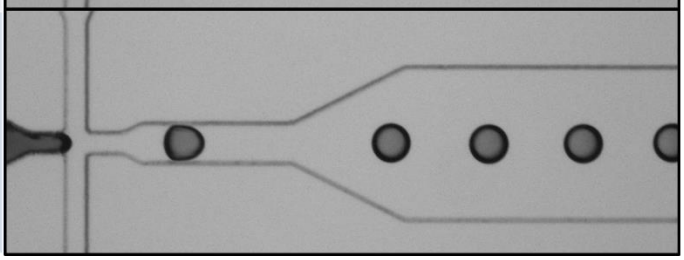

Figure 4.1 Adjusted flowrates during droplet generation

Oil Flow Rate	Water Flow Rate	Droplet generation at constant 20:1 flow ratio with 4x camera
µL/min	µL/min	
1.5	0.075	
2.00	0.100	
2.5	0.125	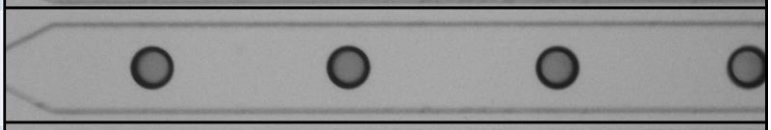
3.00	0.150	
3.50	0.175	
4.00	0.200	
4.50	0.225	
5.00	0.250	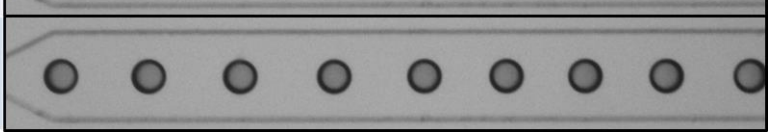

Figure 4.2 Adjusted flow rates after obtaining stable droplet generation

4.1.1 Droplet Generation in X-Channel Device

Droplet generation in microfluidic devices require a delicate design and fabrication procedure. Device design requires the knowledge of the requirements beforehand, so that each fabricated device can be executed as intended. X-channel devices basically consist of 3 inlets and 1 outlet hole, and 4 channels that combine the ports to each other at a junction which has a flow-focusing type of structure. The reason that the device is called X-channel is that there is no other extension or feature in the device other than then the junction, compared to the main experimentation device shown in Figure 3.1 and Figure 3.2, which includes serpentine section and auxiliary channels. The main reason to use X-Channel devices prior to serpentine devices is that serpentine devices are more complex and require additional setup to execute. A basic X-channel device can be used to generate droplets or encapsulate cells very fast, since an additional auxiliary flow channel is not required to control. Also, total channel length is considerably small in X-junction devices, whereas serpentine portion as a total effective length of approximately 1 m, which requires more time to obtain a steady flow at the beginning of experiments.

As can be seen from Figure 4.2, at increased flow rates with constant Q_o/Q_w ratio, droplet size decreases. Therefore, performing a parametric study using a droplet generator device reveals the characteristics of the device. Since the junction size also affects the droplet size while it is forming, using same flow rates in different geometries yield different sized droplets. Figure 4.3 shows three separate X-Channel type device, where the junction widths are 25 µm, 50 µm and 100 µm. In Figure 4.4, the average droplet sizes generated by three different X-channel type devices are plotted. Although the trend of decreased droplet size with increasing flow rate applies to all three devices, narrow junctions provide smaller droplets at the same flow rates. Therefore, determining the application and requirements is important.

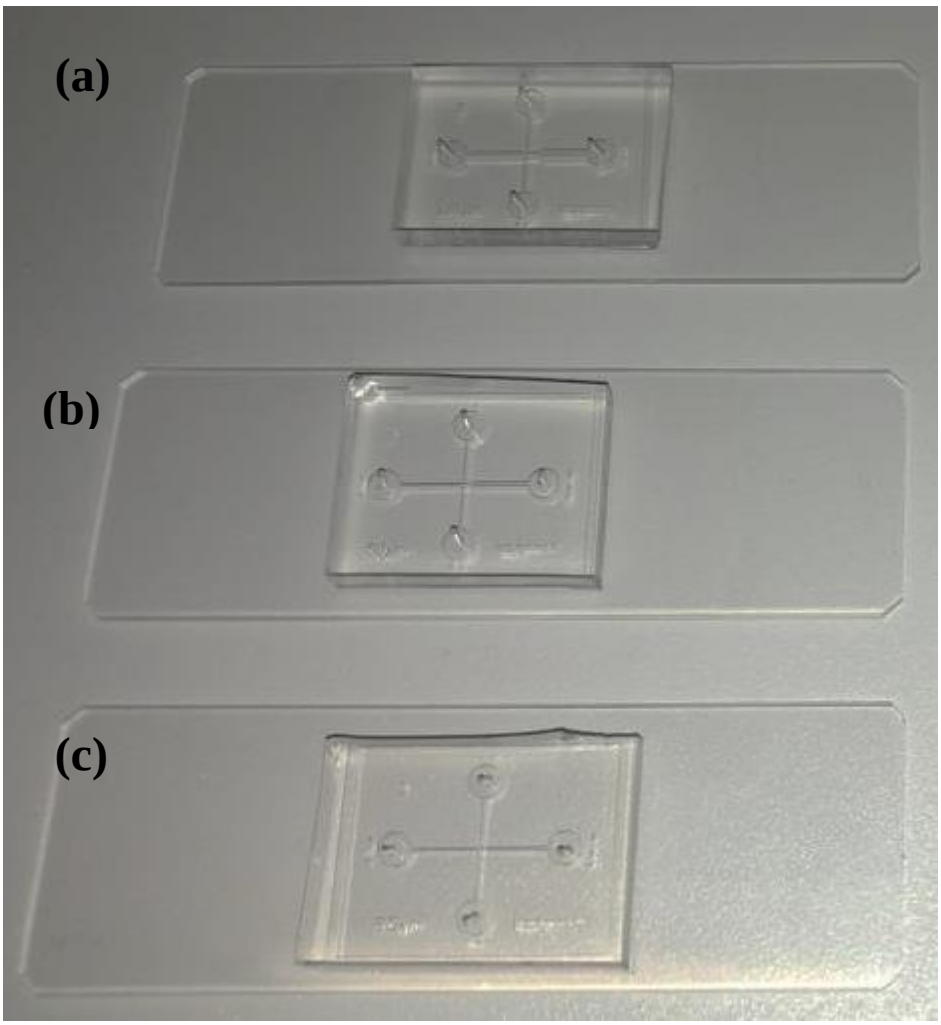

Figure 4.3 X-Channel devices with (a) 100 µm (b) 50µm (c) 25 µm junction width used in the experiments

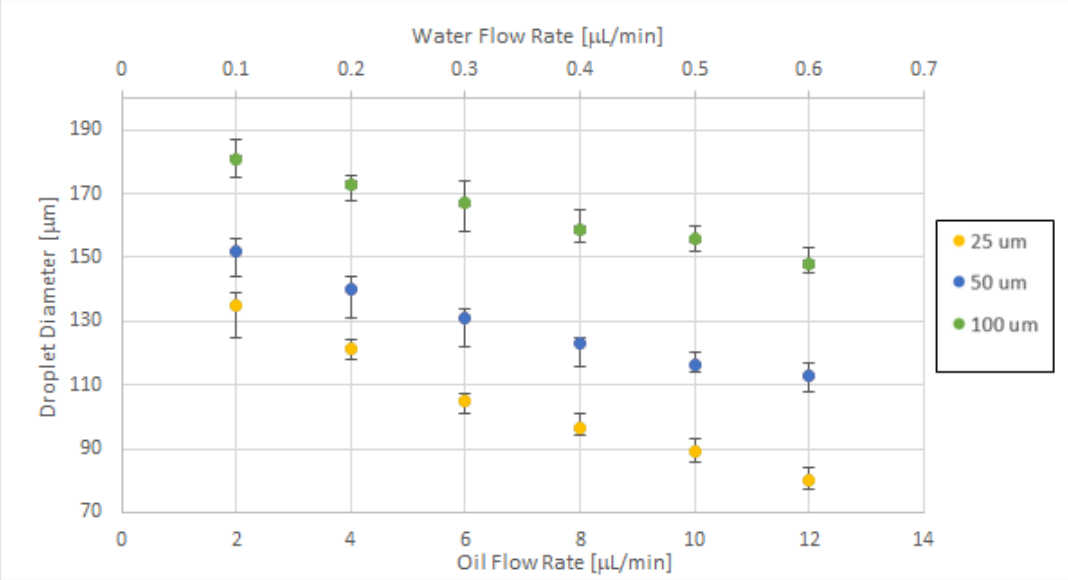

Figure 4.4 Droplet diameter as a function of volumetric flow rate for three junction widths

4.1.2 Droplet Generation in Serpentine Device

Microfluidic devices are the combination of narrow channels with inlet and outlet ports, together with the features in between. Figure 4.5 shows three serpentine devices, which have similar geometrical design but in different sizes. As described in Figure 3.1, the device contains more features than the simple X-junction device. The geometries of the droplet generation region in both X-channel and serpentine devices are identical. Therefore, it is expected to obtain similar sized droplets at same flow rates. However, the total length that fluid should travel between inlet and outlet ports is larger in serpentine devices. In addition, having a serpentine structure with a large number of U-turns bring both major and minor head losses, resulting in disturbance in the monodispersity that can be obtained in a simple X-junction device. Although monodispersed droplets were obtained both in X junction and serpentine devices, it is difficult to maintain monodispersity in serpentine devices if droplets are close to each other. Figure 4.5 shows three different serpentine devices, which were named based on the width of their droplet generation junction (25µm, 50 µm and 100 µm).

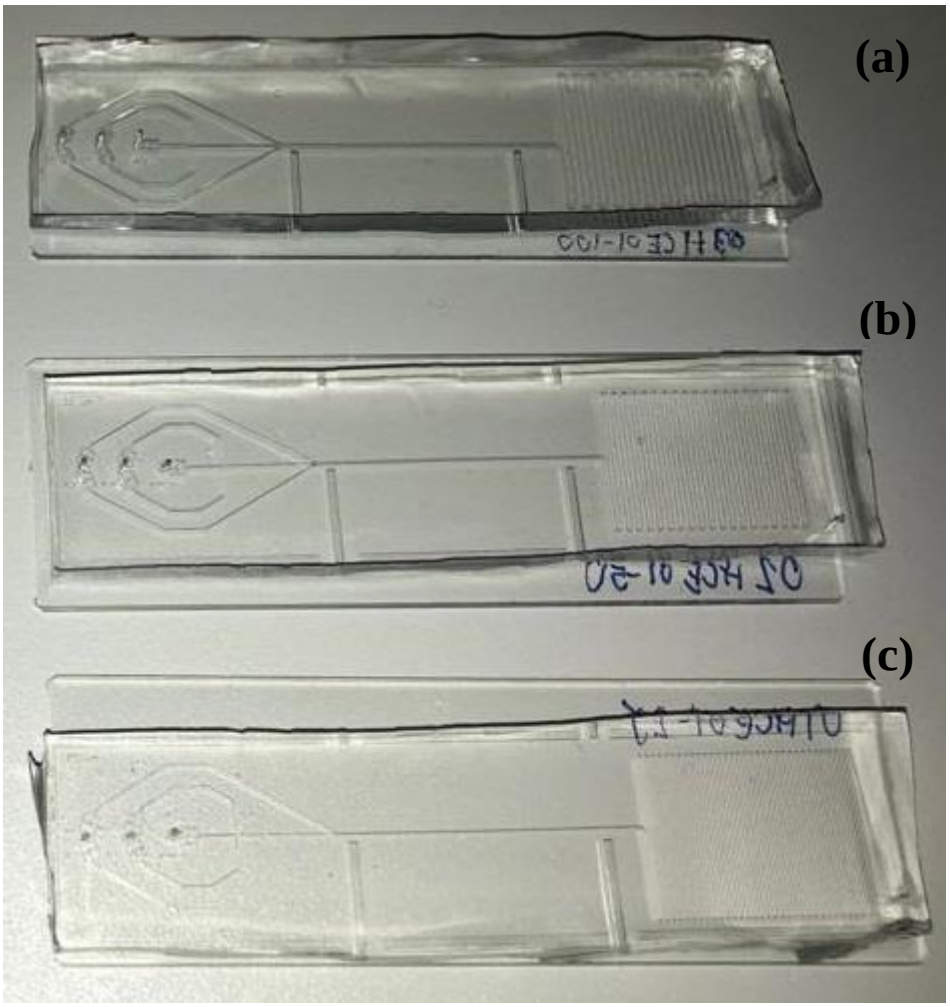

Figure 4.5 Serpentine devices used in the experiments with (a) 100 µm (b) 50µm (c) 25 µm junction width

The segment of the microchannel between droplet generation and auxiliary oil region, which can be seen in Figure 3.1, was modeled in COMSOL to investigate the contribution of auxiliary channel to droplet size. The intention of the auxiliary channel is to adjust interdroplet distances between droplets, which otherwise only dependent to the ratio between flow rates of continuous and dispersed phases. Figure 4.6, Figure 4.7, Figure 4.8 and Figure 4.9 show the alternating flow rates of auxiliary oil channel and the pressure contours inside the channels. Figure 4.6, Figure 4.7, Figure 4.8 and Figure 4.9 have the results of auxiliary flow rates 1µL/min, 5µL/min, 10µL/min and 15µL/min, respectively. COMSOL results of the auxiliary channel effect can be summarized to be highly impactful on the size of droplets even though

these auxiliary channels contribute to the flow after the droplets are already generated. Increased auxiliary flow rate also increases the pressure at the earlier stages of the channel; the maximum pressure in the left portion of the channel is around 420 Pa at 1 µL/min auxiliary oil flow rate, while the pressure increases to 560 Pa when the auxiliary oil flow rate is 15 µL/min. Since the droplet generation is also a result of the flow caused by pressure difference between inlet ports and the droplet generation downstream, increased auxiliary oil flow rate tends to have a negative contribution in the overall flow rate. It is shown that increased flow rates tend to generate smaller droplets in previous chapter. Although the flow rates are controlled, the phenomenon causing to obtain smaller droplets is a larger pressure difference between inlet and outlet. Or, smaller pressure difference would yield larger droplets, like smaller flow rates do. Therefore, an inside effect causing to reduce this pressure difference acts like having a smaller flow rate and provide the similar behavior of having larger droplets.

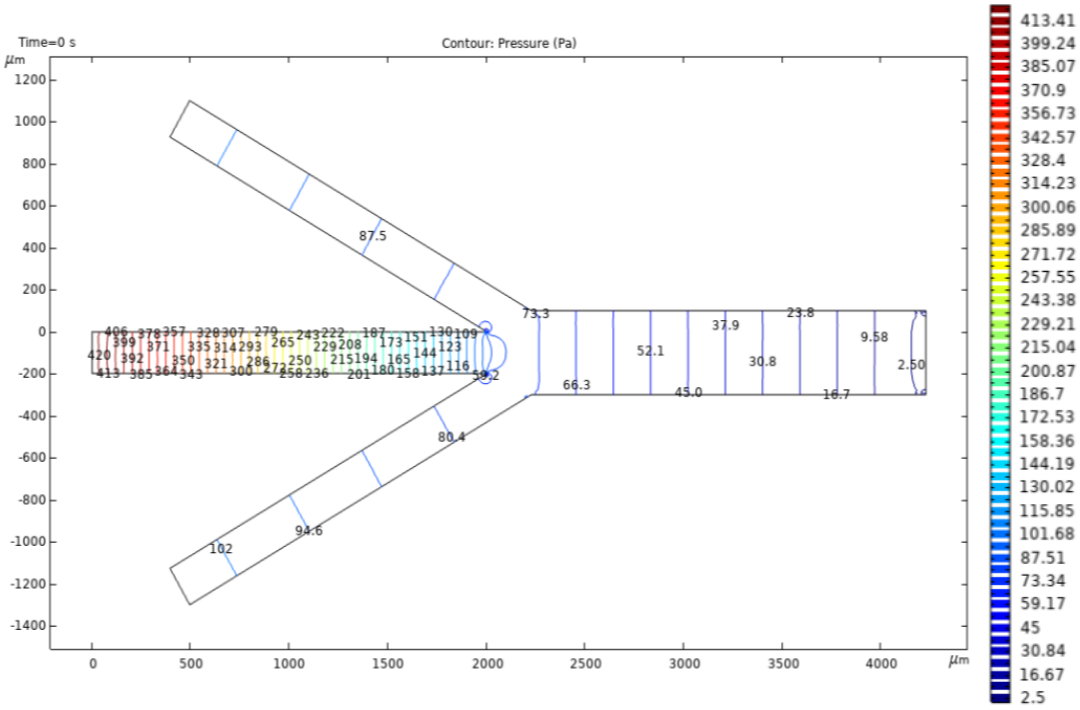

Figure 4.6 Pressure contours at the auxiliary flow channel junction (middle channel flow rate =10 µL/min, each auxiliary channel flow rate = 1 µL/min)

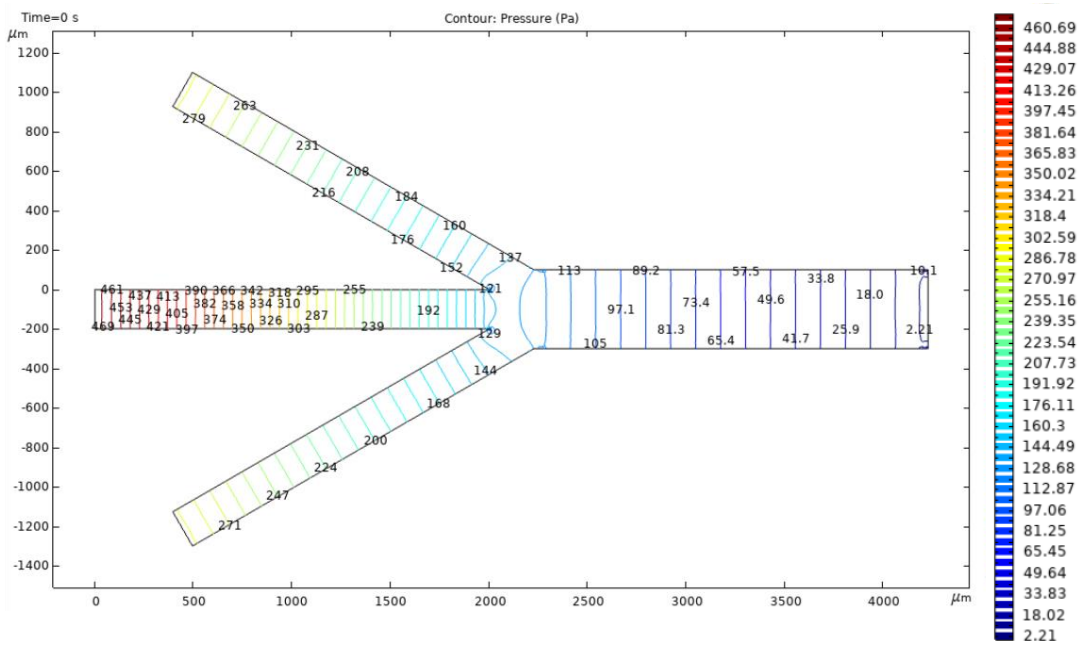

Figure 4.7 Pressure contours at the auxiliary flow channel junction (middle channel flow rate =10μL/min, each auxiliary channel flow rate = 5μL/min)

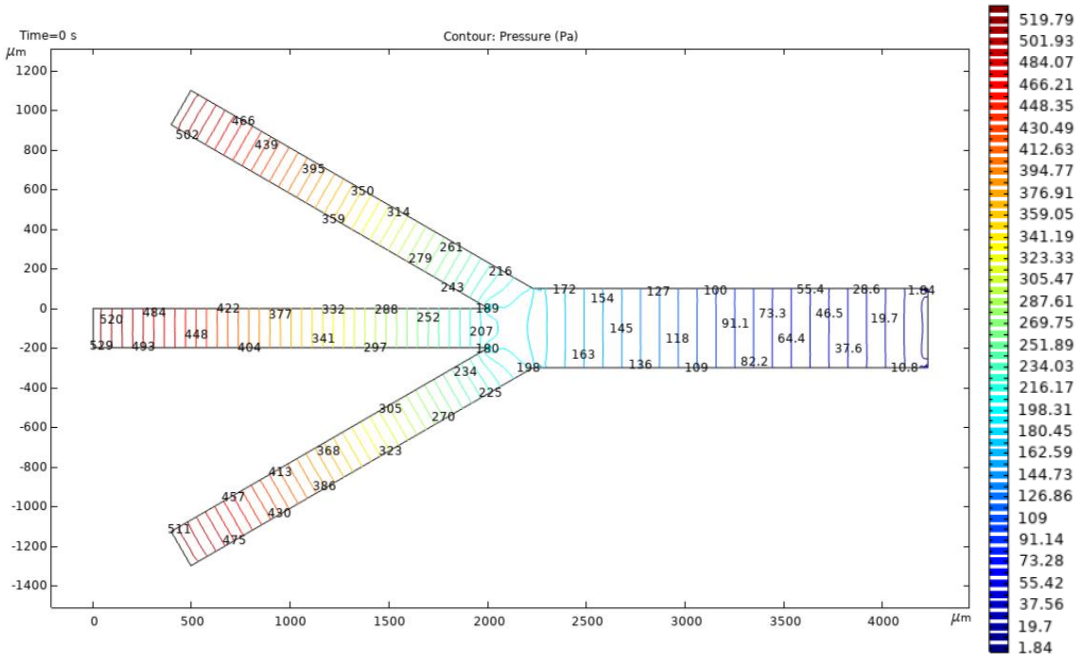

Figure 4.8 Pressure contours at the auxiliary flow channel junction (middle channel flow rate =10μL/min, each auxiliary channel flow rate = 10μL/min)

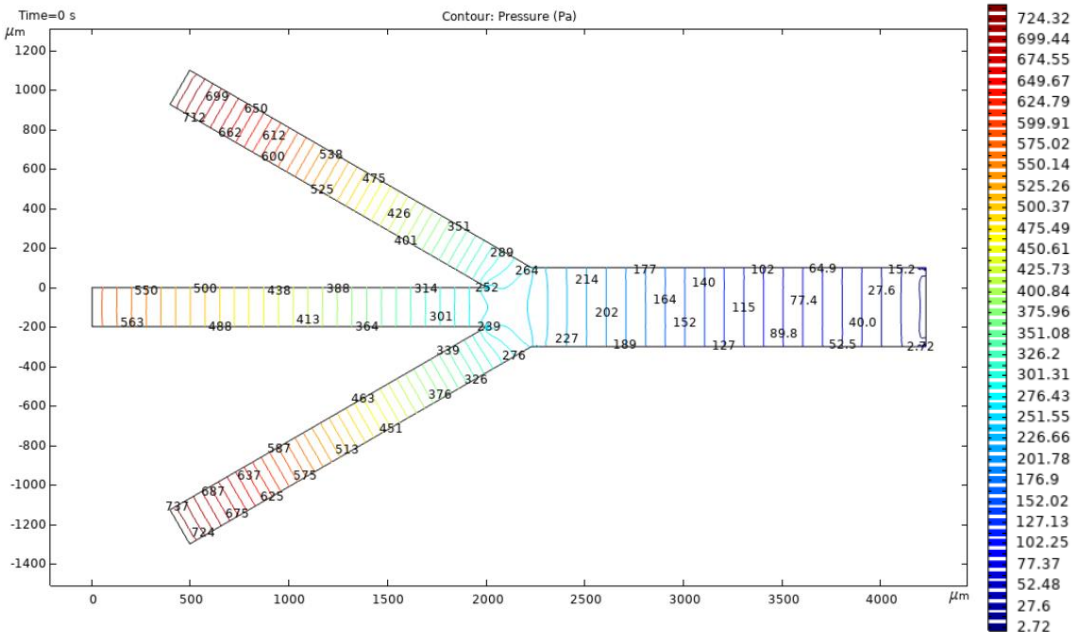

Figure 4.9 Pressure contours at the auxiliary flow channel junction (middle channel flow rate =10 µL/min, each auxiliary channel flow rate = 15 µL/min)

Although droplet size is related to the flow rates which are contributing to the generation of droplet, i.e. dispersed and continuous phases, experimental results in Figure 4.10 showed that axuiliary flow also affecting the droplet size, most probably due to the decreasing pressure difference between inlet ports and the droplet generation region with increasing auxiliary flow rates. It is a surprising outcome at the droplet generation experiments that, given the constant dispersed and continuous phase flow rates, auxiliary oil flow rate has an effect on droplet size and interdroplet distance. In the design of device, channel width is doubled after the auxiliary flow junction, so that using the same flow rates at continuous phase flow rate and auxiliary channel flow rate, linear velocity does not change i.e., both cross sectional area and volumetric flow rate is doubled. Having equal flow rates would maintain the constant interdroplet distance, while use of lower auxiliary flow rate than continuous phase flow rate decreases the interdroplet distance and the use of higher auxiliary flow rate than continuous phase flow rate increases the interdroplet distance, which can be seen in Figure 4.11.

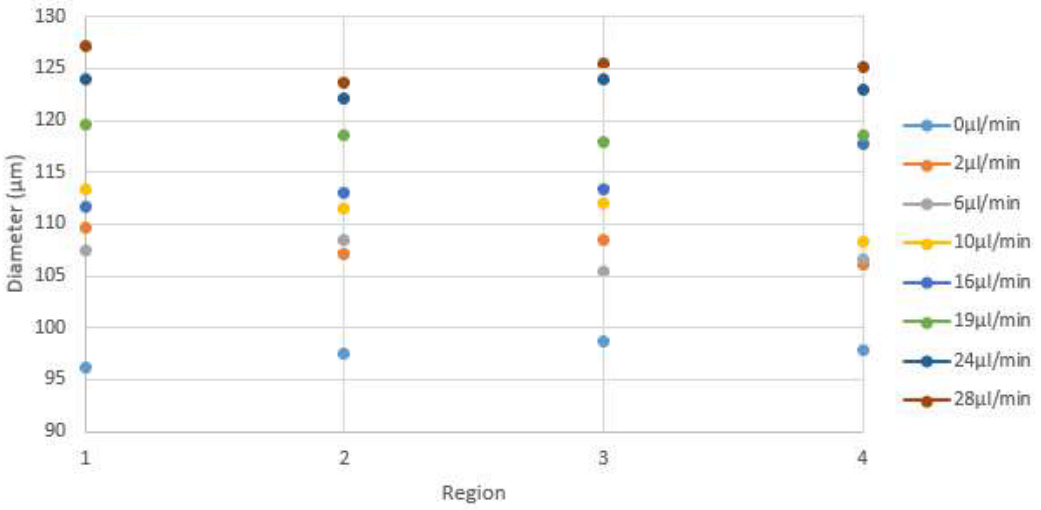

Figure 4.10 Droplet sizes in 100µm-device (Q_w=0.8 µL/min ,Q_o=16 µL/min)

4

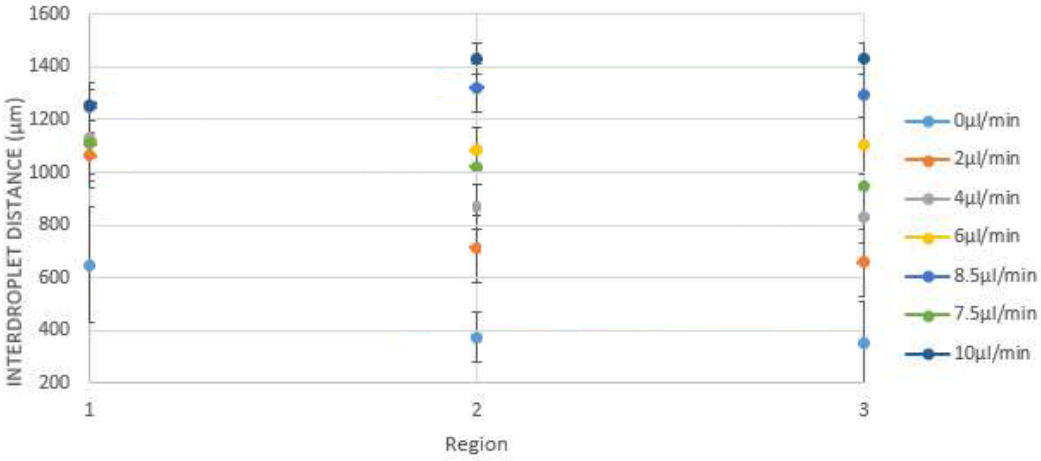

Figure 4.11 Interdroplet distances in 50µm-device (Q_w=0.4 µL/min ,Q_o=8 µL/min)

4.1.3 Aqueous Droplet Solubility in Soybean Oil

It is important to know the behavior of cryoprotectant agents, which should dissolve in water but not in soybean oil. Inside a microchannel where flow velocity is zero, solubility data can be obtained from droplet shrinkage rate in time. The experiment was performed to assess DMSO solubility in soybean oil at 40°C. Since the flow was stationary, solubility is slower than that in a normal flow. Stationary droplet experiments require sudden stop of the flow in channels. Therefore, metal paper clamps were used as shown in Figure 4.12. After droplets are obtained, inlet and outlet ports are clamped immediately to cancel flow in any direction. This way, it is possible to observe stationary droplets up to 5 hours inside the microchannel.

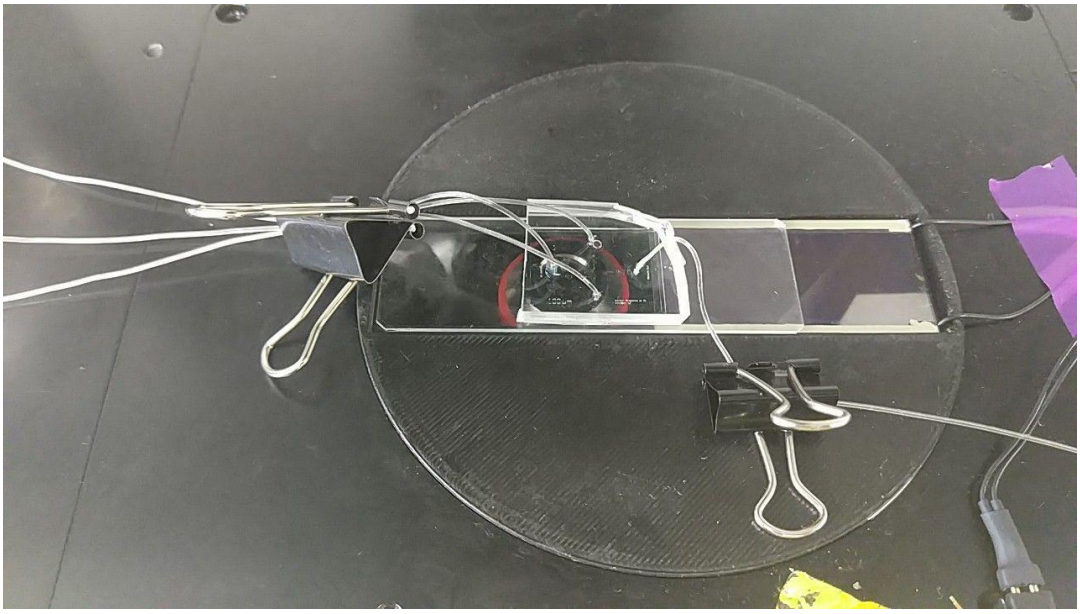

Figure 4.12 X-junction type device and the clamped tubings to stop the flow

Results show that in soybean oil environment, DMSO droplets have a mass loss of 7.2×10^{-6} mg/min. A theoretical calculation can be performed as follows. In the microscope camera frame, there is a fixed volume of oil phase and there are adjacent droplets, all of which are surrounded by equal amount of soybean oil, as shown in Figure 4.13.

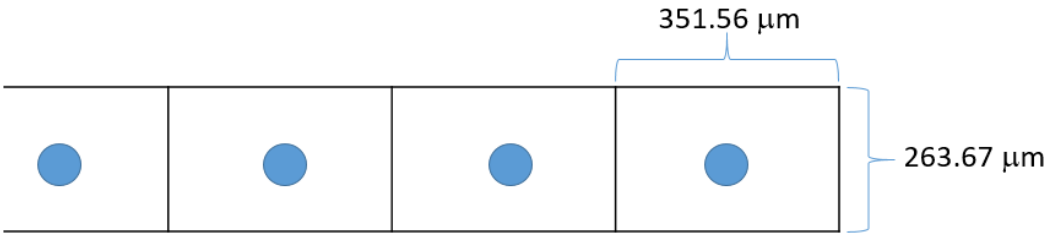

Figure 4.13 Approximate dimensions for the solvent volume and solubility calculation

Droplet volume can be calculated and the volume of surrounding soybean oil phase can be approximately known. Size of DMSO droplets were detected as 96.679 µm at t=85 s, and 53.393 µm at t=3600 s, where $V_{initial}$=473.1 pL, V_{final}=79.7 pL and V_{oil}=8796 pL, yielding

$$\frac{V_{initial} - V_{final}}{V_{oil}} \cdot 100 \ = 4.47\% \qquad (9)$$

Compared to the water solubility of 0.3% in soybean at 25°C [14], DMSO does not seem to be used as cryoprotectant in aqueous droplets inside soybean oil. Figure 4.14 also shows that DMSO and water droplets have a similar trend of shrinkage, meaning that they both dissolve in soybean oil in a similar manner. Therefore, DMSO dissolved in water would be likely to diffuse into soybean oil, and DMSO concentration inside the aqueous droplet is not possible to control. Due to this result, DMSO is not used in experiments where cell encapsulation and cell membrane permeability is investigated.

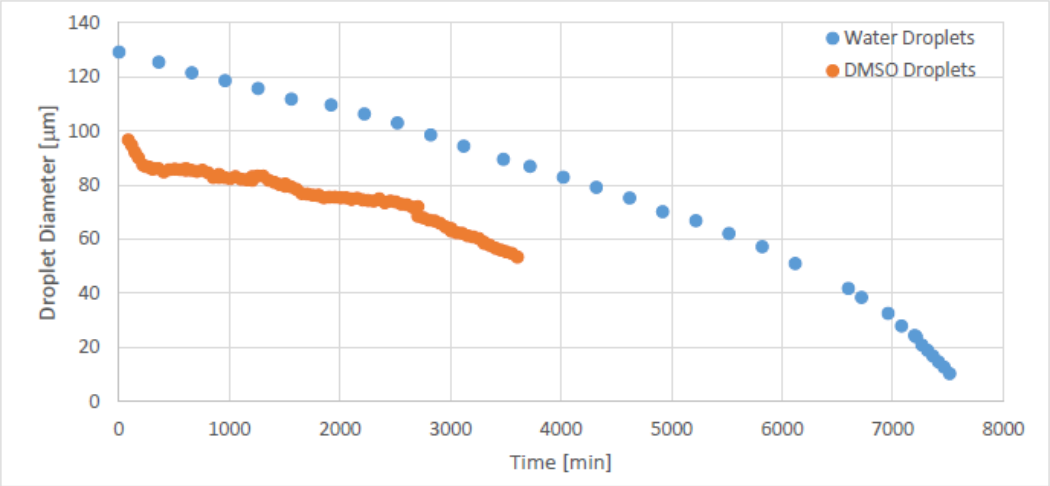

Figure 4.14 DMSO and pure water droplet sizes with respect to time

Another stationary droplet shrinking experiment was performed with glycerol using several molarities and pure water. As seen in Figure 4.15, all 1M, 3M and 5M glycerol droplets stop shrinking after a certain point. This is due to the removal of all water content from droplet and the negligible solubility of glycerol inside soybean oil. Theoretically, after all water leaves the droplet, the remaining sphere is expected to involve only glycerol. From the graph, after shrinking has stopped, final average diameters of 1M, 3M and 5M glycerol droplets are 49.41µm, 72.30 µm and 85.31 µm, respectively. Given that all initial droplet diameters are known, total number of moles of glycerol inside each droplet can be calculated. Removal of water ensures that volume occupied in the spherical droplet 100% belongs to glycerol, therefore the molarity of pure glycerol droplet with the calculated amount of moles of molecules yield theoretical volume and diameter. In Table 4.1, it is shown that theoretical and experimental final diameters are very close. Therefore, glycerol is an ideal CPA to form an aqueous droplet at any molarity, ensuring its solubility in soybean oil is practically zero.

Table 4.1 Shrinking data of droplets with three different molarities

Molarity [mol/L]		5	3	1
Inıtial Diameter [µm]		121.99	124.19	121.02
Final Diameter [µm]	Theoretical	87.19	74.87	50.29
	Experimental	85.31	72.30	49.41

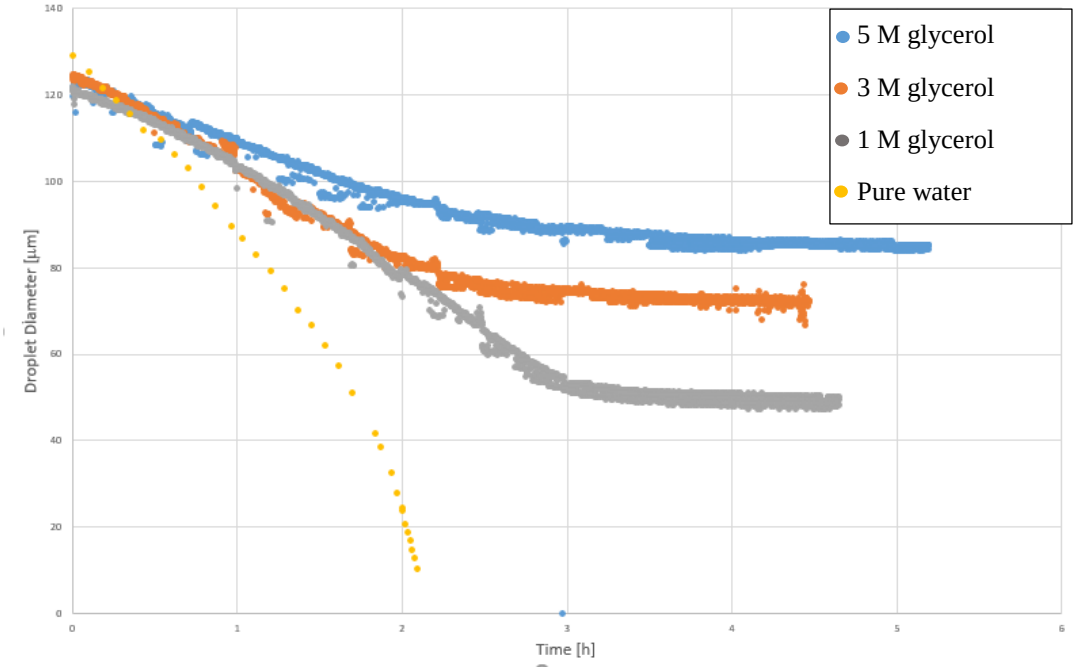

Figure 4.15 Droplet sizes for three different glycerol molarities and pure water

4.2 Droplet Shrinkage in Serpentine Device

Droplet shrinking experiments are based on a study performed by Prof. Dr. Mehmet Toner and his students [14] and its implementation to the microfluidic devices [25] [40]. In a mixture containing two immiscible liquids, it is possible to form emulsions. It is possible to form aqueous droplets by vigorous mixing in a test tube. However,

droplets formed in this way would be polydispersed and not controllable in terms of their sizes. Droplet generator microchannels provide monodispersity and observability under microscope. In the experimental setup, by partial heating of microfluidic device, it is possible to increase temperature of the droplets so that the solubility of water in soybean oil increases, leading to the shrinkage of the droplet. Droplet shrinkage experiments performed at 25°C since it is easier to maintain the temperature at laboratory conditions. Generated droplets were heated to 40°C, which is a reasonable temperature to create a temperature gradient with the initial conditions. So, it is possible to observe the shrinking effect better with higher temperate gradient. However, since the main purpose is to encapsulate cells in droplets (which will be discussed in the next chapter), 40°C does not cause lethal damage to the cells during experiments and increasing the temperature further is dangerous for a living sample.

Figure 4.16 illustrates the results of three microfluidic experiments with different flow rates and the amount of shrinkage in droplets. Droplet sizes obtained at different flow rates was not exactly same but very close to the simulation results [25]. Highest flow rate in the experiment (2333 µm/s) resulted in the most steep decline in droplet radius, as curve fit equations also shows. Gray curve (2333 µm/s) curve fit parameters are $0.0027x^2$ and -0.2122x, while blue curve (1986 µm/s) fit parameters are $0.0008x^2$ and -0.115x, meaning a slower decrease in the droplet size. The no-flow condition, on the other hand, shows the slowest rate of mass transfer to the soybean oil. This experiment, alongside with the simulation [25] agrees with the fact that continuous flow in microchannel enhances the solubility of water into soybean oil greatly, offering an efficient way to manipulate CPA concentration inside the droplets.

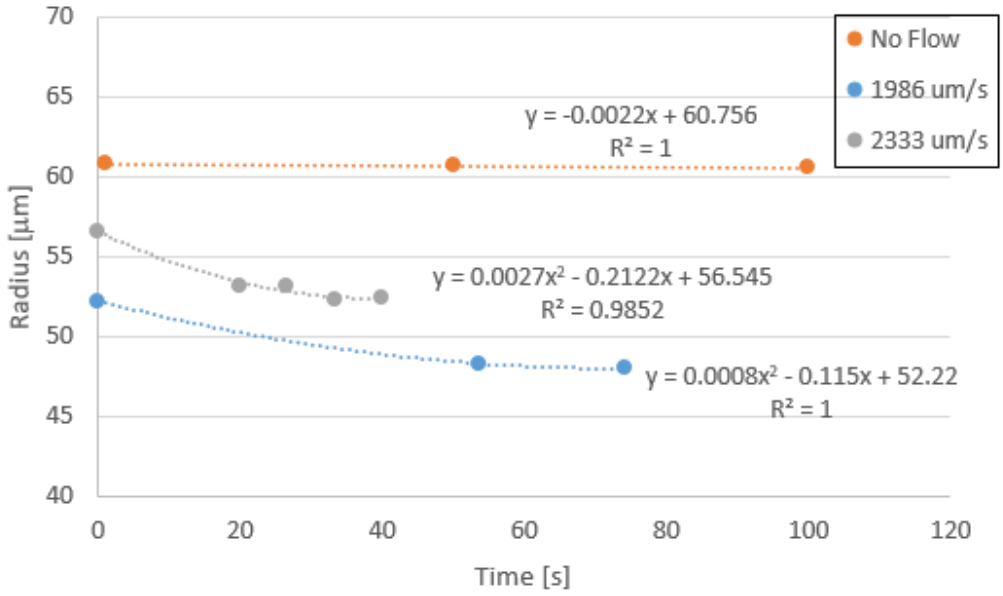

Figure 4.16 Experimental shrinking sdroplet radii at various flow rates

4.2.1 Droplet Shrinkage in 25 µm-Device

25µ-device is the smallest serpentine channel device that were used in the experiments, therefore smallest possible droplets were obtained in this device. Figure 4.17 shows the droplet before and after the heating and shrinking. Using the image processing script, many droplets were detected and plotted as a histogram in Figure 4.18.

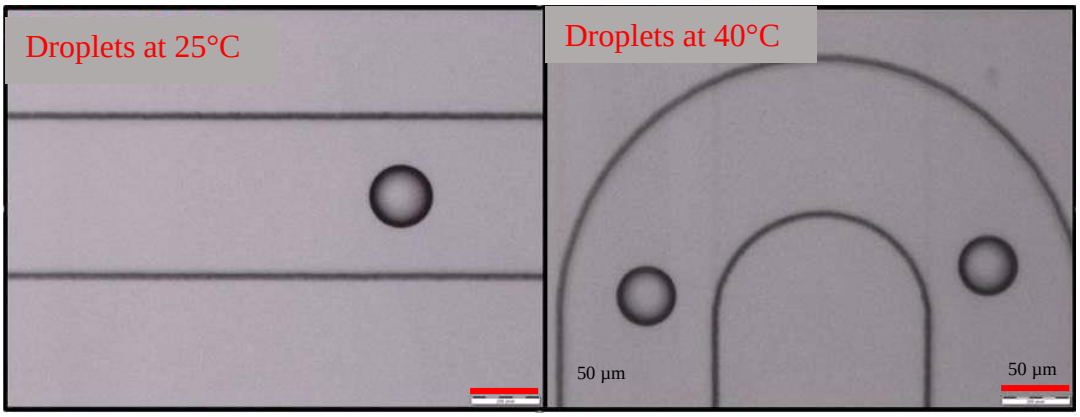

Figure 4.17 Droplets traveling at different regions of the 25 µm device and shrinking

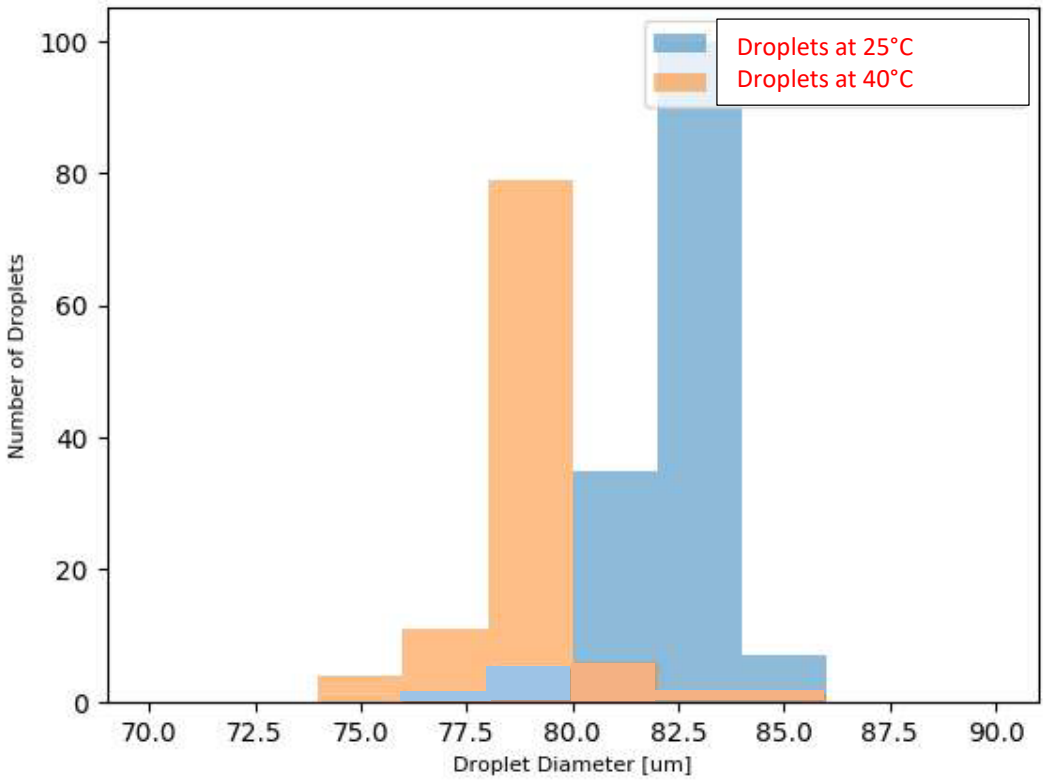

Figure 4.18 Histograms showing the droplet sizes at cold and hot regions

4.2.2 Droplet Shrinkage in 50µm-Device

50µm-device is the intermediate size amongst the three types. Right after the junction, channel width expands to 100 µm. It is followed by the Y-shaped junction where auxiliary oil flow channel joins and channel width becomes 200 µm for the rest of the device. Images of droplets shown in Figure 4.19 is taken from that portion of the channel with 10x magnification (left-side droplet is located before the entrance of serpentine region and right-side droplet is at the serpentine region). Figure 4.20 shows the shrinking droplets with a smaller magnification (4x). Although seeing more droplets at once is possible with 4x camera, the shrinking effect is harder to see with bare eyes and measurement of the droplet size is also limited with the number of pixels. Therefore, most droplet size measurements were performed with 10x and 20x lenses.

Figure 4.21 shows the locations of the droplet size measurements and the respective histograms from the results.

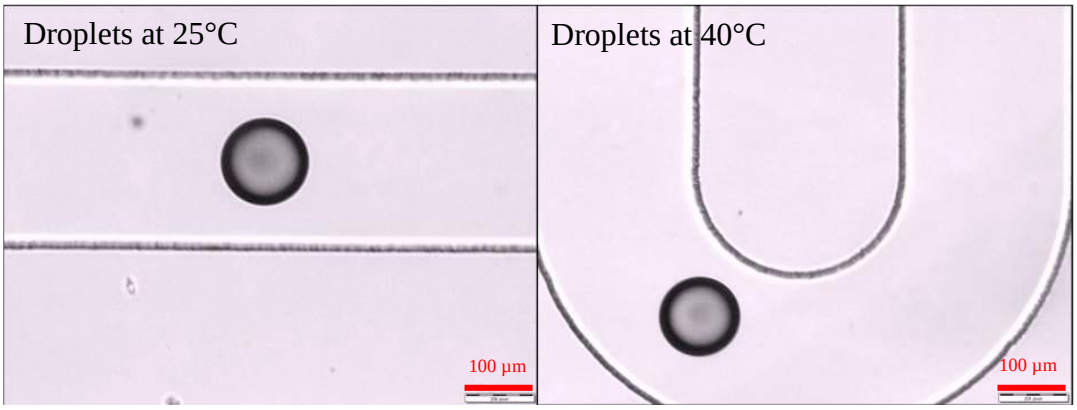

Figure 4.19 Droplets traveling at different regions of the 50 µm device and shrinking recorded with 10x lens

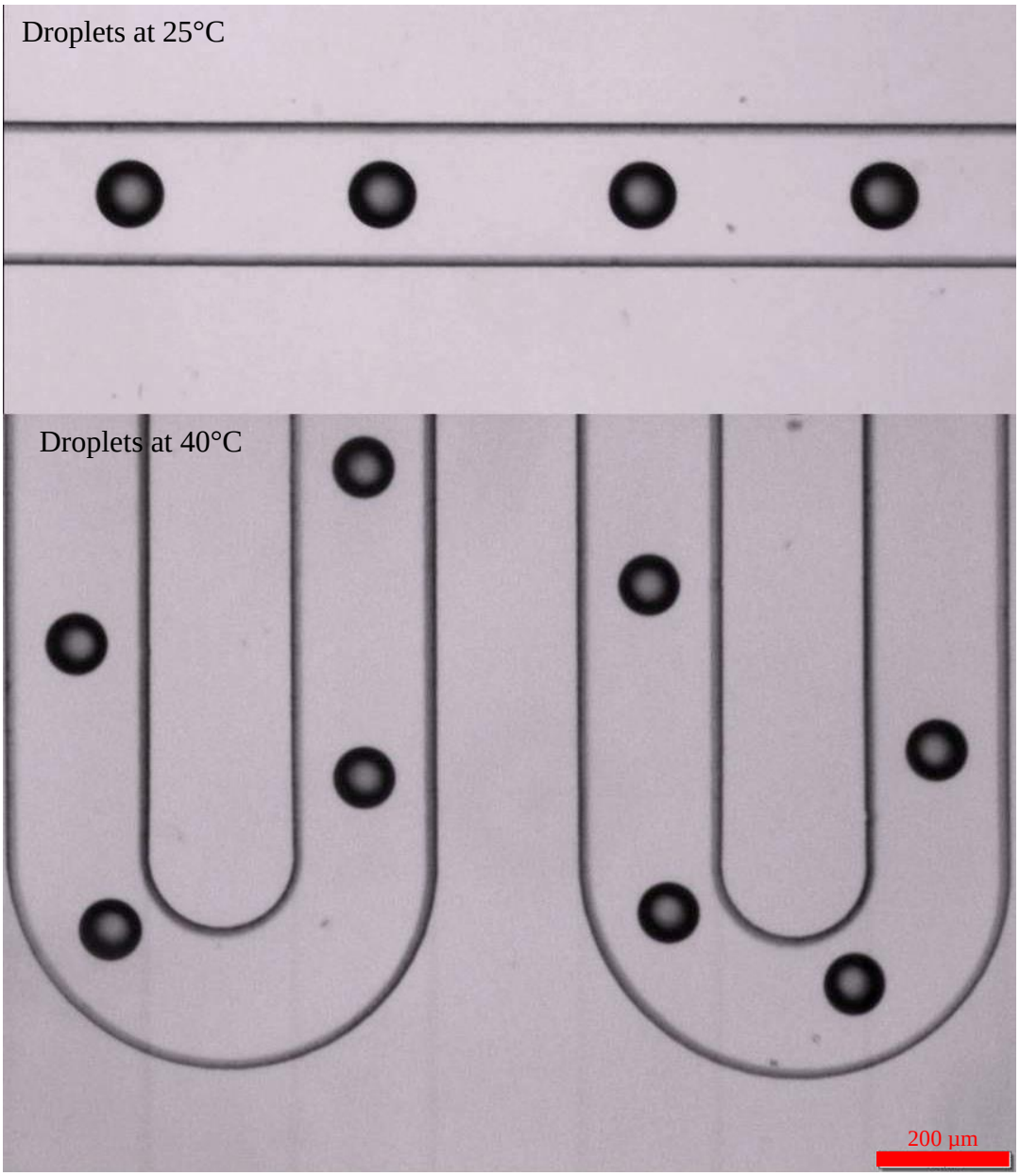

Figure 4.20 Droplets traveling at different regions of the 50 µm device and shrinking recorded with 4x lens

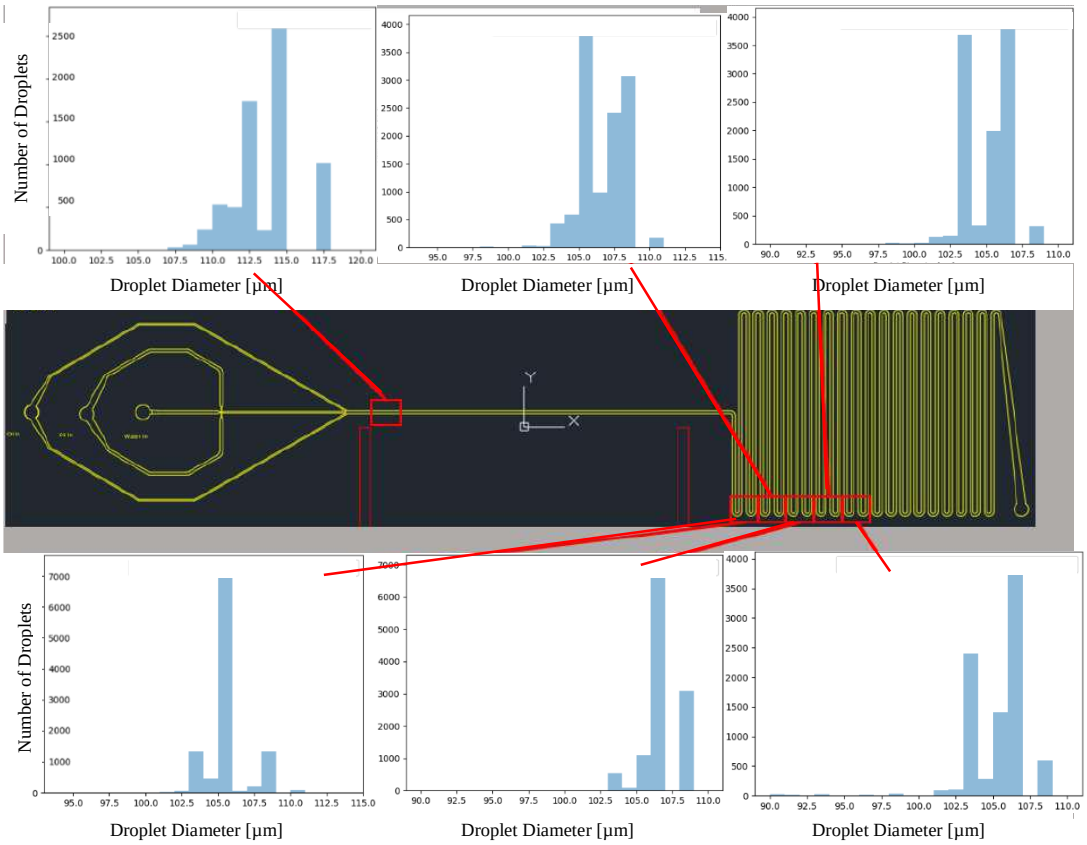

Figure 4.21 Locations of the measurements from 50 µm device and histograms of droplet sizes

Table 4.2 Droplet diameter and volume change across the 50 µm-device

	Junction Region	1st&2nd Serpentine	3rd&4th Serp.	5th&6th Serp.	7th&8th Serp.	9th&10th Serp.
⌀ [µm]	113.1±4.5	105.1±2.5	106.3±2.6	106.3±2.6	104.6±4.0	104.8±3.9
V [pL]	758.11	608.4	629.9	628.57	599.40	601.98
ΔV [%]	0	-19.75	-16.90	-17.09	-20.93	-20.59

4.2.3 Droplet Shrinkage in 100 µm-Device

100 µm-device is the largest channel device amongst the three type. Right after the junction, channel width expands to 200 µm. Droplet at left-side image in Figure 4.22 belongs to that portion of the channel. It is followed by the Y-shaped junction where auxiliary oil flow channel joins and channel width becomes 400 µm for the rest of the device, where right-side image is taken from that portion of the channel.

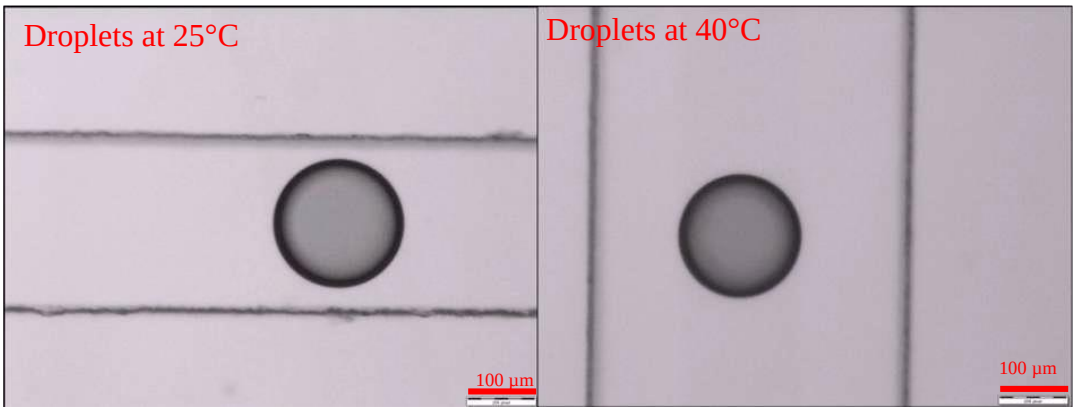

Figure 4.22 Droplets traveling at different regions of the 100 µm device and shrinking

Figure 4.23 shows the histograms taken from droplet size detection script with their respective locations shown on the device schematic. It was possible to detect shrinkages as large as 20% volume decrease around 6th serpentine (Table 4.3), however the numbers are not exactly identical due to the fluctuations in the flow during a long experiment caused by major and minor losses across the long serpentine channel.

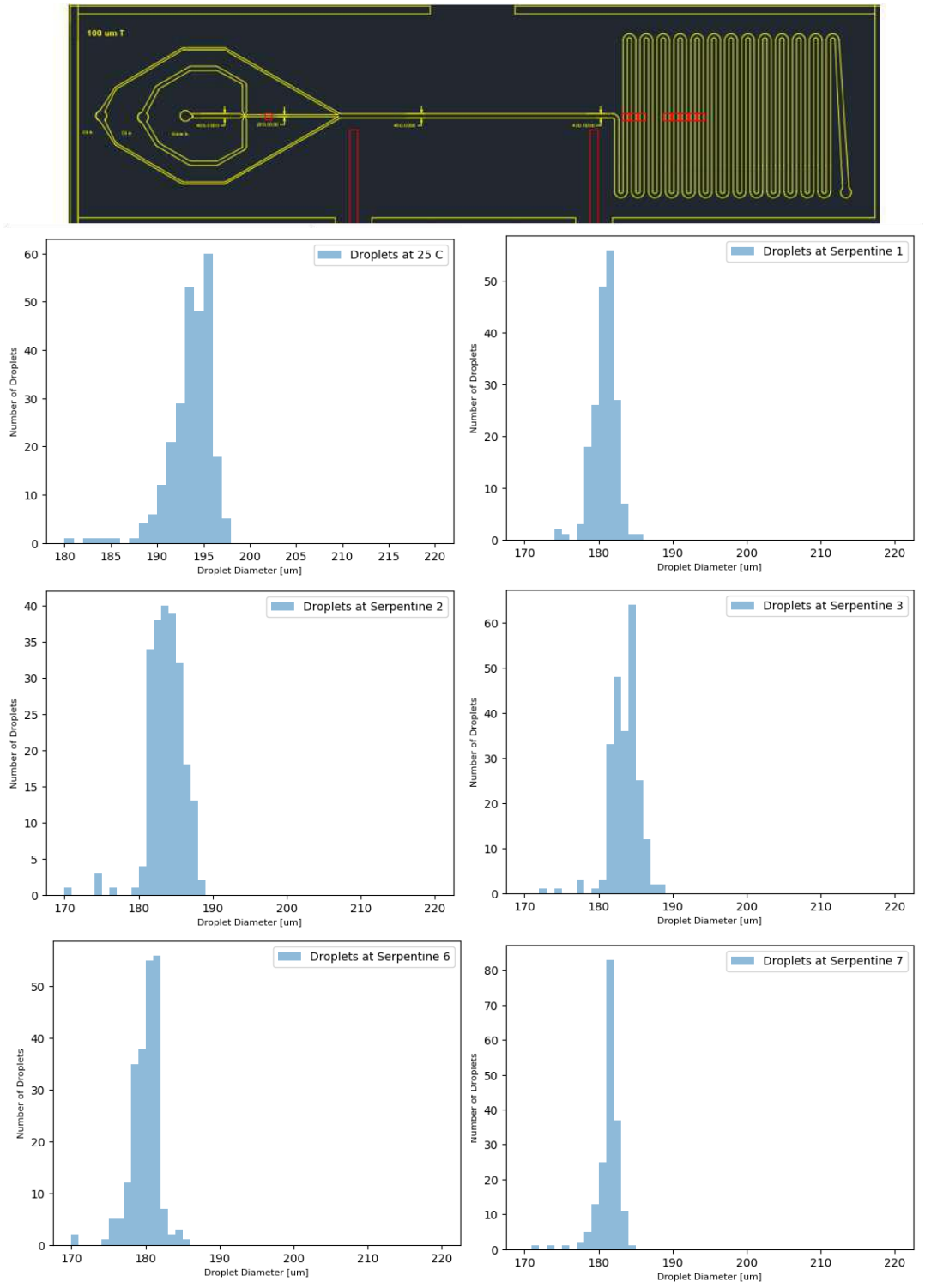

Figure 4.23 Locations of the measurements from 100 µm device and histograms of droplet sizes

Table 4.3 Droplet diameter and volume change across the 100 µm-device

	Junction Region	1st Serp.	2nd Serp.	3rd Serp.	6th Serp.	7th Serp.
⌀ [µm]	193.6±3.9	180.6±4.0	183.8±4.2	183.6±2.4	179.8±4.2	181.3±2.7
V [pL]	3799.4	3086.8	3250.1	3238.9	3044.0	3120.8
ΔV [%]	0	-18.7	-14.5	-14.7	-19.9	-17.9

Droplet generation and shrinkage in different sized microfluidic devices are performed. It is found that increased flow rates help to generate smaller droplets, but channel junction width also affects the size of droplets. It is possible to generate smaller droplets in devices with smaller junctions. In droplet shrinkage experiments, it is shown that microfluidic device is capable of shrinking droplets at 20% volume. Shrinkage of aqueous CPA loaded droplets showed that DMSO, which is a common cryoprotectant used in various studies is not suitable in microfluidic experiments due to its solubility in soybean oil, which makes the concentration uncontrollable. Convection effects are shown to have greater effect in solubility of water in soybean oil as flow rate increases. Compared to no flow conditions, shrinkage of traveling droplets occur faster. It can be also seen in the shrinkage results of serpentine devices that, upon heating volume loss occurs at the early stages of serpentine devices and the diffusion along the serpentine contribute practically no shrinking measureable compared to the initial effect.

4.3 Cell Encapsulation Performance of the Microfluidic Device

Cell encapsulation in microfluidic devices are performed to determine the best conditions for good encapsulation performance based on flow rate, considering the cell sedimentation and multiple cell encapsulation. A conclusion is sought to understand what flow rates are best to encapsulate cells in droplets, so that CPA concentration during droplet shrinkage can be controlled.

In the experiments performed with Jurkat cells, the encapsulation performance of microfluidic devices were assessed. In dispersed phases, cells are moving towards the junction and at the vicinity of the junction, they are forced to move into the droplet thanks to the viscous shear of continuous phase acting on cell solution. Figure 4.25 illustrates the encapsulation process from various timestamps. Table 4.4 and Figure 4.24 represents the number of cells in droplets. Both dispersed and continuous phase flow rates are increased together, by keeping 20:1 ratio contant. In the flow focusing device, continuous phase merges with dispersed phase by joining form two sides, therefore two oil flow rates are written separately, i.e. for the 3/3/0.3 µL/min case, total oil flow rate is 6.0 µL/min and water flow rate is 0.3 µL/min. At higher flow rates, generated droplets are smaller as explained in previous chapters. Also, number of droplets generated in the same time interval is higher, meaning that the droplet generation frequency is high. This tends to have more empty droplets, since oil flow rate is increased from 6.0 µL/min to 18.0 µL/min, where the difference is 6.0 µL/min. However, dispersed phase is increased from 0.3 µL/min to 0.9 µL/min, where the difference is 0.6 µL/min. Considering the volume occupied by the phases inside channels, increase in the dispersed phase is not dominant compared to continuous phase. Since the cells are carried by the dispersed phase, the small amount of increase does not cause cells to arrive at the droplet generation junction as fast as the oil phase. More empty droplets are observed in higher flow rates as shown in Figure 4.24 and Table 4.4, while having less multiple cell encapsulation

cases. Since the CPA concentration in droplets is aimed to control for its transport across cell membrane, the cases where the most single cell encapsulation obtained is more suitable for a better controlled environment. Also, since higher flow rates are associated with better convection effect and shrinkage of droplets in previous chapter, the encapsulation performance at higher flow rates are favored. Figure 4.24 shows a behavior like Poisson distribution as in similar studies [32]. Poisson distribution can be calculated as

$$f(x) = \frac{\mu^x e^{-\mu}}{x!} \tag{10}$$

Where μ is the mean value of occurrences within an interval, (where experimentally 0.1 cells per droplet can be seen) and x is the occurrences (number of cells encapsulated).

Table 4.4 Number of encapsulated cells in droplets at various flow rates

Q_o [µL/min]		Q_w [µL/min]	Droplet Size [µm]	Cells per droplet [%]				
				0	1	2	3	4+
3.00	3.00	0.30	108.7	80.9	17.1	1.96	0.25	0.08
4.50	4.50	0.45	99.2	91.8	7.78	0.40	0.02	0.02
9.00	9.00	0.90	78.6	93.6	6.21	0.17	0.00	0.00

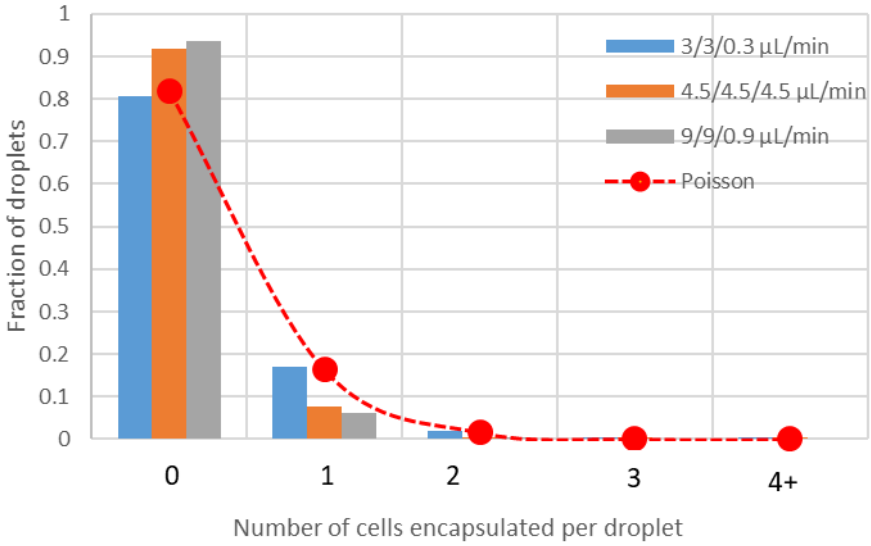

Figure 4.24 Number of encapsulated cells per droplet at flow rates 3/3/0.3 µL/min (blue), 4.5/4.5/0.45 µL/min (orange), 9/9/0.9 µL/min (gray)

Another set of experiments was performed with L929 cells and their encapsulation efficiency in serpentine device. A series of flow rates are used to generate droplets using cell solution, and it was observed that at low flow rates of dispersed phase, cells are more likely to settle down to the bottom of microchannels instead of flowing in suspension. Up to step 5, flow rate of dispersed phase is reduced in each step while keeping other flow rates constant, as in Figure 4.26. After step 5, main oil phase flow rate is increased from 5µL/min to 6µL/min and dispersed phase is increased in each step until step 9, as in Figure 4.27. Step numbers are written at the left top corner of each image with red color and flow rates are given in Table 4.5.

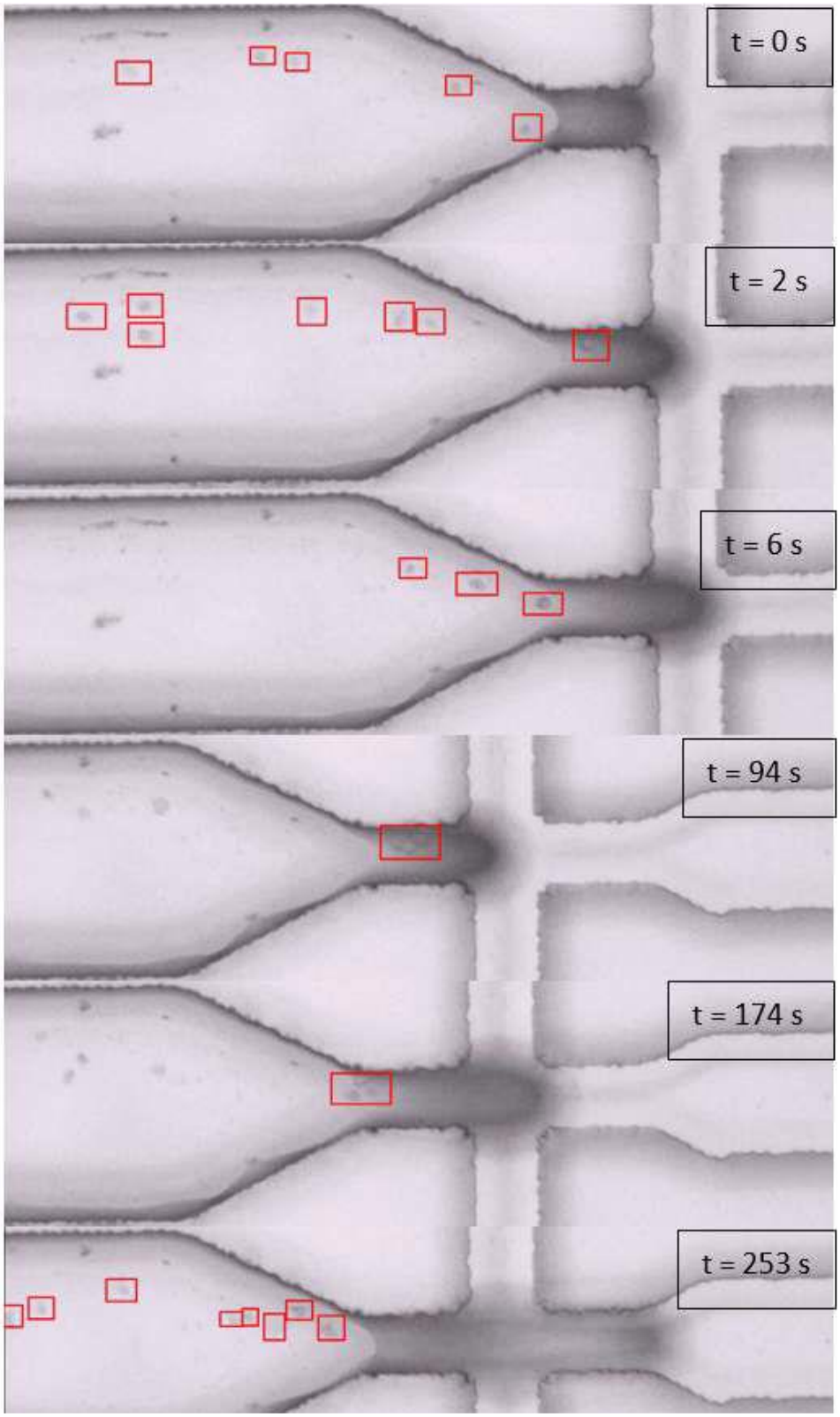

Figure 4.25 Cells traveling inside the dispersed phase just before encapsulation

Table 4.5 Flow rates used in each step

Step	Auxiliary Q_o [µL/min]	Main Q_o [µL/min]	Q_w [µL/min]
1	2	5	2
2	2	5	1.5
3	2	5	1
4	2	5	0.5
5	2	5	0.25
6	2	6	0.3
7	2	6	0.6
8	2	6	1.2
9	2	6	2.4

Dispersed phase flow rates slower than 0.5µL/min shows that a reliable flow to sustain cell movement into encapsulation is difficult. Even though the aqueous cell solution moves with relatively low flow rate, it is not enough to prevent cells sedimentation at the inlet region. Surprisingly, flow rate increase between steps 6-9 recovers the sedimentation problem and cells start to get carried by increased dispersed phase flow rate. Since lowering the flow rate does not permanently clog the device, this set of experiment might be used as a way to find the optimal flow rate for every cell types being used in cell encapsulation in a similar study.

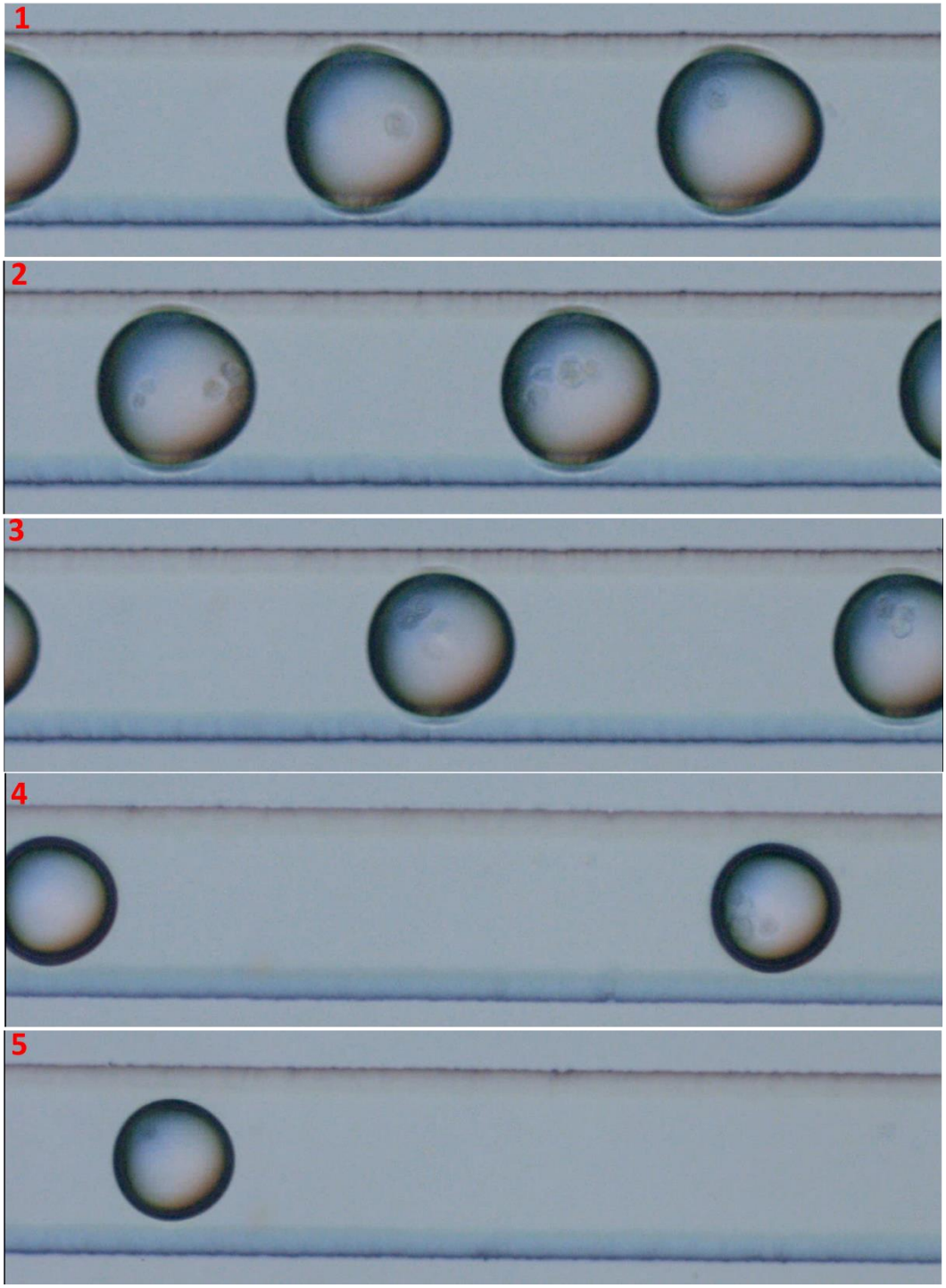

Figure 4.26 Encapsulation during decreased dispersed phase flow rates (steps 1-5)

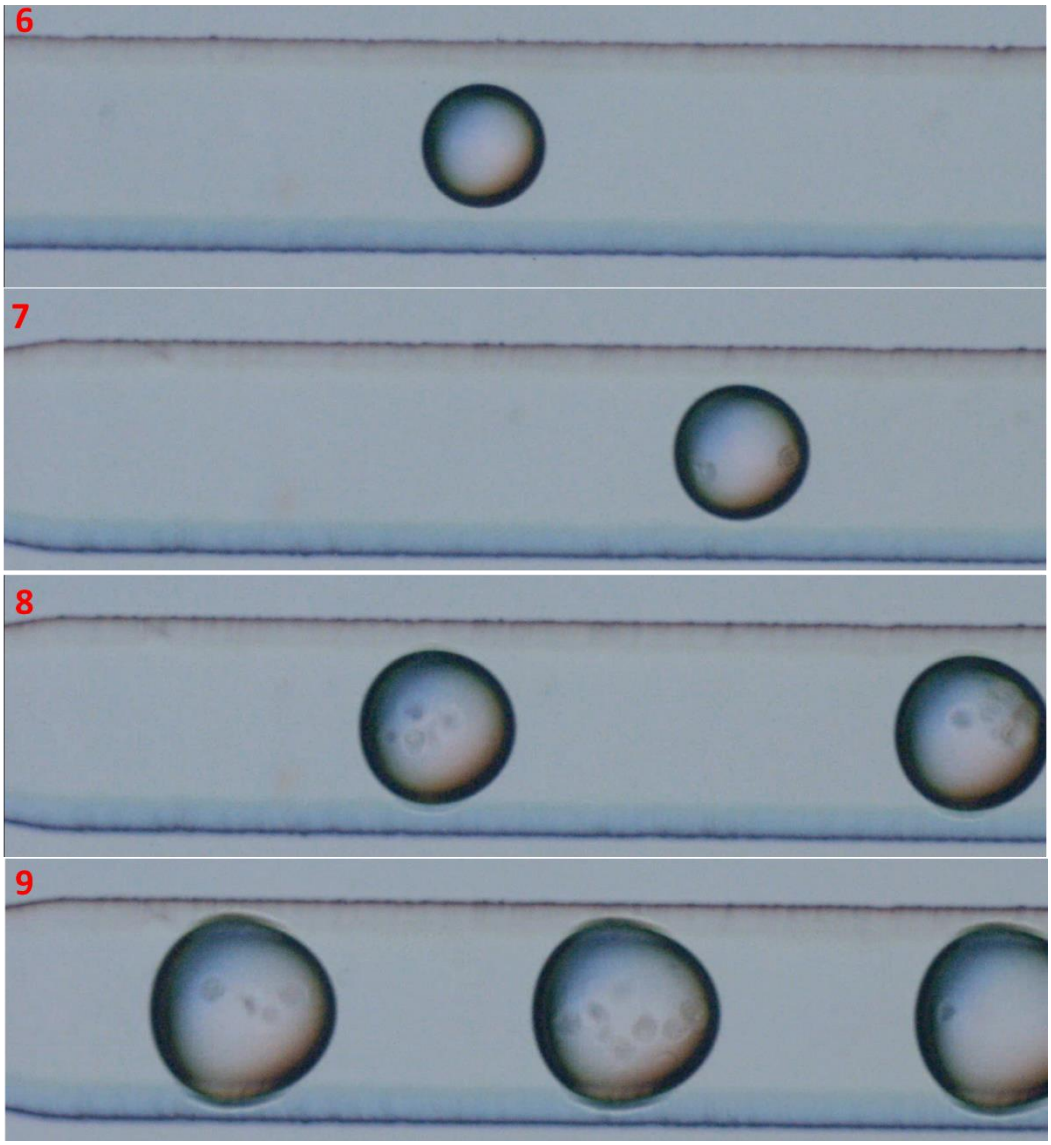

Figure 4.27 Encapsulation during increased dispersed phase flow rates (steps 6-9)

Cell encapsulation is the final step of experiments which are aimed to be done for preconcentrating cells with CPAs using microfluidic device is a continuous manner. All necessary information is obtained to form monodispersed droplets ensuring that cells are not exposed to sedimentation and mostly single cells are encapsulated in droplets. In the next chapter, proposed microfluidic model is explained with the improvements and adaptation to microfluidic environment over the current models. Experiments are performed to obtain shrinkage rates of aqueous droplets with different CPA solutions to be used in the microfluidic model. Representing the dynamic extracellular concentration with experimental shrinkage data cannot be explained with current models.

4.4 Cell Membrane Permeability in Microdroplet Environment

In this chapter, the novel microfluidic model is proposed and the results are presented using the permeability model solver along with two-parameter model and Kedem-Katchalsky model. All models can be used for solution of cell response to a CPA exposure. For microfluidic model only, shrinkage rates of aqueous droplets for three different CPA molecules, glycerol, ethylene glycol and propylene glycol are used as input to represent the dynamic extracellular CPA concentration, as opposed to constant concentrations used in conventional methods. Cell volume change inside a shrinking droplet is observed and the response is correlated to the microfluidic model to obtain membrane permeability parameters.

4.4.1 CPA Concentration in Continuous Media

Purpose of the droplet shrinking and cell encapsulation experiments is to achieve a novel method for CPA loading into cells prior to cryopreservation. Generating aqueous droplets with a certain amount of CPA concentration allows a controllable and confined extracellular environment for encapsulated cells.

MDA-MB231 cell solution was used to perform glycerol loading inside microchannel. 0.159 mL of glycerol was added to cell solution of 2mL in order to obtain 1M glycerol concentration prior to droplet generation. Then, cells were encapsulated in 50µm-device and heated to 40°C in serpentine region in order to expose them to increased concentration of CPA. Figure 4.28 has snapshots taken every 15 seconds from an encapsulated cell in an aqueous droplet with 1M glycerol is used. Figure 4.28 shows glycerol loaded aqueous droplets where the droplet size and cell volume was measured to obtain experimental data points. Images were taken from a recorded video and cell sizes were measured using ImageJ software as surface area, similar to the study performed by Shu [39], shown in Figure 2.4.

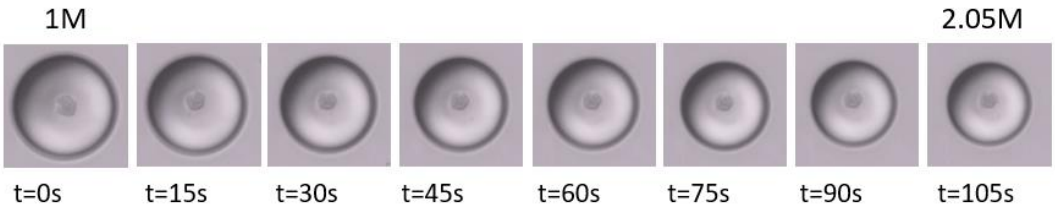

Figure 4.28 MDA-MB231 cells encapsulated in aqueous glycerol droplets with increasing concentration

Figure 4.29 shows the cell volume and diameter calculation from the surface area of pixels representing the cell. In both Shu's work and this experiment, cells were assumed to be spherical and conversion from surface to volume and diameter was performed.

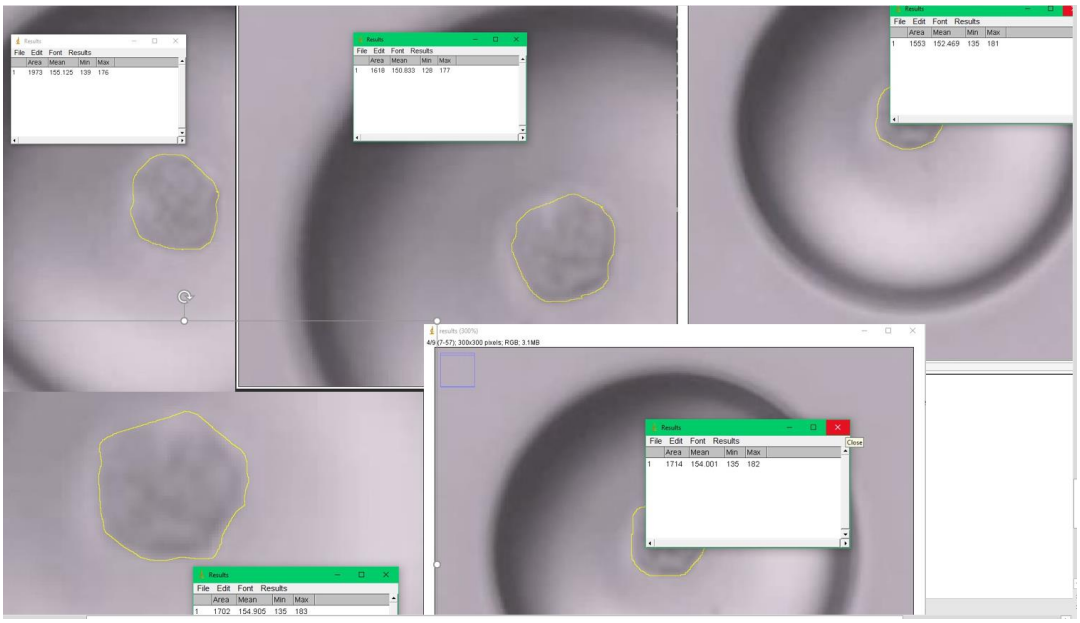

Figure 4.29 Cell size measurement from surface areas in several frames

Glycerol concentration can be calculated and it increased from 1 M to 2.05 M. Eventually, droplets were heavily distorted and lost spherical shape, probably due to some excessive water loss and possible gelations in the content of cell culture at relatively high temperature (40°C) than normal storage conditions of cell culture. Therefore, further images were omitted since a proper measurement were not possbile on them.

The shrinkage rates of glycerol, ethylene glycol and propylene glycol were calculated as volume loss as in Table 4.6.

Table 4.6 Experimental shrinking rates of aqueous droplets in a heated channel

Aqueous Droplets	Shrinking Rate [µm3/s]
1M Glycerol	47.92
1M Ethylene Glycol	169.45
1M Propylene Glycol	7.1

4.4.2 Microfluidic Model for the Cell Membrane Permeability

A new model for cell membrane permeability is proposed here to adjust the membrane permeability behavior to microfluidics environment, where the extracellular concentration is also dynamically changing unlike that in conventional CPA loading procedures, or presented in 2-parameter and Kedem-Katchalsky models. Inside a droplet, which is shrinking due to the water removal upon heating, CPA concentration can be defined as a function of time rather than a constant value, which is more precise given the conditions in microfluidic channels. In the experiments, it is possible to measure the shrinking droplet radius as a function of time, *r(t).* Providing that droplet maintains its spherical shape in a continuous flow, volume of the droplet can be calculated as

$$V(t) = \frac{4}{3}\pi\, r(t)^3 \tag{11}$$

Preparation of solutions prior to experiment ensures that an initial CPA concentration is maintained unless temperature is increased, since the water solubility does not increase and lead to the shrinkage of droplet. Therefore, initial concentration of CPA in droplet also the initial extracellular CPA concentration for an encapsulated cell, which is $C_c^e(0) = C_o$. Total number of CPA molecules in droplet can be found by multiplying initial concentration by the initial droplet volume as

$$N = V_0 C_0 \tag{12}$$

Shrinking rates (δV) for glycerol, ethylene glycol and propylene glycol in aqueous droplets were found experimentally and presented in Table 4.6. So, at any time, starting from *t=0,* concentration of these CPA molecules inside the droplet can be calculated as

$$C(t) = C_c^e(t) = \frac{N}{V_0 - \delta V t} \tag{13}$$

Equation 12 is then used in the microfluidic model as the dynamic extracellular concentration, as follows

$$\frac{dV_c}{dt} = -Lp\ A\ R\ T\left[\left(C_s^e - C_s^i\right) + \sigma\left(C_c^e(t) - C_c^i(t)\right)\right] \quad (14)$$

$$\frac{dN_c}{dt} = P_s A\left(C_c^e(t) - C_c^i(t)\right) + \frac{(1-\sigma)}{2}\frac{dV}{dt}\left(C_c^e(t) + C_c^i(t)\right) \quad (15)$$

Addition of reflection coefficient σ coupled two differential equations by describing solute-solvent interaction during membrane transport [21]. In this microfluidic model, equations involved another parameter requiring the information of current size of droplet diameter and the current CPA concentration, which makes the system continuously increase the CPA concentration upon heating and the shrinkage of droplet, while representing the physical phenomena in the differential equations.

Figure 4.30 compares the different scenarios where human embryonic stem cells are encapsulated in aqueous droplets with 1M glycerol and having diameters of 100µm, 50µm and 35µm, respectively. When the droplet size was 100µm, even though the shrinking rate is constant, increase in concentration is similar to the concentration trend of two-parameter and Kedem-Katchalsky models. As the initial droplet size with 1M initial glycerol concentration is adjusted to 50µm and 35µm, the shrinking effect becomes more dominant and it is possible to reach higher concentration levels without sudden increase occurred.

Figure 4.31 demonstrates a curve fitting using the microfluidic model with calculated shrinking rate of glycerol droplet at 40°C with encapsulated MDA-MB231 cells. Experimental data set do not involve too many data points, however it is enough to observe the volume change trend. Membrane permeability parameters of MDA-MB231 cells are unknown, therefore the model here is demonstrated to find out the L_p, P_s, σ and V_b. Table 4.7 summarizes the approximate values which are close enough to fit the theoretical curve to the experimental curve. These curves are specific to the type of cell, the CPA used and the ambient temperature, therefore for each changing parameter, membrane permeability parameters should be calculated separately.

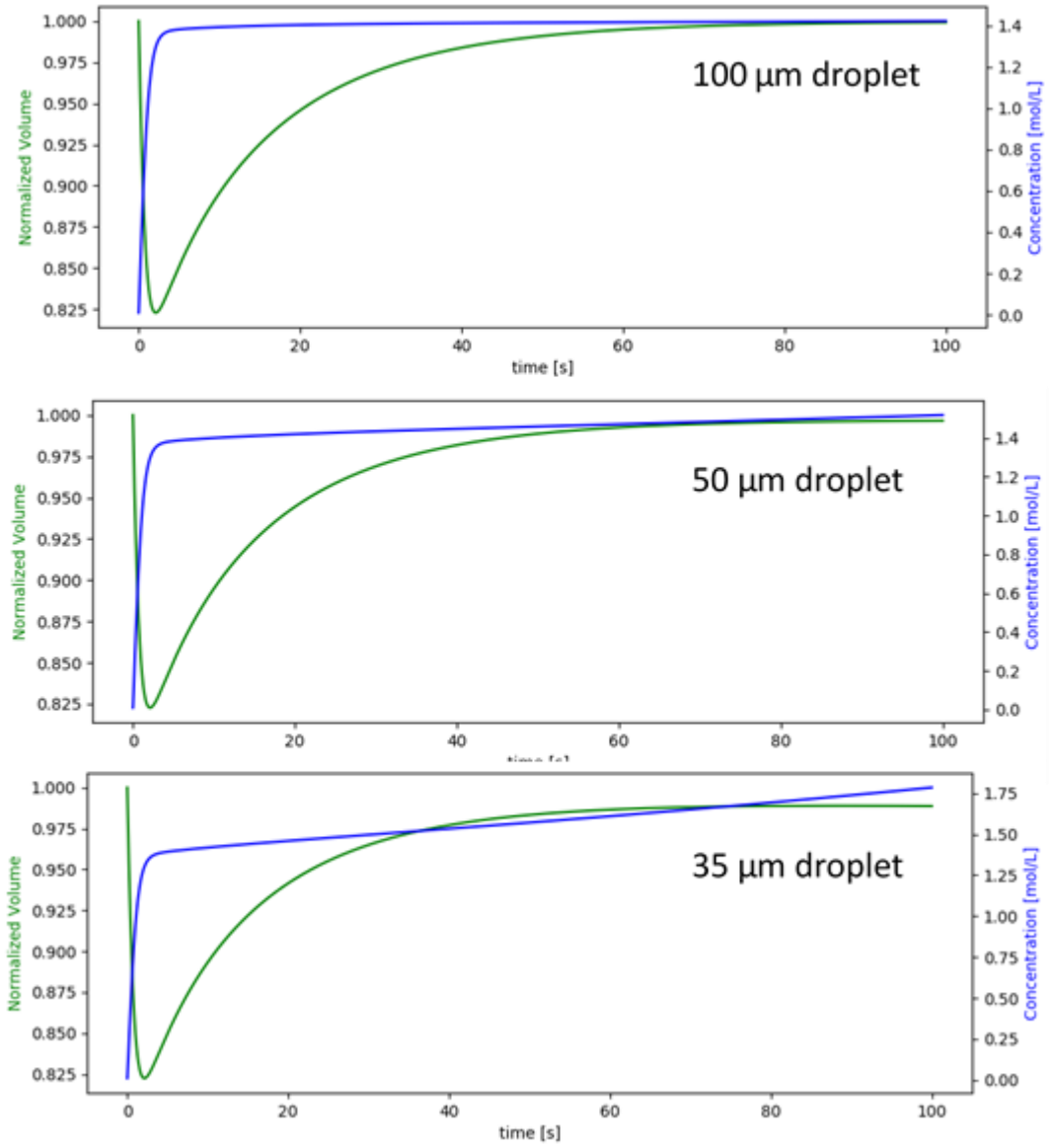

Figure 4.30 Volume change and CPA concentration plots of proposed model with human embriyonic stem cells encapsulated in droplets with diameter of 100µm (top), 50µm (middle) and 35µm (bottom)

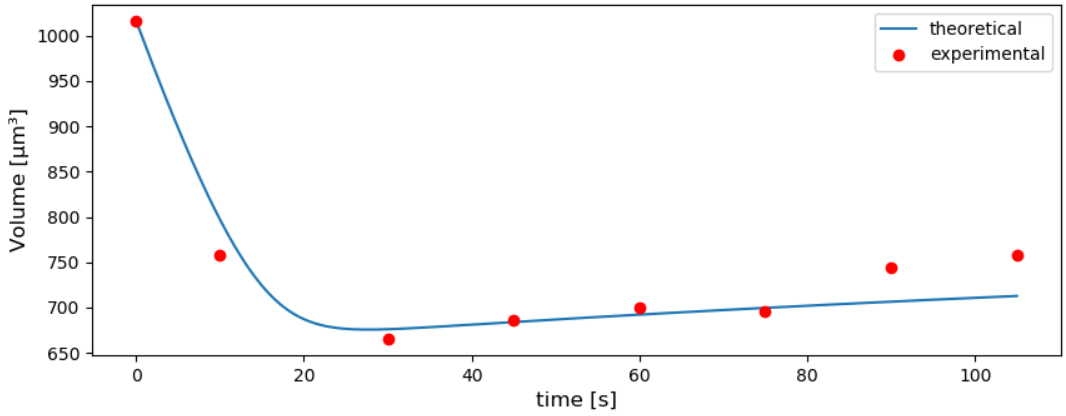

Figure 4.31 Comparison of experimental and theoretical cell volume response to glycerol exposure

Table 4.7 Estimated cell membrane permeability parameters of MDA-MB231 cells at 40°C with 1M glycerol

L_p [µm/atm/min]	0.15
P_s [cm/min]	0.00005
σ [-]	0.79
V_b [-]	0.55

CHAPTER 5

CONCLUSION

In this study, microfluidic devices were used in a series of experiments systematically. First, empty aqueous droplets were generated at various flow rates to determine the limits of sizes of droplets obtainable in each device. Basic X-channel devices were employed for preliminary droplet generation and cell encapsulation experiments to understand the conditions that should be considered, such as required droplet sizes and number of cells encapsulated in each droplet based on flow rate. Droplet generation behavior of microchannels show that, increased flow rates allow to generate smaller droplets. Providing a droplet size plot for various flow rates, one can generate monodispersed droplets of desired diameter knowing the flow rate required, i.e., 10μL/min oil and 0.5μL/min water flow rate is needed to generate 90μm droplet in 25μm X-junction device. Cell encapsulation experiments in basic X-channel devices showed that at lower oil and water flow rates, it is more likely to encapsulate multiple cells inside a droplet compared to higher flow rates. Howevre, higher flow rates are more likely to generate empty droplets, meaning that no cells are encapsulated.

Following experiments required the information of shrinking rates of aqueous droplets which contain CPAs, such as glycerol, ethylene glycol and propylene glycol. Therefore, serpentine device with ITO heater and thermocouples were used to maintain 25°C at droplet generation site and increase the temperature to 40°C at serpentine region to start droplet shrinkage. Experimental results agreed with the simulations that increased flow rates enhances droplet shrinking rate by promoting convective effects. Serpentine devices were able to provide 20% volume shrinkage in water droplets and the volume loss is observed at the early stages of serpentine region, showing that the convective effects are dominant upon the temperature

increase and increased solubility of water in soybean oil at elevated temperature forces water loss so quickly that a further volume loss throughout the serpentine is not recorded in a decreasing trend. Serpentine device after the volume loss in early stages provide a certain residence time based on flow rate for the cell membrane permeability experiments.

It is aimed to encapsulate mammalian cells in aqueous droplets and control the CPA concentration inside droplets using a novel heating method for droplets traveling in serpentine type microchannels. Encapsulated cells are loaded with permeable CPA molecules inside droplets. To achieve this, cell encapsulation performance of serpentine devices are assessed using the knowledge to obtain more single cell encapsulation in higher flow rates. In serpentine devices, dispersed phase flow rates slower than 0.5µL/min is not practically useful due to sedimentation. At higher flow rates, such as 2µL/min, cell solution provide better stream and encapsulation. Higher flow rates associated with the high cell encapsulation performance is favored due to ability to reach higher concentrations without harming the cells. It is possible to eliminate long CPA exposure to cells by continuous loading of CPA (within minutes) compared to step-wise loading in conventional methods (taking several hours). 1M glycerol concentration in droplets was increased to 2.05M due to droplet shrinkage within two minutes, which is a considerable improvement to the conventional preconcentration techniques.

Applying new microfluidic model to literature data showed that using smaller droplets, the confined effect becomes more dominant. Using a 100µm droplet 1.4M glycerol is loaded into hESC, while using a 35µm droplet it is possible to reach 1.75M in 100 seconds. Microfluidic model is used to estimate membrane permeability parameters of MDA-MB231 cells using experimental droplet shrinkage and concentration increase data. However, permeability parameters change with temperature and vary from cell to cell. Being easy-to-use and cheap to fabricate many replicates, microfluidic devices can expand the studies in membrane permeability research and cryopreservation.

Every different microfluidic device design can be tested to determine the best flow rates for the selected cell and culture medium to achieve a good encapsulation performance. Aqueous droplets having a certain amount of CPA concentration can be generated at a desired diameter, providing that the flow rates required are known. In transparent microfluidic devices, any sized droplet with a CPA content can be tracked, measured and recorded for their solubility or shrinking rates while the selective removal and diffusion of water into soybean oil increases the concentration of insoluble CPA molecules, which is a powerful driving force helping to penetrate into cell membrane. Considering conventional mathematical models on cell membrane permeability, the physical event involving all the continuous processes between droplet and cell can be explained with a new model which is adjusted to formulate the dynamic droplet environment better. The proposed new model can also spark new ideas off by representing the powerful microfluidics environment more precisely.

REFERENCES

1. Elmoazzen, H.Y., *Parameters Affecting Water Permeability Across Biological Cell Membranes*. 2000. p. 161.
2. Elliott, J.A.W., R.C. Prickett, H.Y. Elmoazzen, K.R. Porter, and L.E. Mcgann, *A Multisolute Osmotic Virial Equation for Solutions of Interest in Biology*. 2007: p. 1775-1785.
3. Shepherd, V.A., *The Cytomatrix as a Cooperative System of Macromolecular and Water Networks*, in *Current Topics in Developmental Biology*. 2006, Academic Press. p. 171-223.
4. Velikov, V., S. Borick, and C.A. Angell, *The glass transition of water, based on hyperquenching experiments.* Science, 2001. **294**(5550): p. 2335-8.
5. *Ciba Foundation Symposium - The Frozen Cell*. Novartis Foundation Symposia, ed. G. E. W. Wolstenholme and M. O'Connor. 1970.
6. Elliott, G.D., S. Wang, and B.J. Fuller, *Cryoprotectants: A review of the actions and applications of cryoprotective solutes that modulate cell recovery from ultra-low temperatures.* Cryobiology, 2017. **76**: p. 74-91.
7. Brüggeller, P. and E. Mayer, *Complete vitrification in pure liquid water and dilute aqueous solutions.* Nature, 1980. **288**(5791): p. 569-571.
8. Aksan, A. and M. Toner, *Roles of thermodynamic state and molecular mobility in biopreservation*, in *Tissue Engineering*. 2007, CRC Press. p. 169-188.
9. Costanzo, J.P., R.E. Lee, Jr., and M.F. Wright, *Glucose loading prevents freezing injury in rapidly cooled wood frogs.* Am J Physiol, 1991. **261**(6 Pt 2): p. R1549-53.
10. Nash, T., *The chemical constitution of compounds which protect erythrocytes against freezing damage.* J Gen Physiol, 1962. **46**: p. 167-75.
11. Ogura, A., J. Matsuda, T. Asano, O. Suzuki, and R. Yanagimachi, *Mouse oocytes injected with cryopreserved round spermatids can develop into normal offspring.* J Assist Reprod Genet, 1996. **13**(5): p. 431-4.
12. Mazur, P., K.W. Cole, J.W. Hall, P.D. Schreuders, and A.P. Mahowald, *Cryobiological preservation of Drosophila embryos.* Science, 1992. **258**(5090): p. 1932-5.
13. Youm, H.W., J.R. Lee, J. Lee, B.C. Jee, C.S. Suh, and S.H. Kim, *Optimal vitrification protocol for mouse ovarian tissue cryopreservation: effect of cryoprotective agents and in vitro culture on vitrified-warmed ovarian tissue survival.* Hum Reprod, 2014. **29**(4): p. 720-30.
14. Bajpayee, A., J.F. Edd, A. Chang, and M. Toner, *Concentration of glycerol in aqueous microdroplets by selective removal of water.* Anal Chem, 2010. **82**(4): p. 1288-91.
15. Thorsen, T., R.W. Roberts, F.H. Arnold, and S.R. Quake, *Dynamic Pattern Formation in a Vesicle-Generating Microfluidic Device.* Physical Review Letters, 2001. **86**: p. 4163-4166.

16. Utada, A.S., A. Fernandez-Nieves, H.A. Stone, and D.A. Weitz, *Dripping to Jetting Transitions in Coflowing Liquid Streams.* Physical Review Letters, 2007. **99**(9): p. 094502.
17. Anna, S.L., N. Bontoux, and H.A. Stone, *Formation of dispersions using "flow focusing" in microchannels.* Applied Physics Letters, 2003. **82**: p. 364-366.
18. Squires, T.M. and S.R. Quake, *Microfluidics: Fluid physics at the nanoliter scale.* Reviews of Modern Physics, 2005. **77**(3): p. 977-1026.
19. Young, S.S., S. Moon, L. Hulli, S.K. Hasan, E. Kayaalp, and U. Demirci, *Microfluidics for cryopreservation.* Lab on a Chip, 2009. **3**: p. 1874-1881.
20. Kamalakshakurup, G. and A.P. Lee, *High-efficiency single cell encapsulation and size selective capture of cells in picoliter droplets based on hydrodynamic micro-vortices.* Lab on a Chip, 2017. **17**: p. 4324-4333.
21. Kedem, O. and A. Katchalsky, *Thermodynamic analysis of the permeability of biological membranes to non-electrolytes.* Biochimica et Biophysica Acta, 1958. **27**(2): p. 229-246.
22. Folch, A., A. Ayon, O. Hurtado, M.A. Schmidt, and M. Toner, *Molding of Deep Polydimethylsiloxane Microstructures for Microfluidics and Biological Applications.* Journal of Biomechanical Engineering, 1999. **121**(1): p. 28-34.
23. Nie, Z., M. Seo, S. Xu, P.C. Lewis, M. Mok, E. Kumacheva, G.M. Whitesides, P. Garstecki, and H.A. Stone, *Emulsification in a microfluidic flow-focusing device: effect of the viscosities of the liquids.* Microfluidics and Nanofluidics, 2008. **5**(5): p. 585-594.
24. Basu, A.S., *Droplet morphometry and velocimetry (DMV): a video processing software for time-resolved, label-free tracking of droplet parameters.* Lab on a Chip, 2013. **13**(10): p. 1892-1901.
25. Okumuş, U., *Examination and Mathematical Modelling of Shrinkage Rate of Uniform Droplets in a Microfluidic System Designed for Biopreservation*. 2015. p. 66.
26. Jacobs, M.H., *The simultaneous measurement of cell permeability to water and to dissolved substances.* 1933. **2**(4): p. 427-444.
27. Holz, R. and A. Finkelstein, *The water and nonelectrolyte permeability induced in thin lipid membranes by the polyene antibiotics nystatin and amphotericin B.* J Gen Physiol, 1970. **56**(1): p. 125-45.
28. Andreoli, T.E., V.W. Dennis, and A.M. Weigl, *The effect of amphotericin B on the water and nonelectrolyte permeability of thin lipid membranes.* J Gen Physiol, 1969. **53**(2): p. 133-56.
29. Fleming Glass, K.K., E.K. Longmire, and A. Hubel, *Optimization of a microfluidic device for diffusion-based extraction of DMSO from a cell suspension.* International Journal of Heat and Mass Transfer, 2008. **51**: p. 5749-5757.
30. Elmoazzen, H.Y., J.A. Elliott, and L.E. McGann, *Osmotic transport across cell membranes in nondilute solutions: a new nondilute solute transport equation.* Biophys J, 2009. **96**(7): p. 2559-71.

31. Xu, Y., L. Zhang, J. Xu, Y. Wei, and X. Xu, *Membrane permeability of the human pluripotent stem cells to Me(2)SO, glycerol and 1,2-propanediol.* Archives of Biochemistry and Biophysics, 2014. **550-551**: p. 67-76.
32. Edd, J.F., D. Di Carlo, K.J. Humphry, S. Köster, D. Irimia, D.A. Weitz, and M. Toner, *Controlled encapsulation of single-cells into monodisperse picolitre drops.* Lab on a Chip, 2008. **8**: p. 1262-1264.
33. Gilmore, J.A., L.E. McGann, J. Liu, D.Y. Gao, A.T. Peter, F.W. Kleinhans, and J.K. Critser, *Effect of Cryoprotectant Solutes on Water Permeability of Human Spermatozoa'.* Biology of Reproduction, 1995. **53**(5): p. 985-95.
34. Heo, Y.S., H.J. Lee, B.A. Hassell, D. Irimia, T.L. Toth, H. Elmoazzen, and M. Toner, *Controlled loading of cryoprotectants (CPAs) to oocyte with linear and complex CPA profiles on a microfluidic platform.* Lab on a Chip, 2011. **11**: p. 3530-3537.
35. Abraham, R.T. and A. Weiss, *Jurkat T cells and development of the T-cell receptor signalling paradigm.* Nat Rev Immunol, 2004. **4**(4): p. 301-8.
36. Yang, T., J. Peng, Z. Shu, P.K. Sekar, S. Li, and D. Gao, *Determination of the Membrane Transport Properties of Jurkat Cells with a Microfluidic Device.* Micromachines (Basel), 2019. **10**(12).
37. Fang, C., F. Ji, Z. Shu, and D. Gao, *Determination of the temperature-dependent cell membrane permeabilities using microfluidics with integrated flow and temperature control.* Lab on a Chip, 2017. **17**: p. 951-960.
38. Vian, A.M. and A.Z. Higgins, *Membrane permeability of the human granulocyte to water, dimethyl sulfoxide, glycerol, propylene glycol and ethylene glycol.* Cryobiology, 2014. **68**(1): p. 35-42.
39. Shu, Z., S.M. Hughes, C. Fang, J. Huang, B. Fu, G. Zhao, M. Fialkow, G. Lentz, F. Hladik, and D. Gao, *A study of the osmotic characteristics, water permeability, and cryoprotectant permeability of human vaginal immune cells.* Cryobiology, 2016. **72**(2): p. 93-9.
40. Onel, S., U. Okumus, and M. Toner, *Dissolution Modeling of Uniform Aqueous Droplets in Two-Phase Flow in a Microfluidic Device*, in *COMSOL Conference Boston*. 2018, COMSOL: Newton, MA, USA. p. p. 65321

APPENDICES

A. Python script for droplet size detection using image processing

```
import cv2
import numpy as np
import math
import imutils
import matplotlib.pyplot as plt



def player(fname, minR, maxR, check, ):
    cap = cv2.VideoCapture(fname)
    minR = int(minR)
    maxR = int(maxR)
    check = bool(check)
    fname = fname.replace(".avi","")
    scale = 1757.80  #4x kamera icin
    #scale = 703.12  #10x kamera icin
    #scale = 351.56  #20x kamera icin
    #scale = 175.78  #40x kamera icin

    totalFrame = int(cap.get(cv2.CAP_PROP_FRAME_COUNT))
    print (totalFrame)
    font = cv2.FONT_HERSHEY_SIMPLEX
    height = 1200
    width  = 1600

    cnt = 0



    MaxOfInterest = 80 # in micrometers
    MinOfInterest = 60 # in micrometers


    maxR = int(maxR*1600/1757.80) # in pixels
    minR = int(minR*1600/1757.80) # in pixels



    file1 = open("droplet"+fname+"-Droplet.txt", "w")
    file2 = open("droplet"+fname+"-Distance.txt", "w")

    dropletList = []
    distanceList = []
    centerDistanceList = []
    while True:
```

```
        ret,frame = cap.read()
        cnt = cnt + 1

        frame = cv2.medianBlur(frame,5)

        cimg = cv2.cvtColor(frame, cv2.COLOR_BGR2GRAY)

        circles = cv2.HoughCircles(cimg,cv2.HOUGH_GRADIENT,1,maxR,
param1=50,param2=30,minRadius=minR,maxRadius=maxR)
        print ("-------------------------------------------")
        print ("Frame", cnt, "of", totalFrame)
        print (circles)

        if circles is not None:
            circles=circles
            circles=np.uint16(np.around(circles))
            count = 0
            tempList = []
            tempDiameter = []

            for i in circles[0,:]:

                cv2.circle(cimg, (maxR, maxR), minR, (0,0,0), 2)
                cv2.circle(cimg, (maxR, maxR), maxR, (0,0,0), 2)
                cv2.putText(cimg, str("Largest & Smallest"), (maxR+100, maxR),
cv2.FONT_HERSHEY_SIMPLEX, 0.8, (0,255,0),2)
                cv2.putText(cimg, str("Detectable Circles"), (maxR+100, maxR+50),
cv2.FONT_HERSHEY_SIMPLEX, 0.8, (0,255,0),2)
                # draw the outer circle
                cv2.circle(cimg, (i[0], i[1]), i[2], (0,0,0), 2)
                #draw the center of the circle
                cv2.circle(cimg, (i[0], i[1]), 2, (0,0,0), 3)

                diameter = (2*i[2]*scale/1600)
                displayDiameter = truncate(diameter,3)
                print ("Diameter: ", diameter)
                dropletList.append(diameter)

                distance = (i[0]*scale/1600)
                tempList.append(distance)
                tempDiameter.append(diameter)
                print(tempList)
                tempList = sorted(tempList)
                tempDiameter = sorted(tempDiameter)
                #print(tempList)
                cv2.putText(cimg, str(displayDiameter), (i[0]-60, i[1]-80),
cv2.FONT_HERSHEY_SIMPLEX, 0.8, (0,255,0),2)
                cv2.putText(cimg, str("FileName:"+fname), (400, 60),
cv2.FONT_HERSHEY_SIMPLEX, 0.8, (0,255,0),2)
                cv2.putText(cimg, str("Droplet Diameter [um]"), (750, 60),
cv2.FONT_HERSHEY_SIMPLEX, 0.8, (0,255,0),2)
                cv2.putText(cimg, str("Interdroplet Distance [um]"), (1150, 60),
cv2.FONT_HERSHEY_SIMPLEX, 0.8, (0,255,0),2)
```

```
            cv2.putText(cimg, str("_____"), (750, 65),
cv2.FONT_HERSHEY_SIMPLEX, 0.8, (0,255,0),2)
            cv2.putText(cimg, str(displayDiameter), (750, count*50+90),
cv2.FONT_HERSHEY_SIMPLEX, 0.8, (0,255,0),2)
            file1.write(repr(diameter)+"\n")
            count = count+1


        for x in range(len(tempList)-1):

            if abs(tempList[x+1]-tempList[x])<1500:
                file2.write(repr(abs(tempList[x+1]-tempList[x]))+"\n ")
                distanceList.append(abs(tempList[x+1]-tempList[x])-
(tempDiameter[x+1]/2+tempDiameter[x]/2))
                centerDistanceList.append(abs(tempList[x+1]-tempList[x]))
                displayDistance = truncate(abs(tempList[x+1]-tempList[x])-
(tempDiameter[x+1]/2+tempDiameter[x]/2),3)
                print ("Distance \n", abs(tempList[x+1]-tempList[x])-
(tempDiameter[x+1]/2+tempDiameter[x]/2))
                cv2.putText(cimg, str("Interdroplet Distance [um]"), (1150, 60),
cv2.FONT_HERSHEY_SIMPLEX, 0.8, (0,255,0),2)
                cv2.putText(cimg, str("_____"), (1150, 65),
cv2.FONT_HERSHEY_SIMPLEX, 0.8, (0,255,0),2)
                cv2.putText(cimg, str(displayDistance), (1150, x*50+90),
cv2.FONT_HERSHEY_SIMPLEX, 0.8, (0,255,0),2)


    if check == False:
        cv2.imshow('Frame', cimg)

    if cnt == totalFrame-1:
        break
    if cv2.waitKey(300) & 0xFF == ord('q') | cnt==10:
        break
cap.release()
cv2.destroyAllWindows()
file1.close()
file2.close()

file = open("droplet"+fname+"-Report.txt", "w")
file.write( "Number of Frames: " + repr(totalFrame))

file.write("\n Average Droplet Size: " + repr(np.mean(dropletList)))
file.write("\n total droplet amount: " + repr(len(dropletList)))

file.write("\n Average Droplet Distance: " + repr(np.mean(distanceList)))
file.write("\n total droplet distance amount: " + repr(len(distanceList)))

file.close()

fig, ax1 = subplots()
ax2 = ax1.twinx()

bins = np.linspace(MinOfInterest*2, MaxOfInterest*2, MaxOfInterest*2-MinOfInterest*2+1)
```

```
    plt.hist(dropletList, bins, alpha=0.5, label='Droplets @ 25 Celcius')
    plt.xlabel('Droplet Diameter [um]', fontsize=8)
    plt.ylabel('Number of Droplets', fontsize=8)
    plt.legend(loc='upper right')
    plt.savefig(fname+"-Histogram.png")
    plt.clf()

    x1 = np.arange(1,len(distanceList)+1)
    x2 = np.arange(1,len(centerDistanceList)+1)
    x3 = np.arange(1,len(dropletList)+1)
    ax1.plt.plot(x1, distanceList,'.', label='Distance from the surfaces')
    ax1.plt.plot(x2, centerDistanceList,'.', label='Distance from the centers')
    ax2.plt.plot(x3, dropletList, '.')
    ax1.set_xlabel('Droplet Number (based on the detection order)', fontsize=8)
    ax1.set_ylabel('Interdroplet Distance [um]', fontsize=8)
    ax2.set_ylabel("Droplet Size [um]")
    plt.legend(loc='upper right')
    plt.savefig(fname+"-InterDropletDistance.png")
    plt.figure()
    plt.plot(x3, dropletList,'.')
    plt.show()

def truncate(f, n):
    '''Truncates/pads a float f to n decimal places without rounding'''
    s = '{' .format(f)
    if 'e' in s or 'E' in s:
        return '{0:.{1}f}'.format(f, n)
    i, p, d = s.partition('.')
    return '.'.join([i, (d+'0'*n)[:n]])
```

B. Python script for cell membrane permeability solver

```
import tkinter as tk
from PIL import ImageTk, Image
from tkinter import Menu
from tkinter import filedialog
from tkinter import ttk
import tkinter.ttk
import matplotlib
import matplotlib.pyplot as plt
matplotlib.use("TkAgg")
from matplotlib.backends.backend_tkagg import FigureCanvasTkAgg, NavigationToolbar2Tk
```

```
from matplotlib.figure import Figure
import numpy as np
from scipy.optimize import curve_fit
import math
import os


class SampleApp(tk.Tk):
   def __init__(self):
      tk.Tk.__init__(self)

      self.title("Cell Membrane Permeability Solver v1.1")
      frame1_bg = "NavajoWhite3"
      frame1 = tk.Frame(self, bg=frame1_bg).grid(row =0, column=0, rowspan=25, columnspan=8,
sticky=tk.W+tk.E+tk.N+tk.S)
      frame2_bg = "PeachPuff3"
      frame2 = tk.Frame(self, bg=frame2_bg).grid(row =0, column=8, rowspan=25, columnspan=2,
sticky=tk.W+tk.E+tk.N+tk.S)
      entry_bg = "navajo white"
      #tkinter.ttk.Separator(self, orient=tk.HORIZONTAL).grid(columnspan=2, row=11,
sticky='ew')
      tk.Label(self, text = "Cell Parameters", bg=frame1_bg, fg='gray26', font='Helvetica 16
bold').grid(row = 1, column = 1, columnspan=2, sticky = tk.W)
      #tk.Label(self, text = "Select max and min radius",  bg="orange", fg="green").grid(row=1,
column=2, sticky=tk.W)

      tk.Label(self, text = "Cell Radius [µm]", bg=frame1_bg).grid(row = 2, column = 1, sticky =
tk.W)
      tk.Label(self, text = "Lp [um/atm/min]", bg=frame1_bg).grid(row = 3, column = 1, sticky =
tk.W)
      tk.Label(self, text = "Ps [cm/min]", bg=frame1_bg).grid(row = 4, column = 1, sticky = tk.W)
      tk.Label(self, text = "Reflection Coeff.", bg=frame1_bg).grid(row = 5, column = 1, sticky =
tk.W)
      tk.Label(self, text = "Osm. Inactive Vol.", bg=frame1_bg).grid(row = 6, column = 1, sticky =
tk.W)
      tk.Label(self, text = "partial molar volume", bg=frame1_bg).grid(row = 7, column = 1, sticky =
tk.W)
      tk.Label(self, text = "Initial int. CPA con.[mol/m3]", bg=frame1_bg).grid(row = 8, column = 1,
sticky = tk.W)
      tk.Label(self, text = "Initial int. salt con.[mol/m3]", bg=frame1_bg).grid(row = 9, column = 1,
sticky = tk.W)
      tk.Label(self, text = "External CPA con.[mol/m3]", bg=frame1_bg).grid(row = 10, column = 1,
sticky = tk.W)
      tk.Label(self, text = "External salt con.[mol/m3]", bg=frame1_bg).grid(row = 11, column = 1,
sticky = tk.W)

      tkinter.ttk.Separator(self, orient=tk.VERTICAL).grid(column=3, rowspan=12, sticky='ew')
      tk.Label(self, text = "Ambient Parameters", bg=frame1_bg, fg='gray26', font='Helvetica 16
bold').grid(row = 13, column = 1, columnspan=3, sticky = tk.W)
      tk.Label(self, text = "Time step [s]", bg=frame1_bg).grid(row = 14, column = 1, sticky = tk.W)
      tk.Label(self, text = "Total time [s]", bg=frame1_bg).grid(row = 15, column = 1, sticky =
tk.W)
      tk.Label(self, text = "Temperature [K]", bg=frame1_bg).grid(row = 16, column = 1, sticky =
tk.W)
```

```
        tk.Label(self, text = "Boltmann Cons. [J/mol/K]", bg=frame1_bg).grid(row = 17, column = 1,
sticky = tk.W)
        tk.Label(self, text = "Droplet Diameter [µm]", bg=frame1_bg).grid(row = 18, column = 1,
sticky = tk.W)
        tk.Label(self, text = "Shrinking Rate [µm3/s]", bg=frame1_bg).grid(row = 19, column = 1,
sticky = tk.W)

        tk.Label(self, text = "References", bg=frame1_bg, fg='gray26', font='Helvetica 16
bold').grid(row = 1, column = 4, sticky = tk.W)
        tk.Label(self, text = "CPA Used", bg=frame1_bg, fg='gray26', font='Helvetica 16
bold').grid(row = 14, column = 4, sticky = tk.W)
        self.v1 = tk.IntVar()       # cell radius in um
        self.v2 = tk.IntVar()       # hydraulic conductivity in um/atm/min
        self.v3 = tk.IntVar()       # solute permeability in cm/min
        self.v4 = tk.IntVar()       # reflection coefficient
        self.v5 = tk.IntVar()       # Osmotically inactive volume fraction (should be multiplied by V0)
        self.v6 = tk.IntVar()       # partial molar volume in m3/mol
        self.v7 = tk.IntVar()       # Initial internal CPA concentration
        self.v8 = tk.IntVar()       # Initial internal salt concentration
        self.v9 = tk.IntVar()       # External CPA concentration
        self.v10 = tk.IntVar()      # External salt concentration
        self.v11 = tk.IntVar()      # time step
        self.v12 = tk.IntVar()      # total time
        self.v13 = tk.IntVar()      # Ambient Temperature
        self.v14 = tk.IntVar()      # Boltzmann
        self.v15 = tk.IntVar()      # Droplet Diameter
        self.v16 = tk.IntVar()      # Shrinking Rate
        self.paper = tk.StringVar()  # Name of the Article
        self.var1 = tk.IntVar()
        self.var2 = tk.IntVar()


        self.comboRef = ttk.Combobox(textvariable=self.var1, width=60, justify='left')
        self.comboRef.bind("<<ComboboxSelected>>", self.getReferences)
        self.comboRef['value'] = (  "Glycerol Experiment, 40C",
                                    "Yang et al., 2019, %10 DMSO, Jurkat, 22C",
                                    "Xu et al., 2014, %10 Glycerol, hESC, 24C",
                                    "Xu et al., 2014, %10 Glycerol, hiPSC, 24C",
                                    "Vian et al., 2014, 0.7 Osm/kg Glycerol, Human Granulocyte, 21C",
                                    "Fang et al., 2017, %10 DMSO, Jurkat, 22C",
                                    "Fang et al., 2017, %10 DMSO, Jurkat, 37C",
                                    "Shu et al., 2016, 1.5M Ethylene Glycol, Human Vaginal T Cell, 22C",
                                    "Shu et al., 2016, 1.5M Propylene Glycol, Human Vaginal T Cell, 22C",
                                    "Shu et al., 2016, 1.5M Glycerol, Human Vaginal T Cell, 22C",
                                    "Shu et al., 2016, 1.5M Ethylene Glycol, Human Vaginal Macrophage, 22C",
                                    "Shu et al., 2016, 1.5M Propylene Glycol, Human Vaginal Macrophage,
22C",
                                    "Shu et al., 2016, 1.5M Glycerol, Human Vaginal Macrophage, 22C"
                                    "Gilmore et al, 1995, 1M Glycerol, Human Spermatozoa, 22C",
                                    "Gilmore et al, 1995, 1M PG, Human Spermatozoa, 22C",
                                    "Gilmore et al, 1995, 1M DMSO, Human Spermatozoa, 22C",
                                    "Gilmore et al, 1995, 2M EG, Human Spermatozoa, 22C"

                                    )
```

```
        self.comboRef.current(0)
        self.comboRef.grid(column=4, row=2, columnspan=2)

        self.comboRef2 = ttk.Combobox(textvariable=self.var2, width=60, justify='left')
        self.comboRef2.bind("<<ComboboxSelected>>", self.getCPAs)
        self.comboRef2['value'] = (  "",
                                "glycerol",
                                "ethylene glycol",
                                "propylene glycol"
                                )
        self.comboRef2.current(0)
        self.comboRef2.grid(column=4, row=16, columnspan=1)

        tk.Label(self, textvariable = self.paper, bg = entry_bg, wraplength=300).grid(column=3,
row=6, rowspan=3, columnspan=3, sticky=tk.W)
        """
        [1] T. Yang, J. Peng, Z. Shu, P. K. Sekar, S. Li, and D. Gao, “Determination of the membrane
transport properties of jurkat cells with a microfluidic device,” Micromachines, vol. 10, no. 12, pp.
1–13, 2019.
        [2] Y. Xu, L. Zhang, J. Xu, Y. Wei, and X. Xu, “Membrane permeability of the human
pluripotent stem cells to Me2SO, glycerol and 1,2-propanediol,” Arch. Biochem. Biophys., vol.
550–551, pp. 67–76, 2014.
        [3] A. M. Vian and A. Z. Higgins, “Membrane permeability of the human granulocyte to
water, dimethyl sulfoxide, glycerol, propylene glycol and ethylene glycol,” Cryobiology, vol. 68,
no. 1, pp. 35–42, 2014.
        [4] C. Fang, F. Ji, Z. Shu, and D. Gao, “Determination of the temperature-dependent cell
membrane permeabilities using microfluidics with integrated flow and temperature control,” Lab
Chip, vol. 17, no. 5, pp. 951–960, 2017.
        [5] Z. Shu et al., “A study of the osmotic characteristics, water permeability, and
cryoprotectant permeability of human vaginal immune cells,” Cryobiology, vol. 72, no. 2, pp. 93–
99, 2016.
        [6] J. A. Gilmore et al., “Effect of Cryoprotectant Solutes on Water Permeability of Human
Spermatozoa’,” Biol. Reprod., vol. 53, pp. 985–995, 1995.
        """



        self.R = tk.Entry(self,text=self.v1, bg=entry_bg)
            # cell radius in um
        self.Lp = tk.Entry(self,text=self.v2, bg=entry_bg)              # hydraulic conductivity in
um/atm/min
        self.Ps = tk.Entry(self,text=self.v3, bg=entry_bg)             # solute permeability in cm/min
        self.Sgm = tk.Entry(self,text=self.v4, bg=entry_bg)              # reflection coefficient
        self.Vb = tk.Entry(self,text=self.v5, bg=entry_bg)              # Osmotically inactive volume
fraction (should be multiplied by V0)
        self.Nu = tk.Entry(self,text=self.v6, bg=entry_bg)              # partial molar volume in
m3/mol
        self.Cci0 = tk.Entry(self,text=self.v7, bg=entry_bg)             # Initial internal CPA
concentration
        self.Csi0 = tk.Entry(self,text=self.v8, bg=entry_bg)             # Initial internal salt
concentration
        self.Cce = tk.Entry(self,text=self.v9, bg=entry_bg)              # External CPA concentration
        self.Cse = tk.Entry(self,text=self.v10, bg=entry_bg)              # External salt concentration
        self.Timestep = tk.Entry(self,text=self.v11, bg=entry_bg)          # time step
```

```
        self.Timetot = tk.Entry(self,text=self.v12, bg=entry_bg)          # total time
        self.Temp = tk.Entry(self,text=self.v13, bg=entry_bg)             # Ambient Temperature
        self.Rboltz = tk.Entry(self,text=self.v14, bg=entry_bg)           # Boltzmann
        self.drop = tk.Entry(self, text=self.v15, bg=entry_bg)            # Droplet Diameter
        self.shrnk = tk.Entry(self, text=self.v16, bg=entry_bg)           # Shrinking Rate


        self.R.grid(row = 2, column = 2)
        self.Lp.grid(row = 3, column = 2)
        self.Ps.grid(row = 4, column = 2)
        self.Sgm.grid(row = 5, column = 2)
        self.Vb.grid(row = 6, column = 2)
        self.Nu.grid(row = 7, column = 2)
        self.Cci0.grid(row = 8, column = 2)
        self.Csi0.grid(row = 9, column = 2)
        self.Cce.grid (row = 10, column = 2)
        self.Cse.grid (row = 11, column = 2)
        self.Timestep.grid(row = 14, column = 2)
        self.Timetot.grid(row = 15, column = 2)
        self.Temp.grid(row = 16, column = 2)
        self.Rboltz.grid(row = 17, column = 2)
        self.drop.grid(row = 18, column = 2)
        self.shrnk.grid(row = 19, column = 2)


        #c = tk.Checkbutton(self, text="Cancel Video?", variable=self.checkCmd, onvalue=1,
offvalue=0)
        #c.grid(row = 8, column=1, sticky=tk.W)
        tk.Label(self, text = "Solvers", bg=frame1_bg, fg='gray26', font='Helvetica 16 bold').grid(row
= 1, column = 8, columnspan=3, sticky = tk.W)
        tk.Label(self, text = "Two Parameter Model", fg='deep sky blue', bg='NavajoWhite4').grid(row
= 2, column = 8, sticky = tk.W)
        tk.Label(self, text = "Kedem Katchalsky Model", fg='deep sky blue',
bg='NavajoWhite4').grid(row = 9, column = 8, sticky = tk.W)
        tk.Label(self, text = "Microfluidic Model", fg='deep sky blue', bg='NavajoWhite4').grid(row =
16, column = 8, sticky = tk.W)
        tk.Button(self, text = "2P Iterative Solver", command = self.twoParam).grid(row = 7,
column=8, sticky = tk.W)
        tk.Button(self, text = "2P RK4 Solver", command = self.twoParam_RK4).grid(row = 7,
column=9, sticky = tk.W)
        tk.Button(self, text = "KK Model Iterative Solver", command = self.kkModel).grid(row = 15,
column=8, sticky = tk.W)
        tk.Button(self, text = "KK Model RK4 Solver", command = self.kkModel_RK4).grid(row =
15, column=9, sticky = tk.W)
        tk.Button(self, text = "MF Model Iterative Solver", command = self.mfModel).grid(row = 23,
column=8, sticky = tk.W)
        tk.Button(self, text = "MF Model RK4 Solver", command = self.mfModel).grid(row = 23,
column=9, sticky = tk.W)



        load_twoPic = Image.open('twoPic.jpg','r')
        load_kkPic  = Image.open('kkPic.jpg','r')
        load_modelPic  = Image.open('modelPic.jpg','r')
```

```
        render_twoPic = ImageTk.PhotoImage(load_twoPic)
        render_kkPic  = ImageTk.PhotoImage(load_kkPic)
        render_modelPic  = ImageTk.PhotoImage(load_modelPic)
        img_twoPic = tk.Label(self,image=render_twoPic)
        img_kkPic = tk.Label(self,image=render_kkPic)
        img_modelPic = tk.Label(self,image=render_modelPic)
        img_twoPic.image = render_twoPic
        img_kkPic.image = render_kkPic
        img_modelPic.image = render_modelPic
        img_twoPic.grid(row=3, rowspan=4, column=8, columnspan=2, sticky=tk.W, pady=3)
        img_kkPic.grid(row=10, rowspan=4, column=8, columnspan=2, sticky=tk.W, pady=3)
        img_modelPic.grid(row=17, rowspan=4, column=8, columnspan=2, sticky=tk.W, pady=3)

    def twoParam(self):

        r    = float(self.R.get())
        r    = r*(1e-6)
        lp   = float(self.Lp.get())
        lp   = lp/(101325*1e6*60) # 101325 for atm to Pascal, 1e6 for um to meters, 60 for minutes to
seconds
        ps   = float(self.Ps.get())
        ps   = ps*(0.01/60)
        sgm  = float(self.Sgm.get())
        vb   = float(self.Vb.get())
        nu   = float(self.Nu.get())
        cci0 = float(self.Cci0.get())
        csi0 = float(self.Csi0.get())
        cce  = float(self.Cce.get())
        cse  = float(self.Cse.get())

        h  = float(self.Timestep.get())
        tt = float(self.Timetot.get())
        T  = float(self.Temp.get())
        R  = float(self.Rboltz.get())

        V0 = 4/3*math.pi*pow(r,3)
        A = 4*math.pi*pow(r,2)
        Vb = vb*V0

        t = []
        V = []
        N = []
        csi = []

        for i in np.arange(0,tt+2*h,h): # setting up timescale
            t.append(round(i,4))
            #print(i)


        csi = [0]*len(t)
        cci = [0]*len(t)
        delP = [0]*len(t)
        delC = [0]*len(t)
```

```
        dVdt = [0]*len(t)
        dNdt = [0]*len(t)
        V    = [0]*len(t)
        N    = [0]*len(t)
        C    = [0]*len(t)


        V[0] = V0
        N[0] = 0
        delP[0] = cse-csi0
        delC[0] = cce-cci0
        file1 = open("twoParam_Data.txt", "w")
        file1.write("Volume\t\t\t"+"N\t\t\t"+"cci\t\t\t"+"csi\t\t\t"+"delC\t\t\t"+"delP\t\t\t"+"time\n")
        for i in range(len(t)-1):
            csi[0] = csi0
            cci[0] = cci0

            dVdt[i] = -lp*A*R*T*((cse-csi[i])+(cce-cci[i]))
            dNdt[i] = ps*A*(cce-cci[i])
            delP[i] = cse-csi0*((V[0]-Vb)/(V[i]-Vb))
            delC[i] = cce-N[i]/(V[i]-Vb);

            V[i+1] = V[i]+dVdt[i]*h
            N[i+1] = N[i]+dNdt[i]*h
            cci[i+1] = N[i+1]/(V[i+1]-Vb)
            csi[i+1] = csi0*(V[0]-Vb)/(V[i+1]-Vb)


#file1.write(repr(t[i])+"\t"+repr(V[i])+"\t"+repr(N[i])+"\t"+repr(cci[i])+"\t"+repr(csi[i])+"\n")

file1.write(repr(round((V[i]*1e18),1))+"\t\t\t"+repr(round((N[i]*1e18),1))+"\t\t\t"+repr(round((cci[i
]),4))+"\t\t\t"+repr(round((csi[i]),4))+"\t\t\t"+repr(round((delC[i]),4))+"\t\t\t"+repr(round((delP[i]),4
))+"\t\t\t"+repr(round((t[i]),4))+"\n")

        file1.close()

        self.changePlotSize(10,8)

        Vplot = np.array(V)*1e18 # micrometer cube
        Nplot = np.array(N)*1e18 # ...

        Cplot = np.array(cci)/1e3
        t = np.array(t)

        plt.close("all")
        #plt.subplot(211)
        fig = plt.figure()
        ax1 = fig.add_subplot(211)
        ax2 = ax1.twinx()
        ax1.plot(t, Vplot, 'g-')
        ax2.plot(t, Cplot, 'b-')
        ax1.set_xlabel('time [s]')
        ax1.set_ylabel('Volume [um^3]', color='g')
        ax2.set_ylabel('Concentration [mol/L]', color='b')
```

```
    #plt.plot(t,Vplot)
    #plt.plot(t,Nplot)
    #plt.title('volume change')
    #plt.xlabel('time [s]')
    #plt.ylabel('Volume [um^3]')
    plt.subplot(212)
    plt.plot(t,delP)
    plt.plot(t,delC)
    plt.ylabel('driving force')


    plt.show()

def twoParam_RK4(self):

    r    = float(self.R.get())
    r    = r*(1e-6)
    lp   = float(self.Lp.get())
    lp   = lp/(101325*1e6*60)
    ps   = float(self.Ps.get())
    ps   = ps*(0.01/60)
    sgm  = float(self.Sgm.get())
    vb   = float(self.Vb.get())
    nu   = float(self.Nu.get())
    cci0 = float(self.Cci0.get())
    csi0 = float(self.Csi0.get())
    cce  = float(self.Cce.get())
    cse  = float(self.Cse.get())

    h  = float(self.Timestep.get())
    tt = float(self.Timetot.get())
    T  = float(self.Temp.get())
    R  = float(self.Rboltz.get())

    V0 = 4/3*math.pi*pow(r,3)
    A = 4*math.pi*pow(r,2)
    Vb = vb*V0

    file1 = open("twoParam_RK4_Data.txt", "w")
    file1.write("Volume\t\t\t"+"N\t\t\t"+"cci\t\t\t"+"csi\t\t\t"+"delC\t\t\t"+"delP\t\t\t"+"time\n")

    t0 = 0
    N0 = 0
    n = int(tt/h)
    #print(n)
    Tt = [0]*(n+1)
    Vv = [0]*(n+1)
    Nn = [0]*(n+1)
    Cc = [0]*(n+1)

    h = (tt-t0)/float(n)
    Tt[0] = t0
    Vv[0] = V0
```

```
        Nn[0] = N0
        N_i = Nn[0]
        V_i = Vv[0]
        for i in range(1,n+1):
            k1 = h*self.f(lp,A,R,T,cce,cse,csi0,N_i,V_i,Vb,V0)
            m1 = h*self.g(ps,A,cce,N_i,V_i,Vb)

            k2 = h*self.f(lp,A,R,T,cce,cse,csi0, N_i+0.5*m1, V_i+0.5*k1, Vb,V0)
            m2 = h*self.g(ps,A,cce,N_i+0.5*m1,V_i+0.5*k1,Vb)

            k3 = h*self.f(lp,A,R,T,cce,cse,csi0, N_i+0.5*m2, V_i+0.5*k2, Vb,V0)
            m3 = h*self.g(ps,A,cce,N_i+0.5*m2,V_i+0.5*k2,Vb)

            k4 = h*self.f(lp,A,R,T,cce,cse,csi0, N_i+m3, V_i+k3, Vb,V0)
            m4 = h*self.g(ps,A,cce,N_i+m3,V_i+k3,Vb)


            Tt[i] = t = t0+i*h
            Vv[i] = V_i = Vv[i-1]+(k1+2*k2+2*k3+k4)/6
            Nn[i] = N_i = Nn[i-1]+(m1+2*m2+2*m3+m4)/6
            Cc[i] = Nn[i]/Vv[i]/1e3 # from metercube to liter


#file1.write(repr(t[i])+"\t"+repr(V[i])+"\t"+repr(N[i])+"\t"+repr(cci[i])+"\t"+repr(csi[i])+"\n")

file1.write(repr(round((Vv[i]*1e18),1))+"\t\t\t"+repr(round((Nn[i]*1e18),1))+"\t\t\t"+repr(round((Tt
[i]),4))+"\n")

        file1.close()

        self.changePlotSize(10,8)

        Vplot = np.array(Vv)*1e18 #micrometer cube
        t = np.array(Tt)
        Cplot = np.array(Cc)

        plt.close("all")
        fig = plt.figure()
        ax1 = fig.add_subplot(211)
        ax2 = ax1.twinx()
        ax1.plot(t, Vplot, 'g-')
        ax2.plot(t, Cplot, 'b-')

        ax1.set_xlabel('time [s]')
        ax1.set_ylabel('Volume [um^3]', color='g')
        ax2.set_ylabel('Concentration [mol/L]', color='b')



        #plt.subplot(211)

        plt.subplot(212)
        #plt.plot(t,delP)
        #plt.plot(t,delC)
```

```
        #plt.ylabel('driving force')


        plt.show()

    def f(self,lp,A,R,T,cce,cse,csi0,N_i,V_i,Vb,V0):
        dVdt = -lp*A*R*T*((cce-N_i/(V_i-Vb))+(cse-csi0*(V0-Vb)/(V_i-Vb)))
        return dVdt

    def g(self,ps,A,cce,N_i,V_i,Vb):
        dNdt = ps*A*(cce-N_i/(V_i-Vb))
        return dNdt

    def fKK(self,lp,A,R,T,sgm,cce,cse,csi0,N_i,V_i,Vb,V0):
        dVdt = -lp*A*R*T*(sgm*(cce-N_i/(V_i-Vb))+(cse-csi0*(V0-Vb)/(V_i-Vb)))
        return dVdt

    def gKK(self,ps,A,sgm,cce,N_i,V_i,Vb,lp,R,T,cse,csi0,V0):
        dNdt = 0.5*self.fKK(lp,A,R,T,sgm,cce,cse,csi0,N_i,V_i,Vb,V0)*(N_i/(V_i-Vb)+cce)*(1-
sgm)+ps*A*(cce-N_i/(V_i-Vb))
        return dNdt

    def kkModel(self):

        r    = float(self.R.get())
        r    = r*(1e-6)
        lp   = float(self.Lp.get())
        lp   = lp/(101325*1e6*60)
        ps   = float(self.Ps.get())
        ps   = ps*(0.01/60)
        sgm  = float(self.Sgm.get())
        vb   = float(self.Vb.get())
        nu   = float(self.Nu.get())
        cci0 = float(self.Cci0.get())
        csi0 = float(self.Csi0.get())
        cce  = float(self.Cce.get())
        cse  = float(self.Cse.get())

        h  = float(self.Timestep.get())
        tt = float(self.Timetot.get())
        T  = float(self.Temp.get())
        R  = float(self.Rboltz.get())

        V0 = 4/3*math.pi*pow(r,3)
        A = 4*math.pi*pow(r,2)
        Vb = vb*V0

        t = []
        V = []
        N = []
        csi = []

        for i in np.arange(0,tt+2*h,h): # setting up timescale
            t.append(round(i,4))
```

```
        #print(i)


    csi = [0]*len(t)
    cci = [0]*len(t)
    delP = [0]*len(t)
    delC = [0]*len(t)
    dVdt = [0]*len(t)
    dNdt = [0]*len(t)
    V    = [0]*len(t)
    N    = [0]*len(t)
    C    = [0]*len(t)


    V[0] = V0
    N[0] = 0
    delP[0] = cse-csi0
    delC[0] = cce-cci0
    file1 = open("kkModel_Data.txt", "w")
    file1.write("Volume\t\t\t"+"dV\t\t\t"+"cci\t\t\t"+"csi\t\t\t"+"delC\t\t\t"+"delP\t\t\t"+"time\n")
    for i in range(len(t)-1):
        csi[i] = csi0*(V[0]-Vb)/(V[i]-Vb)
        cci[i] = N[i]/(V[i]-Vb)

        dVdt[i] = -lp*A*R*T*((cse-csi[i])+sgm*(cce-cci[i]))
        dNdt[i] = 0.5*dVdt[i]*(cci[i]+cce)*(1-sgm)+ps*A*(cce-cci[i])
        delP[i] = cse-csi0*((V[0]-Vb)/(V[i]-Vb))
        delC[i] = cce-N[i]/(V[i]-Vb)

        V[i+1] = V[i]+dVdt[i]*h
        N[i+1] = N[i]+dNdt[i]*h
        C[i+1] = N[i+1]/(V[i+1]-Vb)/1e3


#file1.write(repr(t[i])+"\t"+repr(V[i])+"\t"+repr(N[i])+"\t"+repr(cci[i])+"\t"+repr(csi[i])+"\n")

file1.write(repr(round((V[i]*1e18),1))+"\t\t\t"+repr(round((dVdt[i]*1e18),1))+"\t\t\t"+repr(round((c
ci[i]),4))+"\t\t\t"+repr(round((csi[i]),4))+"\t\t\t"+repr(round((delC[i]),4))+"\t\t\t"+repr(round((delP[i]
),4))+"\t\t\t"+repr(round((t[i]),4))+"\n")

    file1.close()

    self.changePlotSize(10,8)

    Vplot = np.array(V)*1e18
    Nplot = np.array(N)*1e18
    Cplot = np.array(C)
    t = np.array(t)

    plt.close("all")
    #plt.subplot(211)
    fig = plt.figure()
    ax1 = fig.add_subplot(211)
    ax2 = ax1.twinx()
```

```
    ax1.plot(t, Vplot, 'g-')
    ax2.plot(t, Cplot, 'b-')
    ax1.set_xlabel('time [s]')
    ax1.set_ylabel('Volume [um^3]', color='g')
    ax2.set_ylabel('Concentration [mol/L]', color='b')


    plt.show()

def kkModel_RK4(self):


    r    = float(self.R.get())
    r    = r*(1e-6)
    lp   = float(self.Lp.get())
    lp   = lp/(101325*1e6*60)
    ps   = float(self.Ps.get())
    ps   = ps*(0.01/60)
    sgm  = float(self.Sgm.get())
    vb   = float(self.Vb.get())
    nu   = float(self.Nu.get())
    cci0 = float(self.Cci0.get())
    csi0 = float(self.Csi0.get())
    cce  = float(self.Cce.get())
    cse  = float(self.Cse.get())

    h  = float(self.Timestep.get())
    tt = float(self.Timetot.get())
    T  = float(self.Temp.get())
    R  = float(self.Rboltz.get())

    V0 = 4/3*math.pi*pow(r,3)
    A = 4*math.pi*pow(r,2)
    Vb = vb*V0

    file1 = open("kkMode_RK4_Data.txt", "w")
    file1.write("Volume\t\t\t"+"N\t\t\t"+"cci\t\t\t"+"csi\t\t\t"+"delC\t\t\t"+"delP\t\t\t"+"time\n")

    t0 = 0
    N0 = 0
    n = int(tt/h)
    #print(n)
    Tt = [0]*(n+1)
    Vv = [0]*(n+1)
    Nn = [0]*(n+1)
    Cc = [0]*(n+1)

    h = (tt-t0)/float(n)
    Tt[0] = t0
    Vv[0] = V0
    Nn[0] = N0
    N_i = Nn[0]
    V_i = Vv[0]
    for i in range(1,n+1):
```

```
            k1 = h*self.fKK(lp,A,R,T,sgm,cce,cse,csi0,N_i,V_i,Vb,V0)
            m1 = h*self.gKK(ps,A,sgm,cce,N_i,V_i,Vb,lp,R,T,cse,csi0,V0)

            k2 = h*self.fKK(lp,A,R,T,sgm,cce,cse,csi0, N_i+0.5*m1, V_i+0.5*k1, Vb,V0)
            m2 = h*self.gKK(ps,A,sgm,cce,N_i+0.5*m1,V_i+0.5*k1,Vb,lp,R,T,cse,csi0,V0)

            k3 = h*self.fKK(lp,A,R,T,sgm,cce,cse,csi0, N_i+0.5*m2, V_i+0.5*k2, Vb,V0)
            m3 = h*self.gKK(ps,A,sgm,cce,N_i+0.5*m2,V_i+0.5*k2,Vb,lp,R,T,cse,csi0,V0)

            k4 = h*self.fKK(lp,A,R,T,sgm,cce,cse,csi0, N_i+m3, V_i+k3, Vb,V0)
            m4 = h*self.gKK(ps,A,sgm,cce,N_i+m3,V_i+k3,Vb,lp,R,T,cse,csi0,V0)


            Tt[i] = t = t0+i*h
            Vv[i] = V_i = Vv[i-1]+(k1+2*k2+2*k3+k4)/6
            Nn[i] = N_i = Nn[i-1]+(m1+2*m2+2*m3+m4)/6
            Cc[i] = Nn[i]/Vv[i]/1e3 # from metercube to liter


#file1.write(repr(t[i])+"\t"+repr(V[i])+"\t"+repr(N[i])+"\t"+repr(cci[i])+"\t"+repr(csi[i])+"\n")

file1.write(repr(round((Vv[i]*1e18),1))+"\t\t\t"+repr(round((Nn[i]*1e18),1))+"\t\t\t"+repr(round((Tt
[i]),4))+"\n")

        file1.close()

        self.changePlotSize(10,8)

        Vplot = np.array(Vv)*1e18
        t = np.array(Tt)
        Cplot = np.array(Cc)

        plt.close("all")
        fig = plt.figure()
        ax1 = fig.add_subplot(211)
        ax2 = ax1.twinx()
        ax1.plot(t, Vplot, 'g-')
        ax2.plot(t, Cplot, 'b-')

        ax1.set_xlabel('time [s]')
        ax1.set_ylabel('Volume [um^3]', color='g')
        ax2.set_ylabel('Concentration [mol/L]', color='b')
        plt.subplot(212)
        #plt.plot(t,delP)
        #plt.plot(t,delC)
        #plt.ylabel('driving force')


        plt.show()

    def mfModel(self):

        r    = float(self.R.get())
        r    = r*(1e-6)
```

```
lp   = float(self.Lp.get())
lp   = lp/(101325*1e6*60)
ps   = float(self.Ps.get())
ps   = ps*(0.01/60)
sgm  = float(self.Sgm.get())
vb   = float(self.Vb.get())
nu   = float(self.Nu.get())
cci0 = float(self.Cci0.get())
csi0 = float(self.Csi0.get())
cce  = float(self.Cce.get())
cse  = float(self.Cse.get())

h  = float(self.Timestep.get())
tt = float(self.Timetot.get())
T  = float(self.Temp.get())
R  = float(self.Rboltz.get())
D  = float(self.drop.get())
D  = D*(1e-6)
ds = float(self.shrnk.get())


V0 = 4/3*math.pi*pow(r,3)
A = 4*math.pi*pow(r,2)
Vb = vb*V0
dropVolume = (4/3*math.pi*pow(D/2,3))
nTotal = (cce*dropVolume) # number of moles of CPA in initial droplet (mol/m3  * m3)
t = []
V = []
N = []
csi = []
cceDynamic = []
volumeDroplet = []
Texp = [0,10,30,45,60,75,90,105]
Vexp = [1016.43, 757.27, 665.11, 685.51, 699.43, 695.18, 743.60, 757.89]

for i in np.arange(0,tt+2*h,h): # setting up timescale
   t.append(round(i,4))
   #print(i)

for i in np.arange(0,tt+2*h,h): # setting up dynamic concentration
   volumeDroplet.append(dropVolume-ds*1e-18*round(i,4))
   cceDynamic.append(nTotal/(dropVolume-ds*1e-18*round(i,4)))

csi = [0]*len(t)
cci = [0]*len(t)
delP = [0]*len(t)
delC = [0]*len(t)
dVdt = [0]*len(t)
dNdt = [0]*len(t)
V    = [0]*len(t)
N    = [0]*len(t)
C    = [0]*len(t)
```

```
        V[0] = V0
        N[0] = 0
        delP[0] = cse-csi0
        delC[0] = cce-cci0
        file1 = open("mfModel_Data.txt", "w")
        file1.write("time\t\t"+"VCell\t\t"+"N\t\t"+"dNdt\t\t"+"cci\t\t"+"cceDynamic\t\t"+"\n")
        for i in range(len(t)-1):
            csi[0] = csi0
            cci[0] = cci0
            dVdt[i] = -lp*A*R*T*((cse-csi[i])+sgm*(cceDynamic[i]-cci[i]))
            dNdt[i] = 0.5*dVdt[i]*(cci[i]+cceDynamic[i])*(1-sgm)+ps*A*(cceDynamic[i]-cci[i])

            #delP[i] = cse-csi0*((V[0]-Vb)/(V[i]-Vb))
            #delC[i] = cceDynamic[i]-N[i]/(V[i]-Vb)

            V[i+1] = V[i]+dVdt[i]*h
            N[i+1] = N[i]+dNdt[i]*h
            cci[i+1] = N[i+1]/(V[i+1]-Vb)
            csi[i+1] = csi0*(V[0]-Vb)/(V[i+1]-Vb)

#file1.write(repr(t[i])+"\t"+repr(V[i])+"\t"+repr(N[i])+"\t"+repr(cci[i])+"\t"+repr(csi[i])+"\n")

#file1.write(repr(round((cceDynamic[i]),2))+"\t\t\t"+repr(round((N[i]*1e18),2))+"\t\t\t"+repr(round(
(cci[i]),2))+"\t\t\t"+repr(round((cceDynamic[i]),2))+"\t\t\t"+repr(round((delC[i]),2))+"\t\t\t"+repr(ro
und((delP[i]),2))+"\t\t\t"+repr(round((t[i]),2))+"\n")


file1.write(repr(round((t[i]),1))+"\t\t"+repr(round((V[i]*1e18),1))+"\t\t"+repr(round((dVdt[i]*1e18),
1))+"\t\t"+repr(round((N[i]*1e18),1))+"\t\t"+repr(round((dNdt[i]*1e18),1))+"\t\t"+repr(round((cci[i
]),1))+"\t\t"+repr(round((cceDynamic[i]),1))+"\n")
        file1.close()


        self.changePlotSize(10,8)

        Vplot = np.array(V)*1e18
        Nplot = np.array(N)*1e18

        Texp = np.array(Texp)
        Vexp = np.array(Vexp)
        cciplot = np.array(cci)/1e3
        cceDplot = np.array(cceDynamic)/1e3
        t = np.array(t)

        plt.close("all")
        #plt.subplot(211)
        fig = plt.figure()
        ax1 = fig.add_subplot(211)
        ax2 = ax1.twinx()
        ax1.plot(t, Vplot, 'g-', label='volume')
        ax2.plot(t, cciplot, 'b-', label='V/N')
        ax1.set_xlabel('time [s]')
        ax1.set_ylabel('Volume [um^3]', color='g')
        ax2.set_ylabel('Concentration [mol/L]', color='b')
```

```
    plt.subplot(212)
    plt.plot(t,Vplot, label='theoretical')
    plt.plot(Texp,Vexp,label='experimental')
    plt.legend()
    plt.ylabel('Volume [µm^3]')
    plt.xlabel('time [s]')
    #plt.xlim(0,tt)

    plt.show()

    np.set_printoptions(threshold=np.inf)


def changePlotSize(self, x,y):
    fig_size = plt.rcParams["figure.figsize"]
    fig_size[0] = x
    fig_size[1] = y
    plt.rcParams["figure.figsize"] = fig_size

def client_exit(self):
    exit()
def refresh(self):
    self.lbox.delete(0,tk.END)
    label1 = tk.Label(self, text = "Select a folder again",  bg="orange", fg="green")
    label1.grid(row=1, column=1, sticky = tk.W)
def getFolder(self):
    self.dirname = filedialog.askdirectory()
    print(self.dirname)

    label1 = tk.Label(self, text = self.dirname,  bg="orange", fg="green")
    label1.grid(row=1, column=1, sticky = tk.W)
    self.lbox.grid(rowspan=3,columnspan=3)
    files = os.listdir(self.dirname)
    for item in files:
        if item.endswith(".avi"):
            self.lbox.insert(tk.END,item)

def getReferences(self, event):
    refName = str(self.comboRef.get())

    if refName == "Glycerol Experiment, 40C":
        self.v1.set(6.2373)         # cell radius in um
        self.v2.set(0.15)          # hydraulic conductivity in um/atm/min
        self.v3.set(0.00001)        # solute permeability in cm/min
        self.v4.set(0.79)           # reflection coefficient
        self.v5.set(0.55)         # Osmotically inactive volume fraction (should be multiplied by V0)
        self.v6.set(0.0000713)      # partial molar volume in m3/mol
        self.v7.set(10)            # Initial internal CPA concentration
        self.v8.set(297)            # Initial internal salt concentration
        self.v9.set(1000)           # External CPA concentration
        self.v10.set(297)           # External salt concentration
        self.v11.set(0.01)          # time step
        self.v12.set(105)          # total time
```

```
            self.v13.set(313.15)        # Ambient Temperature
            self.v14.set(8.314)         # Boltzmann
            self.v15.set(57.749)        # Droplet Diameter
            self.v16.set(47.92)         # Shrinking Rate
            self.paper.set("Glycerol Experiment, 40C")

        elif refName == "Yang et al., 2019, %10 DMSO, Jurkat, 22C":
            self.v1.set(7.1)            # cell radius in um
            self.v2.set(0.148)          # hydraulic conductivity in um/atm/min
            self.v3.set(0.00034)        # solute permeability in cm/min
            self.v4.set(0.8)            # reflection coefficient
            self.v5.set(0.496)          # Osmotically inactive volume fraction (should be multiplied by
V0)
            self.v6.set(0.000071)       # partial molar volume in m3/mol
            self.v7.set(10)             # Initial internal CPA concentration
            self.v8.set(297)            # Initial internal salt concentration
            self.v9.set(0.1/0.0000713)  # External CPA concentration
            self.v10.set(297)           # External salt concentration
            self.v11.set(0.01)          # time step
            self.v12.set(200)           # total time
            self.v13.set(295.15)        # Ambient Temperature
            self.v14.set(8.314)         # Boltzmann
            self.paper.set("T. Yang, J. Peng, Z. Shu, P. K. Sekar, S. Li, and D. Gao, “Determination of
the membrane transport properties of jurkat cells with a microfluidic device,” Micromachines, vol.
10, no. 12, pp. 1–13, 2019.")

        elif refName == "Xu et al., 2014, %10 Glycerol, hESC, 24C":
            self.v1.set(7.80)           # cell radius in um
            self.v2.set(0.0204*60)          # hydraulic conductivity in um/atm/min
            self.v3.set(1.47*60/1e4)        # solute permeability in cm/min
            self.v4.set(0.92)           # reflection coefficient
            self.v5.set(0.32)           # Osmotically inactive volume fraction (should be multiplied by V0)
            self.v6.set(0.000071)           # partial molar volume in m3/mol
            self.v7.set(10)             # Initial internal CPA concentration
            self.v8.set(297)            # Initial internal salt concentration
            self.v9.set(0.1/0.000071)           # External CPA concentration
            self.v10.set(297)           # External salt concentration
            self.v11.set(0.01)          # time step
            self.v12.set(200)               # total time
            self.v13.set(297.15)        # Ambient Temperature
            self.v14.set(8.314)         # Boltzmann
            self.paper.set("Y. Xu, L. Zhang, J. Xu, Y. Wei, and X. Xu, “Membrane permeability of the
human pluripotent stem cells to Me2SO, glycerol and 1,2-propanediol,” Arch. Biochem. Biophys.,
vol. 550–551, pp. 67–76, 2014.")

        elif refName == "Xu et al., 2014, %10 Glycerol, hiPSC, 24C":
            self.v1.set(8.44)           # cell radius in um
            self.v2.set(0.137*60)           # hydraulic conductivity in um/atm/min
            self.v3.set(0.77*60/1e4)        # solute permeability in cm/min
            self.v4.set(0.86)           # reflection coefficient
            self.v5.set(0.42)           # Osmotically inactive volume fraction (should be multiplied by V0)
            self.v6.set(0.000071)           # partial molar volume in m3/mol
            self.v7.set(10)             # Initial internal CPA concentration
            self.v8.set(297)            # Initial internal salt concentration
```

```
        self.v9.set(0.1/0.000071)           # External CPA concentration
        self.v10.set(297)          # External salt concentration
        self.v11.set(0.01)          # time step
        self.v12.set(200)          # total time
        self.v13.set(297.15)        # Ambient Temperature
        self.v14.set(8.314)         # Boltzmann
        self.paper.set("Y. Xu, L. Zhang, J. Xu, Y. Wei, and X. Xu, “Membrane permeability of the
human pluripotent stem cells to Me2SO, glycerol and 1,2-propanediol,” Arch. Biochem. Biophys.,
vol. 550–551, pp. 67–76, 2014.")

    elif refName == "Vian et al., 2014, 0.7 Osm/kg Glycerol, Human Granulocyte, 21C":
        self.v1.set(4.485)           # cell radius in um
        self.v2.set(0.18)          # hydraulic conductivity in um/atm/min
        self.v3.set(0.0001)         # solute permeability in cm/min
        self.v4.set(1)           # reflection coefficient
        self.v5.set(0.44)          # Osmotically inactive volume fraction (should be multiplied by V0)
        self.v6.set(0.0000713)          # partial molar volume in m3/mol
        self.v7.set(10)            # Initial internal CPA concentration
        self.v8.set(297)           # Initial internal salt concentration
        self.v9.set(0.7/0.001)           # External CPA concentration
        self.v10.set(297)          # External salt concentration
        self.v11.set(0.01)          # time step
        self.v12.set(200)              # total time
        self.v13.set(294.15)        # Ambient Temperature
        self.v14.set(8.314)         # Boltzmann
        self.paper.set("A. M. Vian and A. Z. Higgins, “Membrane permeability of the human
granulocyte to water, dimethyl sulfoxide, glycerol, propylene glycol and ethylene glycol,”
Cryobiology, vol. 68, no. 1, pp. 35–42, 2014.")

    elif refName == "Fang et al., 2017, %10 DMSO, Jurkat, 22C":
        self.v1.set(5)           # cell radius in um
        self.v2.set(0.158)          # hydraulic conductivity in um/atm/min
        self.v3.set(0.00042)         # solute permeability in cm/min
        self.v4.set(1)           # reflection coefficient
        self.v5.set(0.6741)          # Osmotically inactive volume fraction (should be multiplied by
V0)
        self.v6.set(0.0000713)          # partial molar volume in m3/mol
        self.v7.set(10)            # Initial internal CPA concentration
        self.v8.set(297)           # Initial internal salt concentration
        self.v9.set(0.1/0.0000713)   # External CPA concentration
        self.v10.set(297)          # External salt concentration
        self.v11.set(0.01)          # time step
        self.v12.set(200)              # total time
        self.v13.set(295.15)        # Ambient Temperature
        self.v14.set(8.314)         # Boltzmann
        self.paper.set("C. Fang, F. Ji, Z. Shu, and D. Gao, “Determination of the temperature-
dependent cell membrane permeabilities using microfluidics with integrated flow and temperature
control,” Lab Chip, vol. 17, no. 5, pp. 951–960, 2017.")

    elif refName == "Fang et al., 2017, %10 DMSO, Jurkat, 37C":
        self.v1.set(5)           # cell radius in um
        self.v2.set(0.4336)          # hydraulic conductivity in um/atm/min
        self.v3.set(0.000675)         # solute permeability in cm/min
        self.v4.set(1)           # reflection coefficient
```

```
        self.v5.set(0.6741)          # Osmotically inactive volume fraction (should be multiplied by
V0)
        self.v6.set(0.0000713)          # partial molar volume in m3/mol
        self.v7.set(10)             # Initial internal CPA concentration
        self.v8.set(297)            # Initial internal salt concentration
        self.v9.set(0.1/0.0000713)            # External CPA concentration
        self.v10.set(297)           # External salt concentration
        self.v11.set(0.01)          # time step
        self.v12.set(200)               # total time
        self.v13.set(310.15)        # Ambient Temperature
        self.v14.set(8.314)         # Boltzmann
        self.paper.set("C. Fang, F. Ji, Z. Shu, and D. Gao, “Determination of the temperature-
dependent cell membrane permeabilities using microfluidics with integrated flow and temperature
control,” Lab Chip, vol. 17, no. 5, pp. 951–960, 2017.")

    elif refName == "Shu et al., 2016, 1.5M Ethylene Glycol, Human Vaginal T Cell, 22C":
        self.v1.set(8.43)           # cell radius in um
        self.v2.set(0.099)          # hydraulic conductivity in um/atm/min *** son tabloda hatali
verilmis
        self.v3.set(0.000469)        # solute permeability in cm/min
        self.v4.set(1)            # reflection coefficient
        self.v5.set(0.516)          # Osmotically inactive volume fraction (should be multiplied by
V0)
        self.v6.set(0.0000713)          # partial molar volume in m3/mol
        self.v7.set(10)             # Initial internal CPA concentration
        self.v8.set(297)            # Initial internal salt concentration
        self.v9.set(1500)             # External CPA concentration
        self.v10.set(297)           # External salt concentration
        self.v11.set(0.01)          # time step
        self.v12.set(200)               # total time
        self.v13.set(295.15)        # Ambient Temperature
        self.v14.set(8.314)         # Boltzmann
        self.paper.set("Z. Shu et al., “A study of the osmotic characteristics, water permeability, and
cryoprotectant permeability of human vaginal immune cells,” Cryobiology, vol. 72, no. 2, pp. 93–
99, 2016.")

    elif refName == "Shu et al., 2016, 1.5M Propylene Glycol, Human Vaginal T Cell, 22C":
        self.v1.set(8.43)           # cell radius in um
        self.v2.set(0.077)          # hydraulic conductivity in um/atm/min *** son tabloda hatali
verilmis
        self.v3.set(0.000635)        # solute permeability in cm/min
        self.v4.set(1)            # reflection coefficient
        self.v5.set(0.516)          # Osmotically inactive volume fraction (should be multiplied by
V0)
        self.v6.set(0.0000713)          # partial molar volume in m3/mol
        self.v7.set(10)             # Initial internal CPA concentration
        self.v8.set(297)            # Initial internal salt concentration
        self.v9.set(1500)             # External CPA concentration
        self.v10.set(297)           # External salt concentration
        self.v11.set(0.01)          # time step
        self.v12.set(200)               # total time
        self.v13.set(295.15)        # Ambient Temperature
        self.v14.set(8.314)         # Boltzmann
```

```
        self.paper.set("Z. Shu et al., “A study of the osmotic characteristics, water permeability, and cryoprotectant permeability of human vaginal immune cells,” Cryobiology, vol. 72, no. 2, pp. 93–99, 2016.")

    elif refName == "Shu et al., 2016, 1.5M Glycerol, Human Vaginal T Cell, 22C":
        self.v1.set(8.43)           # cell radius in um
        self.v2.set(0.055)          # hydraulic conductivity in um/atm/min *** son tabloda hatali verilmis
        self.v3.set(0.000005)       # solute permeability in cm/min
        self.v4.set(1)          # reflection coefficient
        self.v5.set(0.516)          # Osmotically inactive volume fraction (should be multiplied by V0)
        self.v6.set(0.0000713)          # partial molar volume in m3/mol
        self.v7.set(10)             # Initial internal CPA concentration
        self.v8.set(297)            # Initial internal salt concentration
        self.v9.set(1500)           # External CPA concentration
        self.v10.set(297)           # External salt concentration
        self.v11.set(0.01)          # time step
        self.v12.set(200)               # total time
        self.v13.set(295.15)        # Ambient Temperature
        self.v14.set(8.314)         # Boltzmann
        self.paper.set("Z. Shu et al., “A study of the osmotic characteristics, water permeability, and cryoprotectant permeability of human vaginal immune cells,” Cryobiology, vol. 72, no. 2, pp. 93–99, 2016.")

    elif refName == "Shu et al., 2016, 1.5M Ethylene Glycol, Human Vaginal Macrophage, 22C":
        self.v1.set(9.62)           # cell radius in um
        self.v2.set(0.241)          # hydraulic conductivity in um/atm/min
        self.v3.set(0.000418)       # solute permeability in cm/min
        self.v4.set(1)          # reflection coefficient
        self.v5.set(0.457)          # Osmotically inactive volume fraction (should be multiplied by V0)
        self.v6.set(0.0000713)          # partial molar volume in m3/mol
        self.v7.set(10)             # Initial internal CPA concentration
        self.v8.set(297)            # Initial internal salt concentration
        self.v9.set(1500)           # External CPA concentration
        self.v10.set(297)           # External salt concentration
        self.v11.set(0.01)          # time step
        self.v12.set(200)               # total time
        self.v13.set(295.15)        # Ambient Temperature
        self.v14.set(8.314)         # Boltzmann
        self.paper.set("Z. Shu et al., “A study of the osmotic characteristics, water permeability, and cryoprotectant permeability of human vaginal immune cells,” Cryobiology, vol. 72, no. 2, pp. 93–99, 2016.")

    elif refName == "Shu et al., 2016, 1.5M Propylene Glycol, Human Vaginal Macrophage, 22C":
        self.v1.set(9.62)           # cell radius in um
        self.v2.set(0.221)          # hydraulic conductivity in um/atm/min
        self.v3.set(0.001168)       # solute permeability in cm/min
        self.v4.set(1)          # reflection coefficient
        self.v5.set(0.457)          # Osmotically inactive volume fraction (should be multiplied by V0)
        self.v6.set(0.0000713)          # partial molar volume in m3/mol
```

```
        self.v7.set(10)            # Initial internal CPA concentration
        self.v8.set(297)           # Initial internal salt concentration
        self.v9.set(1500)          # External CPA concentration
        self.v10.set(297)          # External salt concentration
        self.v11.set(0.01)         # time step
        self.v12.set(200)              # total time
        self.v13.set(295.15)       # Ambient Temperature
        self.v14.set(8.314)        # Boltzmann
        self.paper.set("Z. Shu et al., “A study of the osmotic characteristics, water permeability, and cryoprotectant permeability of human vaginal immune cells,” Cryobiology, vol. 72, no. 2, pp. 93–99, 2016.")

    elif refName == "Shu et al., 2016, 1.5M Glycerol, Human Vaginal Macrophage, 22C":
        self.v1.set(9.62)          # cell radius in um
        self.v2.set(0.192)         # hydraulic conductivity in um/atm/min
        self.v3.set(0.000008)      # solute permeability in cm/min
        self.v4.set(1)           # reflection coefficient
        self.v5.set(0.457)         # Osmotically inactive volume fraction (should be multiplied by V0)
        self.v6.set(0.0000713)         # partial molar volume in m3/mol
        self.v7.set(10)            # Initial internal CPA concentration
        self.v8.set(297)           # Initial internal salt concentration
        self.v9.set(1500)          # External CPA concentration
        self.v10.set(297)          # External salt concentration
        self.v11.set(0.01)         # time step
        self.v12.set(200)              # total time
        self.v13.set(295.15)       # Ambient Temperature
        self.v14.set(8.314)        # Boltzmann
        self.paper.set("Z. Shu et al., “A study of the osmotic characteristics, water permeability, and cryoprotectant permeability of human vaginal immune cells,” Cryobiology, vol. 72, no. 2, pp. 93–99, 2016.")

    elif refName == "Gilmore et al, 1995, 1M Glycerol, Human Spermatozoa, 22C":
        self.v1.set(1.89)          # cell radius in um
        self.v2.set(0.77)          # hydraulic conductivity in um/atm/min
        self.v3.set(0.0021)        # solute permeability in cm/min
        self.v4.set(0.93)          # reflection coefficient
        self.v5.set(0.5)         # Osmotically inactive volume fraction (should be multiplied by V0)
        self.v6.set(0.0000713)         # partial molar volume in m3/mol
        self.v7.set(10)            # Initial internal CPA concentration
        self.v8.set(297)           # Initial internal salt concentration
        self.v9.set(1000)          # External CPA concentration
        self.v10.set(297)          # External salt concentration
        self.v11.set(0.01)         # time step
        self.v12.set(200)              # total time
        self.v13.set(295.15)       # Ambient Temperature
        self.v14.set(8.314)        # Boltzmann
        self.paper.set("J. A. Gilmore et al., “Effect of Cryoprotectant Solutes on Water Permeability of Human Spermatozoa’,” Biol. Reprod., vol. 53, pp. 985–995, 1995.")

    elif refName == "Gilmore et al, 1995, 1M PG, Human Spermatozoa, 22C":
        self.v1.set(1.89)          # cell radius in um
        self.v2.set(1.23)          # hydraulic conductivity in um/atm/min
        self.v3.set(0.0023)        # solute permeability in cm/min
```

```
            self.v4.set(0.95)           # reflection coefficient
            self.v5.set(0.5)          # Osmotically inactive volume fraction (should be multiplied by V0)
            self.v6.set(0.0000713)          # partial molar volume in m3/mol
            self.v7.set(10)             # Initial internal CPA concentration
            self.v8.set(297)            # Initial internal salt concentration
            self.v9.set(1000)             # External CPA concentration
            self.v10.set(297)           # External salt concentration
            self.v11.set(0.01)          # time step
            self.v12.set(200)               # total time
            self.v13.set(295.15)         # Ambient Temperature
            self.v14.set(8.314)         # Boltzmann
            self.paper.set("J. A. Gilmore et al., “Effect of Cryoprotectant Solutes on Water Permeability
of Human Spermatozoa’,” Biol. Reprod., vol. 53, pp. 985–995, 1995.")

        elif refName == "Gilmore et al, 1995, 1M DMSO, Human Spermatozoa, 22C":
            self.v1.set(1.89)           # cell radius in um
            self.v2.set(0.84)          # hydraulic conductivity in um/atm/min
            self.v3.set(0.0008)         # solute permeability in cm/min
            self.v4.set(0.98)           # reflection coefficient
            self.v5.set(0.5)          # Osmotically inactive volume fraction (should be multiplied by V0)
            self.v6.set(0.0000713)          # partial molar volume in m3/mol
            self.v7.set(10)             # Initial internal CPA concentration
            self.v8.set(297)            # Initial internal salt concentration
            self.v9.set(1000)             # External CPA concentration
            self.v10.set(297)           # External salt concentration
            self.v11.set(0.01)          # time step
            self.v12.set(200)               # total time
            self.v13.set(295.15)         # Ambient Temperature
            self.v14.set(8.314)         # Boltzmann
            self.paper.set("J. A. Gilmore et al., “Effect of Cryoprotectant Solutes on Water Permeability
of Human Spermatozoa’,” Biol. Reprod., vol. 53, pp. 985–995, 1995.")

        elif refName == "Gilmore et al, 1995, 2M EG, Human Spermatozoa, 22C":
            self.v1.set(1.89)           # cell radius in um
            self.v2.set(0.74)          # hydraulic conductivity in um/atm/min
            self.v3.set(0.0079)         # solute permeability in cm/min
            self.v4.set(0.77)           # reflection coefficient
            self.v5.set(0.5)          # Osmotically inactive volume fraction (should be multiplied by V0)
            self.v6.set(0.0000713)          # partial molar volume in m3/mol
            self.v7.set(10)             # Initial internal CPA concentration
            self.v8.set(297)            # Initial internal salt concentration
            self.v9.set(2000)             # External CPA concentration
            self.v10.set(297)           # External salt concentration
            self.v11.set(0.01)          # time step
            self.v12.set(200)               # total time
            self.v13.set(295.15)         # Ambient Temperature
            self.v14.set(8.314)         # Boltzmann
            self.paper.set("J. A. Gilmore et al., “Effect of Cryoprotectant Solutes on Water Permeability
of Human Spermatozoa’,” Biol. Reprod., vol. 53, pp. 985–995, 1995.")



    def getCPAs(self, event):
        CPAName = str(self.comboRef2.get())
```

```
        if CPAName == "glycerol":
            self.v16.set(47.92)             # Shrinking Rate
        elif CPAName == "ethylene glycol":
            self.v16.set(169.45)            # Shrinking Rate
        elif CPAName == "propylene glycol":
            self.v16.set(7.1)             # Shrinking Rate

app = SampleApp()

app.mainloop()
```